SAFETY SYSTEMS

FOR

WATER PUMPING WINDMILLS

A. KRAGTEN

April 1989 R 999 D

WIND ENERGY GROUP
Technical University Eindhoven
Faculty of Physics
Laboratory of Fluid Dynamics and Heat Transfer
P.O. Box 513
5600 MB Eindhoven, the Netherlands

CWD
Consultancy Services
Wind Energy
Developing Countries

p.o. box 85
3800 ab amersfoort
holland

CONTENTS

	Page
List of symbols	
1. GENERAL	1
2. THE PURPOSE OF A SAFETY SYSTEM	3
3. OVERVIEW OF SAFETY SYSTEMS	5
3.1 Systems acting on the rotor blades	5
3.2 Systems acting on the whole rotor	5
4. SAFETY SYSTEMS WHICH TURN THE ROTOR SIDEWAYS	7
4.1 General	7
4.2 Non-automatic system	8
4.3 System activated by sideforce only	9
4.4 Ecliptic with eccentrically placed rotor	10
4.5 Ecliptic with auxiliary vane	11
4.6 Inclined hinge main vane with eccentrically placed rotor	11
4.7 Inclined hinge main vane with auxiliary vane	11
4.8 Hinged side vane with eccentrically placed rotor	12
4.9 Hinged side vane with auxiliary vane	14
5. THE IDEAL SAFETY SYSTEM	15
6. DEVIATION FROM THE IDEAL SAFETY SYSTEM	25
6.1 Rotor is placed before the tower axis	25
6.2 Rotor is provided with auxiliary vane in stead of eccentricity	25
6.3 Main vane has no constant moment	31
6.4 Other disturbing effects	34
6.5 Combination of deviations	35

7. DETAILED DESCRIPTION OF THREE SYSTEMS 37
7.1 General 37
7.2 Moment of eccentrically placed rotor around the tower axis 38
7.3 Moment of centrically placed rotor plus auxiliary vane around the tower axis 45
7.4 The ecliptic system 50
7.4.1 General 50
7.4.2 Ecliptic system with eccentrically placed rotor for $V \leq V_{rated}$ 50
7.4.3 Ecliptic system with auxiliary vane for $V \leq V_{rated}$ 54
7.4.4 Ecliptic system with eccentrically placed rotor $V > V_{rated}$ 56
7.4.5 Ecliptic system with auxiliary vane for $V > V_{rated}$ 58
7.4.6 Example 59
7.5 The inclined hinge main vane system 69
7.5.1 General 69
7.5.2 Example 73
7.6 The hinged side vane system 79
7.6.1 General 79
7.6.2 The hinged side vane system for low wind speeds 85
7.6.3 The hinged side vane system for high wind speeds 86
7.6.4 The hinged side vane system for moderate wind speeds 88
7.6.5 Example 89

8. FIELD MEASUREMENTS 99

9. SCALE LAWS 101

10. CONCLUSIONS 105

LITERATURE 107

ANNEX I (TUE internal note 03.89)

LIST OF SYMBOLS

$(1 - a)$	reduction factor of wind speed behind the rotor	–
A_{av}	auxiliary vane area	m^2
A_v	vane area	m^2
A_{mv}	main vane area	m^2
A_{va}	vane arm area	m^2
B	number of blades	–
C	blade chord	m
C_d	drag coefficient	–
$C_{d_{va}}$	vane arm drag coefficient	–
C_l	lift coefficient	–
C_m	pitch moment coefficient	–
C_{m_r}	rotor moment coefficient (around tower axis)	–
$C_{m_{av}}$	auxiliary vane moment coefficient	–
$C_{m_{r+av}}$	coefficient of rotor moment + auxiliary vane moment	–
C_n	normal force coefficient	–
$C_{n_{av}}$	auxiliary vane normal force coefficient	–
$C_{n_{mv}}$	main vane normal force coefficient	–
C_q	rotor torque coefficient	–
C_s	rotor side force coefficient	–
C_{so}	rotor self orientating moment coefficient	–
C_t	rotor thrust coefficient	–
d	pipe diameter	m
d_p	vane arm pipe diameter	m
D	rotor diameter	m
D	drag	N
e	eccentricity (distance between rotor axis and tower axis)	m
f	distance between rotor plane and tower axis	m
f_1 , f_2	specific values for f	m
F_s	rotor side force	N
F_t	rotor thrust	N
F_{t_δ}	rotor thrust at yaw angle δ	N
$F_{t_{rated}}$	rotor thrust at rated wind speed	N
F_{va}	vane arm drag force	N

g	acceleration of gravity (9.81)	m/s^2
g	distance between vane axis and tower axis	m
G	vane weight	N
h	vane chord perpendicular to vane axis	m
i	scale factor	-
i	aspect ratio	-
i	distance between aerodynamic center and leading edges of a vane	m
i_1	value for i at low wind speeds	m
i_2	value for i at high wind speeds	m
k	grain size (of pipe roughness)	m
l	blade length	m
L	lift	N
M	pitch moment (of hinged side vane)	Nm
M_{av}	auxiliary vane moment (around tower axis)	Nm
M_g	moment of vane weight (around vane axis)	Nm
M_{gmax}	maximum moment of vane weight (at $\gamma = 90^o$)	Nm
M_{mv}	main vane moment (around vane axis)	Nm
$M_{mv_{ta}}$	main vane moment around tower axis	Nm
$M_{mv_{va}}$	main vane moment around vane axis	Nm
M_r	rotor moment (around tower axis)	Nm
M_{r+av}	moment of rotor + auxiliary vane (around tower axis)	Nm
M_{spring}	spring moment	Nm
$M_{s_{max}}$	maximum spring moment	Nm
$M_{s_{min}}$	minimum spring moment	Nm
M_{s_γ}	spring moment at certain angle γ	Nm
M_{so}	rotor self orientating moment	Nm
M_v	vane moment (around tower axis)	Nm
M_{va}	vane arm moment	Nm
n	rotor speed	rev/s
N	normal force	N
N_{av}	auxiliary vane normal force	N
N_{mv}	main vane normal force	N
o	distance between spring axis and vane axis	m
P	rotor power	W
Q	rotor torque	Nm

R	rotor radius (half rotor diameter)	m
R_{av}	auxiliary vane radius	m
Re	Reynolds number	-
R_g	radius of vane weight in center of gravity	m
R_{mv}	main vane radius	M
R_v	vane radius	M
t	vane thickness	m
V	wind speed	m/s
V_{rated}	rated wind speed (wind speed at maximum power)	m/s
w	vane chord parallel to vane axis	m

α	angle of attack	–
α_1	angle between vane chord w and wind direction (at low wind speeds)	–
α_2	angle between vane chord h and wind direction (at high wind speeds)	–
α_{av}	angle of attack auxiliary vane	–
α_{mv}	angle of attack main vane	–
β	angle which determines position of auxiliary vane blade before tower axis	–
γ	angle of rotation of the main vane around its axis	–
γ_{max}	maximum angle of rotation of the main vane around its axis	–
δ	yaw angle (angle between rotor axis and wind direction)	–
δ_o	pre-angle between main vane and rotor axis	–
ϵ	angle between vane axis and vertical	–
θ	angle between vane blade and vertical	–
λ	tip speed ratio (ratio between tip speed and wind speed)	–
$\lambda_{unloaded}$	unloaded tip speed ratio	–
ν	kinematic viscosity	m^2/s
ξ	pre-angle of auxiliary vane	–
π	pi (3.1416)	–
ρ	air density	kg/m^3
ρ_v	vane density	kg/m^3
ϕ_1	angle between vane arm axis and rotor axis	–
ϕ_2	angle between vane arm axis and vane axis	–
ω	rotational speed of the head	rad/s
Ω	rotational speed (angular velocity) of the rotor	rad/s
Ω_{max}	maximum rotational speed	rad/s
Ω_δ	rotational speed at yaw angle δ	rad/s

1. GENERAL

Most literature available about safety systems for water pumping windmills has been written by CWD in particular by the Wind Energy Group of the University of Technology Eindhoven.
An overview of all literature about this subject available within CWD has been presented in TUE internal note 03–89 [1] (see annex I).
In chapter 11 of the CWD publication 82–1. Introduction to wind energy [2] some information has been given about safety systems especially about the inclined hinge main vane system based upon the knowledge available up to 1981. It is found to be necessary to write this separate publication about safety systems to cover the knowledge and experience gained by CWD in the period 1981–1989.
However, even this publication can not claim to be a complete collection of all information available in all separate reports as mentioned in annex I. Chapter 2 till 6 and chapter 8 till 10 give more general information about safety systems and can be understood by under graduates.
Chapter 7 in which three safety systems have been described is more complicated and has a more mathematical orientation.

2. THE PURPOSE OF A SAFETY SYSTEM

Windmills without a safety system usually have a short life. An exception can be made for very small windmills with a diameter less then one meter which can be made so strong or have a tower which is so low, that they can survive heavy storms.
Normally a well designed safety system is required which must perform three functions:

1. Limitation of the axial force or thrust on the rotor.

Too high a thrust can cause the following problems:

a. The bending moment and therefore the bending stress in the rotor spars becomes too high which results in blades snapping off.
b. The bending moment in a tubular tower. or the buckling force in the guy wires of a guyed tower can become too high which can cause collapse of the tower or pulling the foundation out of the ground.

2. Limitation of the rotational speed of the rotor.

Too high a rotational speed can cause the following problems:

a. High centrifugal forces in the blades resulting in high tensile forces in the blade spars. This can result in launching of one of the blades, leaving behind an unbalanced machine which soon will loose other blades or even the total head.
b. A high rotational speed in combination with a small unbalance of the rotor causes strong vibrations which can result in high fatigue loads in several windmill components like blades, rotor shaft, head bearing, vane arms etc.
c. A combination of a high rotor speed and a high yawing speed of the head gives rise to high gyroscopic moments in the blades and the rotor shaft.
d. High tip speeds can introduce a dangerous aero-elastic behaviour called "flutter". This is a combination of severe torsional and bending vibrations in the blade. It specially occurs in tall blades with a small torsion stiffness of fast running rotors.
e. In case of water pumping windmills the high pump frequencies lead to a high pump rod force in the transmission from pump rod to rotor shaft. The high pump rod force is caused by high acceleration forces and shock forces due to delayed closure of the valves.

3. Limitation of the yawing speed (rotation of the head around the tower axis).

A high yawing speed results in a high gyroscopic moment (see pt 2c).

Most safety systems have a direct influence on the axial force on the rotor and on the rotational speed.
The influence on the yawing speed is more indirect. It depends on the Ω–V curve of the system (see chapter 7), the inertia of head and vane and the variation in wind speed and wind direction.

3. OVERVIEW OF SAFETY SYSTEMS

The safety system can act either on each of the blades or on the rotor as a whole.
The first method is mostly used for fast running two- or three-bladed wind turbines for the generation of electricity.
The second method is usually used for multiblade rotors for water pumping windmills.

3.1 Systems acting on the rotor blades

a. Pitch control (changing setting angle of the blades, positive or negative).
   The torque to turn the blade can be generated by centrifugal weights, the axial force on the blades or by an external device (for instance using a hydraulic system).
b. Turning only the blade tip.
c. Centrifugal force activated brake flaps at the blade tip.
d. Spoilers (movable ridges that spoil a part the blade's performance).
e. Parachutes in the blade tips (only for an emergency brake).

3.2 Systems acting on the whole rotor

a. Mechanical brake on the rotor shaft to stop the rotor if a certain wind speed or rotor speed is reached.
b. Mechanical brake on the rotor shaft or heavy generator with which the rotor speed is kept constant above a certain wind speed.
c. Centrifugal force activated brake flaps on separate arms.
   For systems b en c stall is introduced in the blades at high wind speeds causing a decrease in power and thrust coefficient of the rotor.
d. Turning the rotor upward out of the wind around a horizontal axis.
e. Turning the rotor sideways out of the wind around the vertical axis of the head bearing which lays in the tower center. Most water pumping windmills use a system according to this principle and it is the focus of this publication.
   Guidelines for safety systems for medium scale electricity generating windmills are given in [22] part 6 of IEA publication Structural Safety.
   Safety systems for water pumping windmills according to 3.2.e are mentioned in chapter four.

4. SAFETY SYSTEMS WHICH TURN THE ROTOR SIDEWAYS

4.1 General

Safety systems which turn the rotor sideways may have the following characteristics:

a. The system is automatic; this means the rotor turns out of the wind above a certain wind speed and turns back into the wind at low wind speeds automatically.
b. The system is non-automatic; this means the rotor turns out of the wind above a certain wind speed and must be turned back into the wind manually.
c. The moment which turns the rotor out of the wind is caused by an auxiliary vane.
d. The moment which turns the rotor out of the wind is caused by the axial force on the rotor (thrust) in combination with an eccentricity "e" between rotor shaft and head axis.
e. The moment which turns the rotor out of the wind is caused by the side force on the rotor in combination with the distance "f" between rotor plane and tower axis.
f. The main vane axis is vertical and the vane is pulled against a stop by a spring or by a weight.
   This is called the **ecliptic system**.
g. The main vane axis makes a certain angle ϵ with the vertical and the vane has a lowest position in which it tends to go by its own weight. This is called the inclined **hinge main vane system**.
h. The main vane can rotate around a horizontal axis and is placed beside and behind the rotor plane. This is called the **hinged side vane system**.
i. The main vane axis is vertical but there is no spring like in the ecliptic system and the vane is kept in position by something else, for example by a side vane activated clutch.

A system now can be characterised by a combination of point a to i.
Most known systems are automatic so according to point a; only one non-automatic system (point b) will be described.
Since a certain distance "f" between rotor plane and tower axis is always required, point e is valid for all systems. The following combinations are more or less common:
(If commercial windmills are mentioned they can be found in CWD publication 84-2 Catalogue of wind machines [3]).

4.2 Non-automatic system b + c + e + i (see fig. 1)

This system was used on the earlier 12PU500 windmill developed by the WOT for the Ghazipur windmill project in India.

Here the auxiliary vane locks the main vane at low wind speeds.

The auxiliary vane moves a bit backwards if the moment of the wind pressure on the vane blade around the vane axis becomes larger than the moment of the spring. Then the main vane is unlocked and the rotor turns out of the wind by the moment of the auxiliary vane around the tower axis. At larger yaw angles δ the side force on the rotor gives an extra moment which is added to the moment of the auxiliary vane.

The main disadvantage of this system is that it can only be used in low wind regimes because it needs only one big gust to turn out of the wind definitively and setting it in the wind again must be done manually. Therefore systems which come back automatically are preferred.

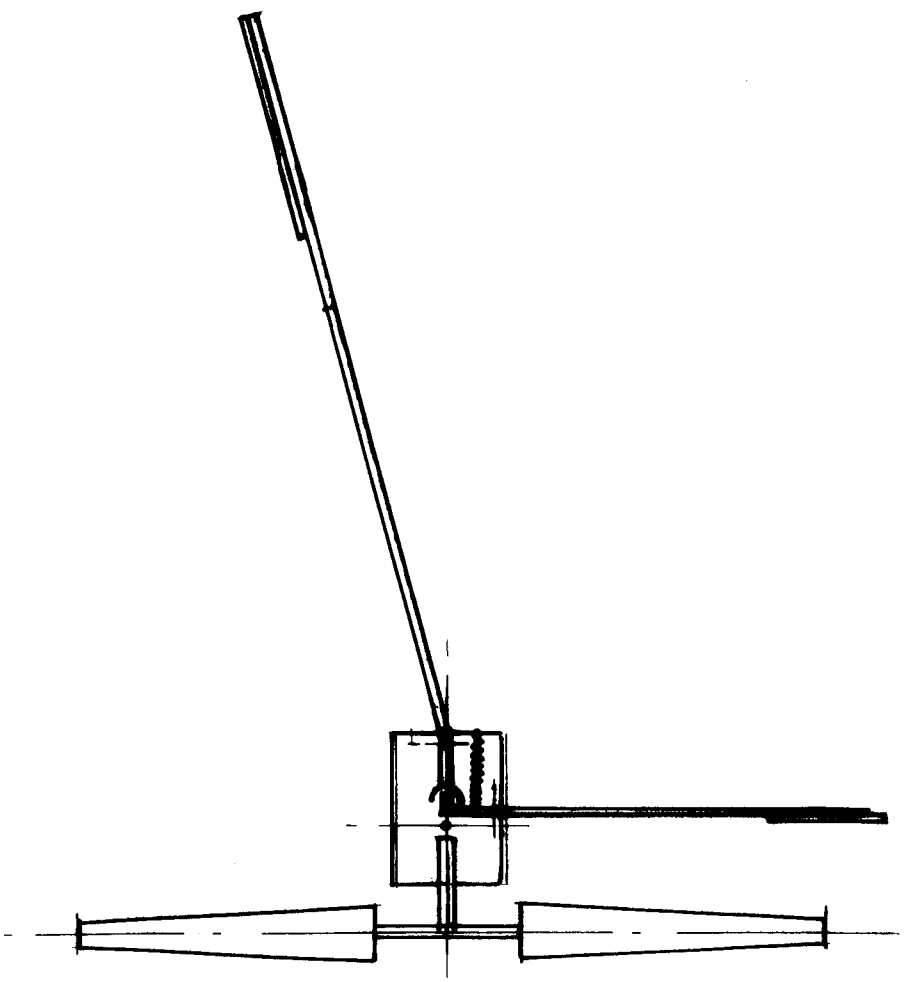

Figure 1 Non-automatic system

4.3 Systems activated by side force only a + e + f (see fig. 2)

This system is used by the Finnish Akrobaatti windmill (see TUE report R 871 D [4]). Because the side force is increasing at an increasing yaw angle the system will be very unstable and will start turning out of the wind only by a sudden change in wind direction. If no such wind shift occurs the rotor speed may increase too much.

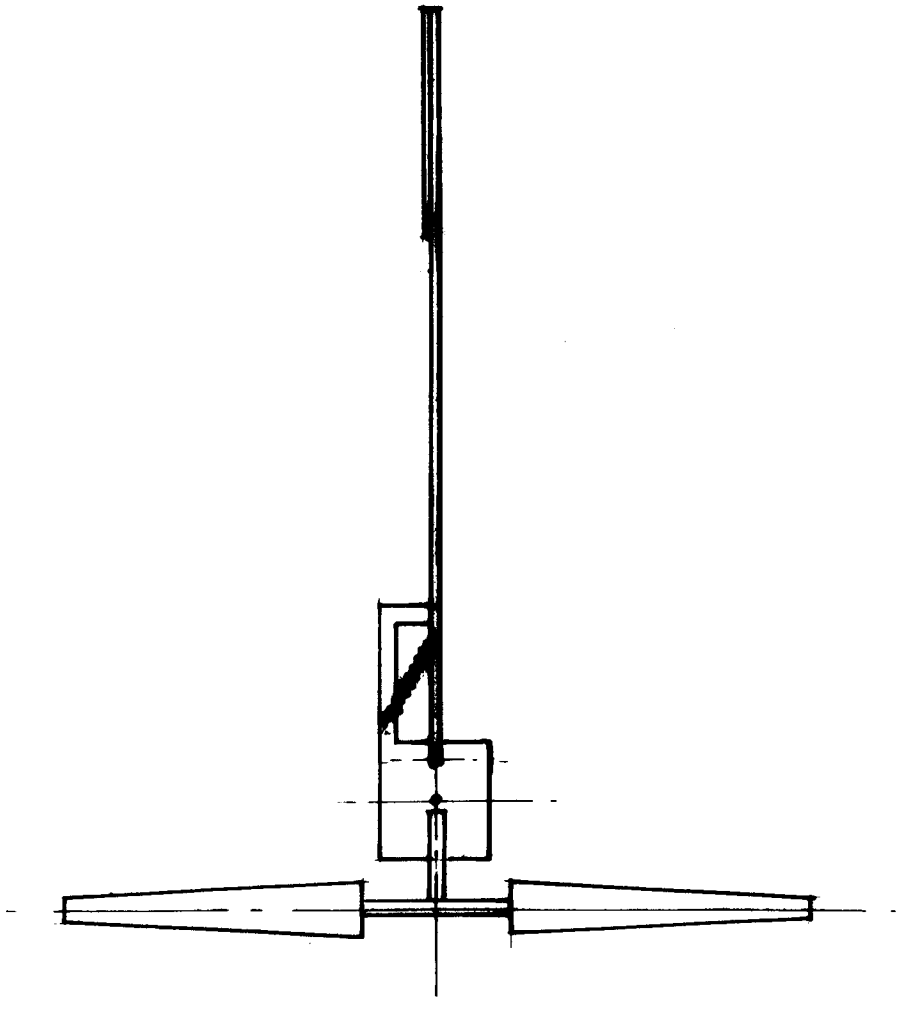

Figure 2 System activated by side force only

4.4 Ecliptic with eccentrically placed rotor a + d + e + f (see fig. 3)

This system is used on almost all commercial windmills especially if they have a gearbox. In that case the eccentricity is determined by the distance between the rotor shaft and the pump rod.

At a low wind speed the main vane is pulled against a stop by a spring or a weight and the moment of rotor thrust times the eccentricity around the tower axis is counter-balanced by the moment of the aerodynamic force on the main vane. To keep the rotor perpendicular to the wind at low wind speeds the main vane must make a pre-angle δ_o with the rotor axis.

The rotor starts turning out of the wind at the wind speed where the moment of the main vane around the vane axis is larger than the moment of the spring or the weight.

A disadvantage of the ecliptic system is that damping on the main vane is required to prevent a large shock if the vane hits the stop.

This system is used on for instance the Dempster, Tozzi and Bardi, Fiasa and many other commercial windmills. For more detailed information about the ecliptic safety system see chapter 7.

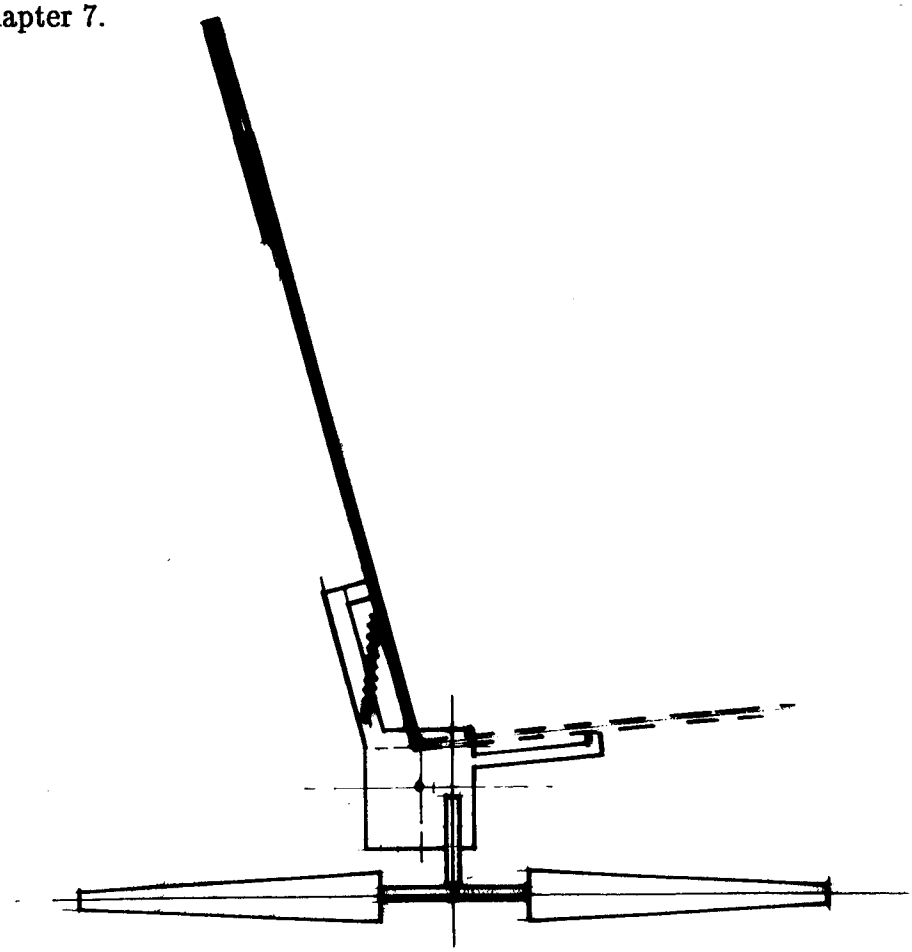

Figure 3 Ecliptic system with eccentrically placed rotor

4.5 Ecliptic with auxiliary vane a + c + e + f

An auxiliary vane has a less favourable effect on the control characteristics than an eccentrically placed rotor (see chapter 6.2). However placing the rotor centrically may result in a simple head construction and transmission.

This system is used on the CWD 5000 HW (see TUE report R 418 D [5]), the Humblot, the Oasis and many other commercial windmills.

4.6 Inclined hinge main vane with eccentrically placed rotor a + d + e + g

The advantage of this system above the ecliptic system is that it has no spring nor stop. The main vane axis is inclined and therefore the vane tends to go to the lowest position by the vane weight. A sinusoidal moment is required to push it out this lowest position. For more detailed information see chapter 7 and lit. [2].

A disadvantage of this system is that the rotor starts turning out of the wind at low wind speeds where it is not yet necessary. The system is used on the CWD 1000 EL, the Southern Cross and others.

4.7 Inclined hinge main vane with auxiliary vane a + c + e + g (fig. 4)

Also for the inclined hinge main vane system an auxiliary vane is less favourable than an eccentrically placed rotor.

This system is used on the CWD 2740, CWD 5000, CWD 8000 and WEU I–3. It is described in lit. [2] and in TUE report R 592 D [6].

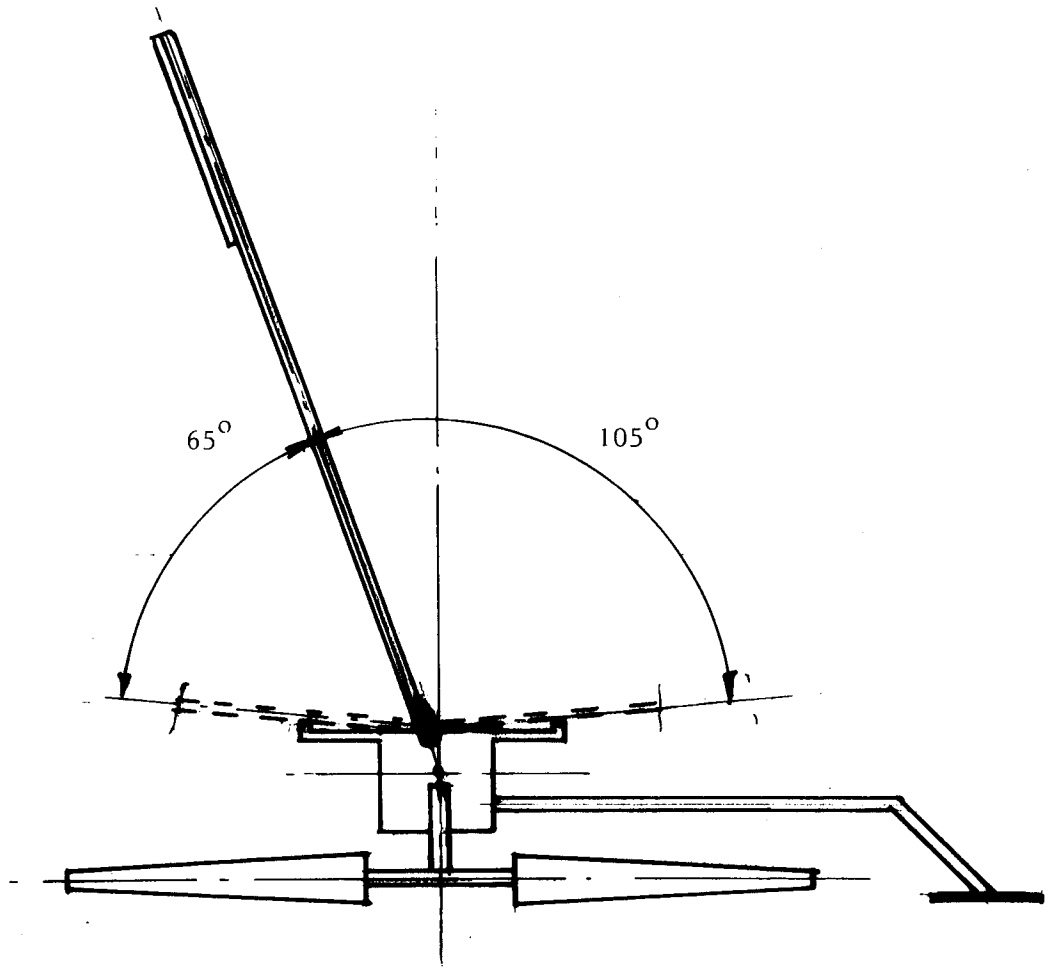

Figure 4 inclined hinge main vane with auxiliary vane

4.8 Hinged side vane with eccentrically placed rotor a + d + e + h (see fig. 5)

The hinged side vane system is a new system which recently has been developed in the first instance for an electricity generating windmill type VIRYA-3 and later on also for the water pumping windmill CWD 2000. It has been described in TUE report R 515 D [7]. The dynamic behaviour has been described in TUE report R 728 D [21].

At low wind speeds the vane blade hangs in an almost vertical position and the moment of the horizontal component of the aerodynamic force on the vane blade around the head axis is in balance with the moment of the thrust on the rotor.

At high wind speed the vane is lifted to an almost horizontal position and the rotor is pushed out of the wind by a combination of thrust and side force.

The characteristic lays close to the theoretical optimum and the system is very stable mainly caused by the large eccentricity of the rotor, the large moment of inertia of the head and the fact that the vane is in the undisturbed wind speed.
For more detailed information about the hinged side vane system see chapter 7.

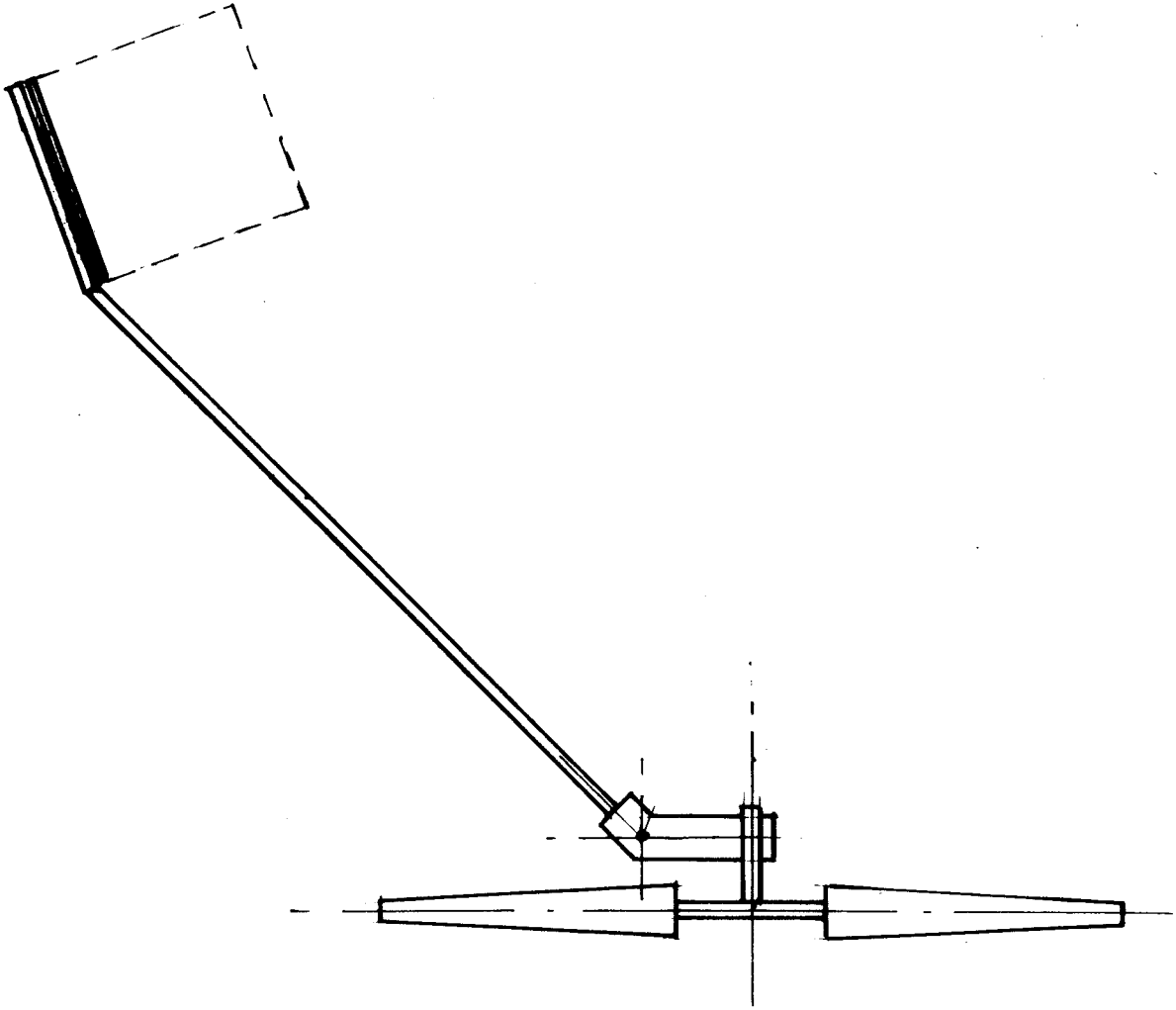

Figure 5 Hinged side vane with eccentrically placed rotor

4.9 Hinged side vane with auxiliary vane a + c + e + h

This system never has been built on full scale but wind tunnel tests have been done for a prototype of the Sri Lankian WEU–4 windmill (see TUE report R 743 D [8]). The system appeared to be unstable which probably was caused by the large distance between the rotor and the tower axis (large influence of the rotor side force) and by the choice of a square auxiliary vane.

The system is not advised unless enough knowledge is available to prevent instability.

5. THE IDEAL SAFETY SYSTEM

To understand the functioning of the various systems a simplified theory is given and based on this theory a theoretical optimal system is designed.
As mentioned in chapter 2 the purpose of a safety system is 1e to limit the thrust and 2e to limit the rotational speed.
The rotational speed Ω for a certain rotor depends on:

1. the wind speed V
2. the yaw angle δ
3. the load torque Q

water pumping windmills generally have low design wind speeds which means that the optimal rotor-pump efficiency is reached at a low wind speed of about 4 m/s.
At wind speeds above 8 m/s where proper functioning of safety systems is important the pump torque is much lower than the optimal rotor torque and therefore the rotor runs at almost the unloaded tip speed ratio $\lambda_{unloaded}$.
Uncoupling of the load at high wind speeds will result only in a small increase of the rotor speed.
Because this situation can happen in reality for instance if the pump rod breaks or if the well is empty the unloaded tip speed ratio is used in the calculations and the influence of the load torque Q on the rotor speed is neglected.
So now the rotational speed only depends on the wind speed V and the yaw angle δ.
The ideal characteristic of the rotational speed Ω versus the wind speed V is given in figure 6.

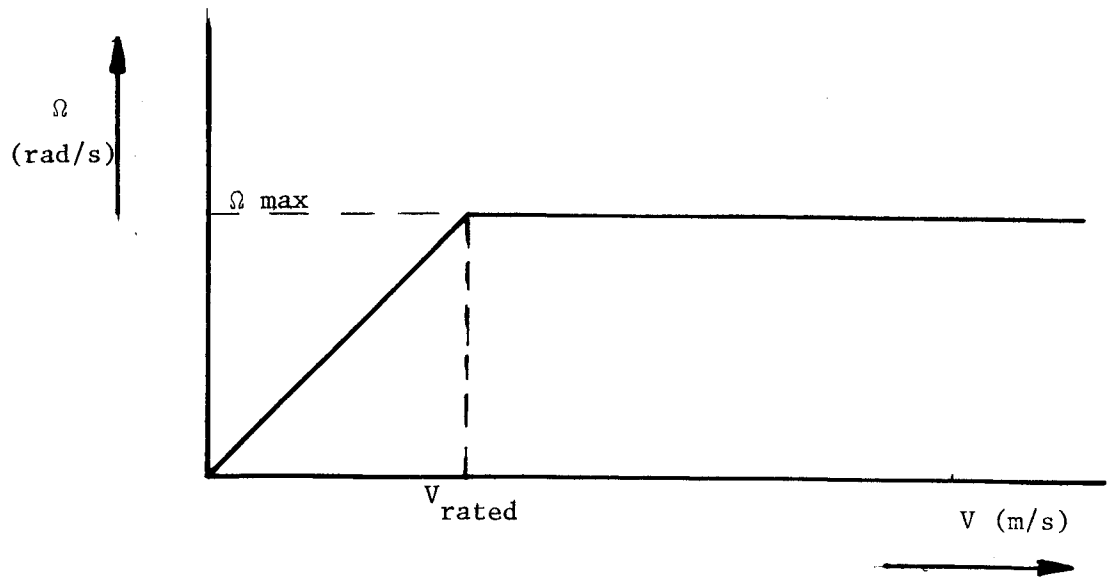

Figure 6 Ideal V - Ω characteristic

At V_{rated} the maximum allowable rotational speed Ω_{max} is reached.
For $V < V_{rated}$ the rotor is perpendicular to the wind to generate the maximum power and Ω is proportional with V (for $\lambda = \lambda_{unloaded}$).
For $V > V_{rated}$ Ω is Ω_{max} to prevent the problems as mentioned in chapter 2.

To solve the question of how the rotor must be turned out of the wind to realise this curve, first the relation between rotor speed and yaw angle δ for a certain wind speed must be known.

In figure 7 a rotor has been drawn at an angle δ with the wind direction.

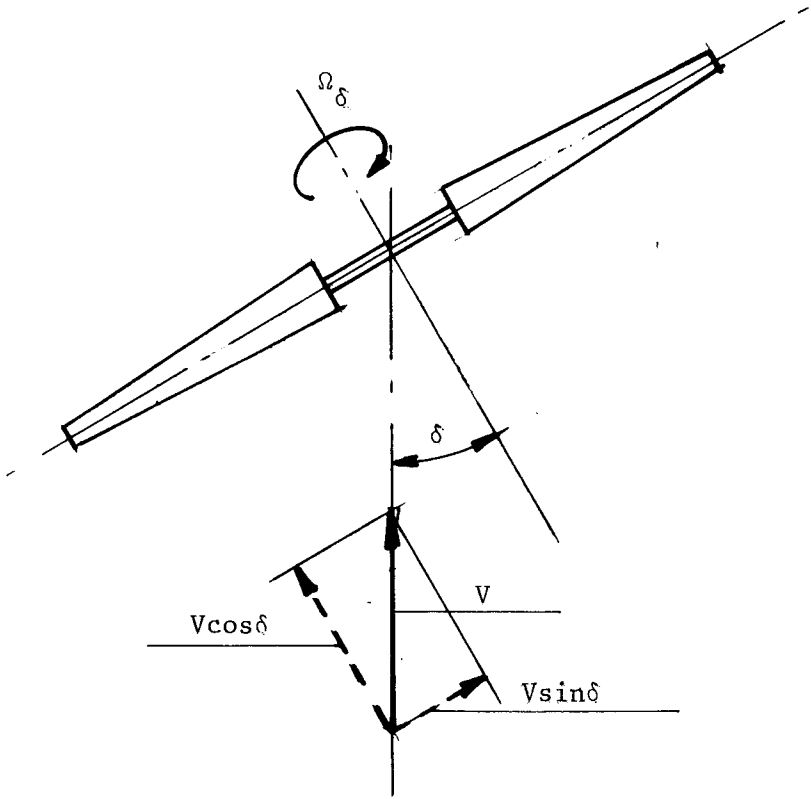

Figure 7 Resolving V in components Vcosδ and Vsinδ

The wind speed V can be resolved into a factor $V\cos\delta$ perpendicular to the rotor plane and a factor $V\sin\delta$ in the direction of the rotor plane.
Several windtunnel measurements indicate that if the factor $V\cos\delta$ is used to calculate the rotational speed Ω, the torque Q, the thrust F_t and the power P only a small mistake is made compared with the measurements (see TUE report R 408 S [9]).
However calculation of the side force F_s on the rotor using the factor $V\sin\delta$ yields a force which is much lower than what is measured, especially for low values of δ.
For the rotor perpendicular to the wind Ω is given by:

$$\Omega = \frac{\lambda \times V}{R} \tag{1}$$

For a certain yaw angle δ one must use $V\cos\delta$ instead of V:

$$\Omega_\delta = \frac{\lambda \times V\cos\delta}{R} \tag{2}$$

For the rotor perpendicular to the wind F_t is given by:

$$F_t = C_t \times 0.5\rho V^2 \pi R^2 \tag{3}$$

For a certain yaw angle δ one must use $V\cos\delta$ instead of V:

$$F_{t_\delta} = C_t \times 0.5\rho V^2 \cos^2\delta \pi R^2 \tag{4}$$

Now the question how to turn the rotor out of the wind to keep Ω constant for $V \geq V_{rated}$ can be answered as follows:

$$(1) \rightarrow \Omega = \frac{\lambda \times V}{R}$$

$$\Omega = \Omega_{max} \text{ for } V = V_{rated}$$

$$\Omega_{max} = \frac{\lambda}{R} \times V_{rated}$$

$$V_{rated} = V\cos\delta$$

or

$$\delta = \arccos \frac{V_{rated}}{V} \quad (5)$$

for $V \geq V_{rated}$

$$(2) \rightarrow \Omega_\delta = \frac{\lambda \times V\cos\delta}{R}$$

$$\Omega_\delta = \Omega_{max} \text{ for } V \geq V_{rated}$$

$$\Omega_{max} = \frac{\lambda \times V\cos\delta}{R}$$

This relation is presented graphically in figure 8.

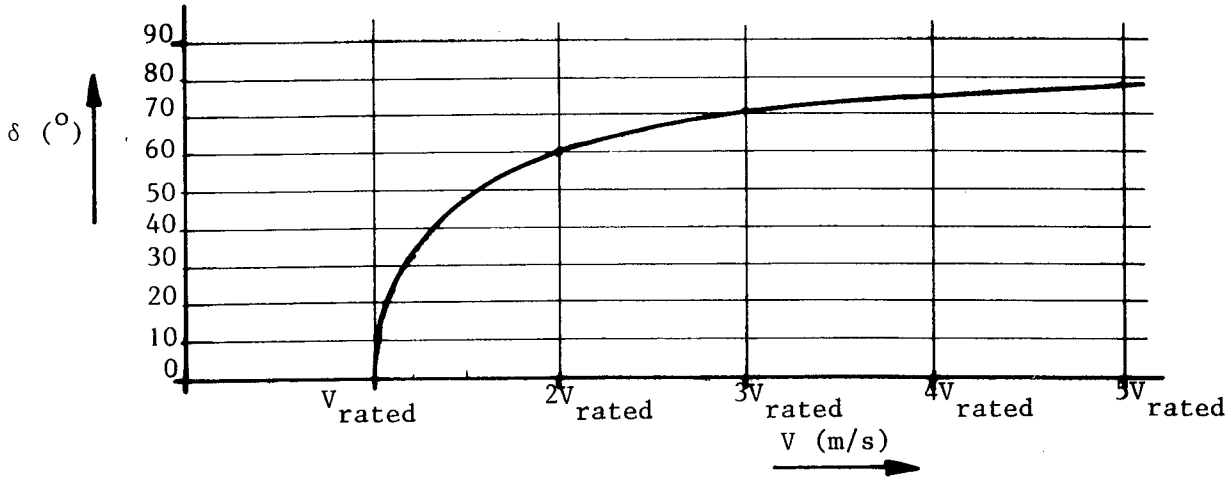

Figure 8 The ideal V – δ curve

In chapter 2 it has been explained that not only the rotor speed but also the rotor thrust F_t must be limited above V_{rated}. The question how to turn the rotor out of the wind to to keep F_t constant for $V \geq V_{rated}$ can be answered as follows:

$$(3) \rightarrow F_t = C_t \times 0.5\rho V^2 \pi R^2 \qquad V = V_{rated}$$

$$F_{t_{rated}} = C_t \times 0.5\rho V^2_{rated} \pi R^2$$

$$(4) \rightarrow F_{t_\delta} = C_t \times 0.5\rho V^2 \cos^2\delta \pi R^2 \qquad F_{t_\delta} = F_{t_{rated}} \text{ for } V > V_{rated}$$

$$F_{t_{rated}} = C_t \times 0.5\rho V^2 \cos^2\delta \pi R^2$$

$$V^2_{rated} = V^2\cos^2\delta \quad \text{or} \quad V_{rated} = V\cos\delta \quad \text{or} \quad \delta = \arccos \frac{V_{rated}}{V} \text{ for } V \geq V_{rated}.$$

This is again formula 5.

So this means that if the rotor is turned out of the wind in a way that the rotor thrust is constant for $V \geq V_{rated}$ automatically the rotor speed will be constant too!!

This knowledge can be used to design a safety system which has an ideal characteristic.

To realise this, the moment which turns the head out of the wind must be caused only by the thrust.

In general the moment produced by the aerodynamic forces on a yawing rotor M_r around the lower axis is given by the formula:

$$M_r = F_t \times e + F_s \times f - M_{so} \qquad (6)$$

(see figure 9)

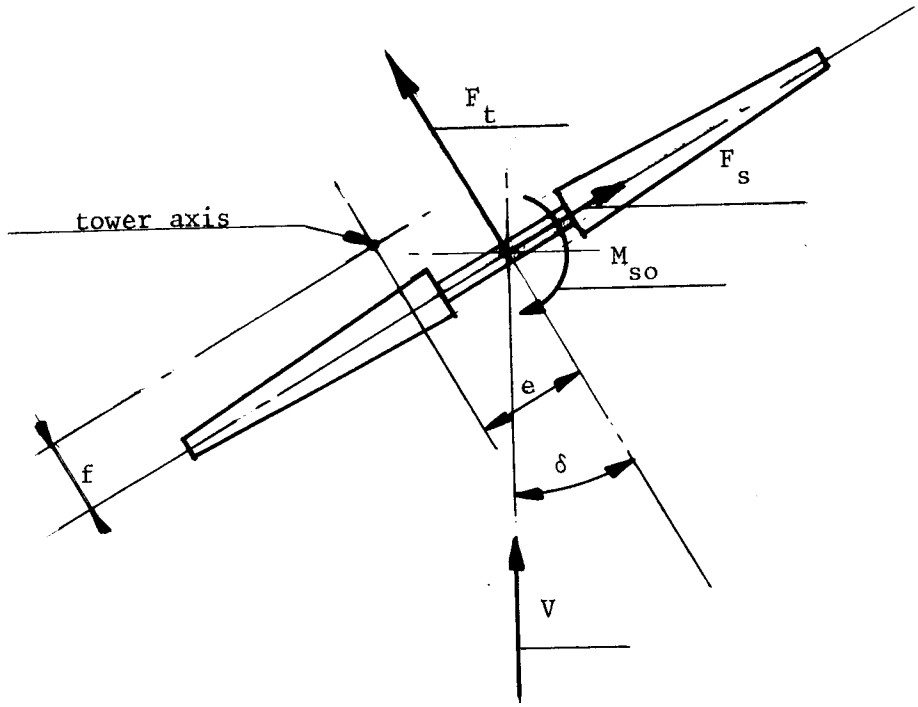

Figure 9 Forces and moments acting on a rotor in yaw

More information about the so called self orientating moment M_{so} is given in chapter 7.2.

If the eccentricity e is taken not too small M_{so} can be neglected with respect to $F_t \times e$.

The influence of F_s on M_r becomes zero for $f = 0$ so for a tower axis which lays in the rotor plane.

Although this requires an unusual head construction it is chosen to be able to describe the most simple system.

Now formula 6 changes into:

$$M_r = F_t \times e \qquad (7)$$

M_r is counterbalanced by the moment produced by the vane M_v around the tower axis.

For static conditions: $M_v = M_r$ (8)

$$(7) + (8) \rightarrow M_v = F_t \times e \qquad (9)$$

(see figure 10)

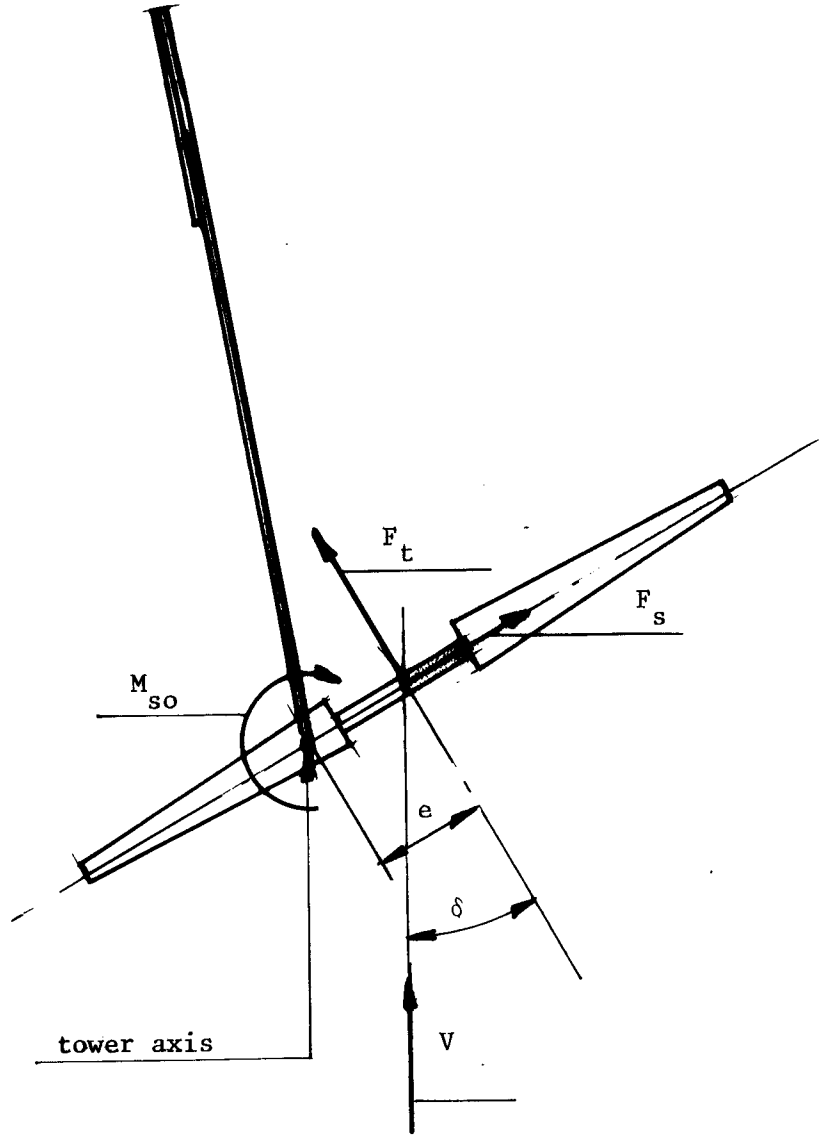

Figure 10 Balance of moments around tower axis for ideal safety system

Now a constant rotor speed and a constant thrust is obtained if M_v is constant for $V \geq V_{rated}$.
Technically this can be realised if the vane is lifting a weight.

A sketch of such a safety system with an ideal characteristic is given in figure 11.

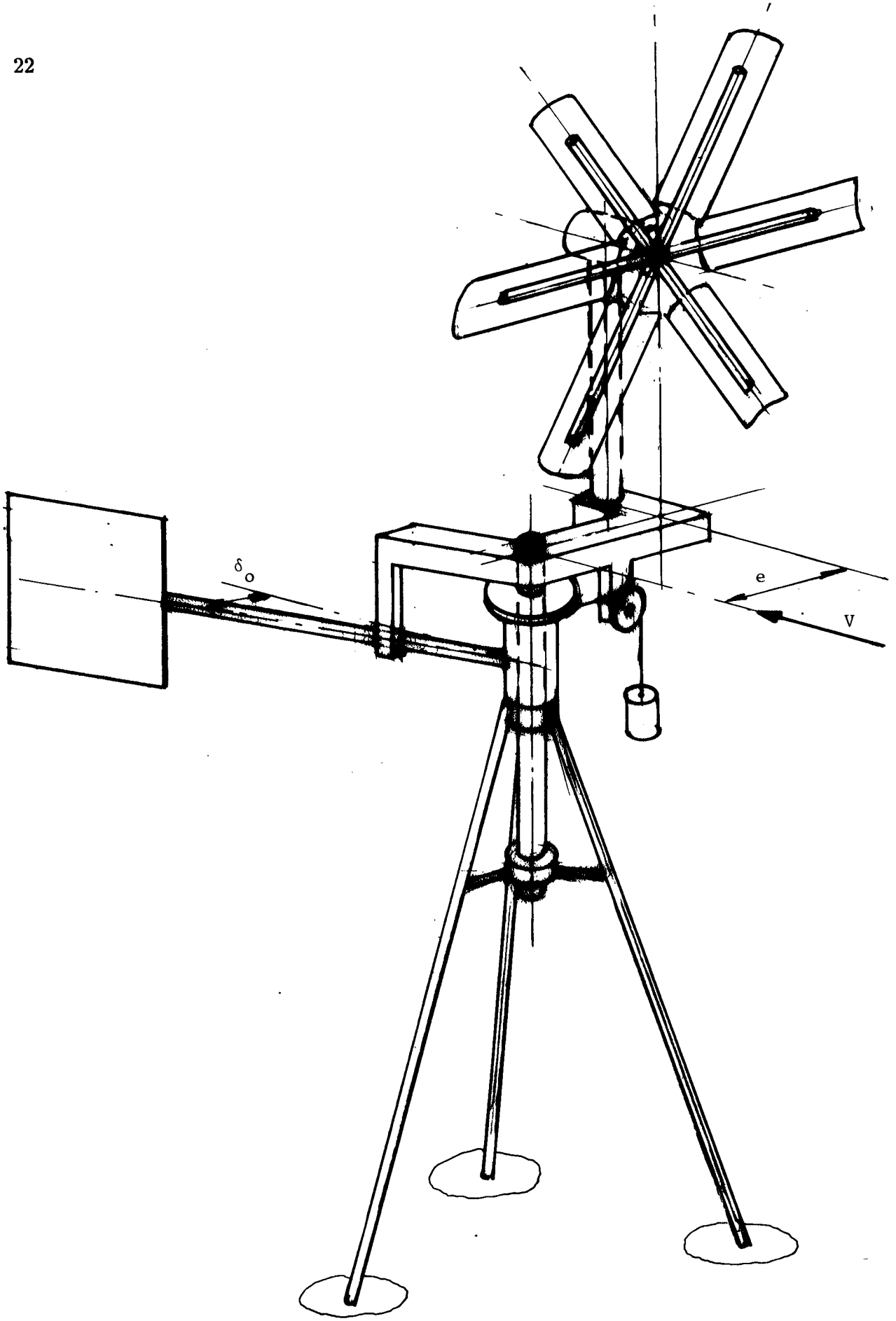

Figure 11 Artist impression of the ideal safety system

The head pipe rotates in the upper and lower head bearing of the tower.
Also the vane rotates around the head pipe so the vane axis and the head axis coincide.
The vane hub is provided with a pully over which the cable of the weight is guided.
On the head frame a second pully guides the cable from a horizontal to a vertical position.

The rotor hub is connected to the head frame in such a way that the head axis lays in the rotor plane. The head is provided with a stop to which the vane is resting for $V < V_{rated}$.
In this position the vane makes a pre-angle δ_0 with the rotor shaft which is necessary to create lift on the vane to counter balance the thrust on the rotor.
For $V > V_{rated}$ the rotor turns out of the wind and the weight is lifted creating a constant moment M_v independent of the position of the vane.

6. DEVIATION FROM THE IDEAL SAFETY SYSTEM

For practical reasons real safety systems deviate strongly from the ideal system as shown in figure 6.
The deviation can involve the rotor moment M_r or the vane moment M_v.
The following deviations are more or less common.

6.1 Rotor is placed before the tower axis

This is done in all CWD and commercial windmills to create a simple head construction and transmission from rotor shaft to pump rod. It also limits the reaction forces on the head bearings.
The consequence of this is that now the side force has an influence on M_r especially if f is chosen large with respect to e. The side force is an unfavourable force because it increases at increasing δ and increasing tip speed ratio λ.
At larger yaw angles δ its influence on M_r can become larger than the influence of F_t.
The result can be that the rotor turns more out of the wind even if there is no increase in wind speed. If this happens it means that the head can have two positions for one wind speed and this results in unstable behaviour.
If e is taken large with respect to f the rotor thrust is the major driving force.
The only influence on the $\Omega - V$ characteristic of figure 1 is that Ω becomes somewhat lower for high wind speeds but that is no problem because it has only a small influence on the total output of the windmill.

6.2 Rotor is provided with auxiliary vane instead of eccentricity

If an auxiliary vane is placed a bit before the rotor plane the rotor shadow causes no hindrance for larger yaw angles, see figure 12.

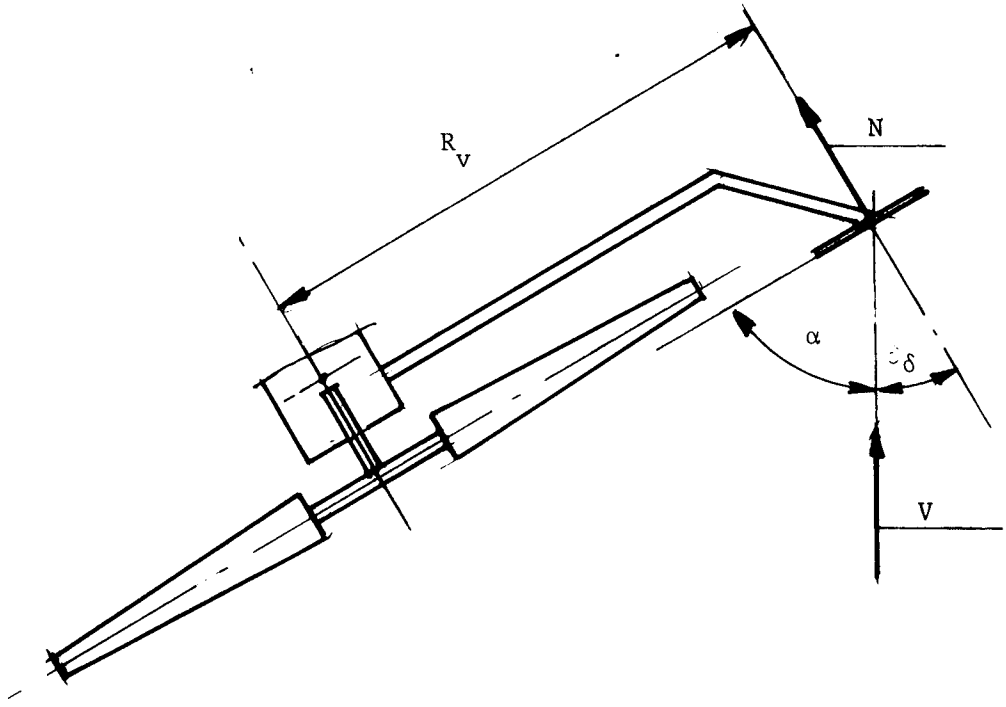

Figure 12 Auxiliary vane placed before the rotor plane

To compare the auxiliary vane with an eccentrically placed rotor the vane dimensions and the eccentricity have to been taken such, that the same moment is produced at a certain wind speed V for the rotor perpendicular to the wind.
The moment produced by the auxiliary vane can be written as:

$$\left.\begin{aligned} M_{av} &= N \times R_v \\ N &= C_n \times 0.5\rho V^2 \times A_v \end{aligned}\right\} \quad M_{av} = C_n \times 0.5\rho V^2 \times A_v \times R_v \qquad (10)$$

The normal coefficient C_n is a function of the shape (aspect ratio) of the vane and the angle α between vane and wind direction.
The $C_n - \alpha$ curves for a square plate and for plates with an aspect ratio i = 1 : 5 and i = 5 : 1 as a function of α, derived out of lift and drag coefficients as measured by Flachsbart (see TUE report R 443 D) are given in figure 13.
The aspect ratio i is the profile length divided by the profile chord.

For a vane the chord is the side of the vane in the wind direction. A vane with i = 5 : 1 means that the long side of the vane is vertical.

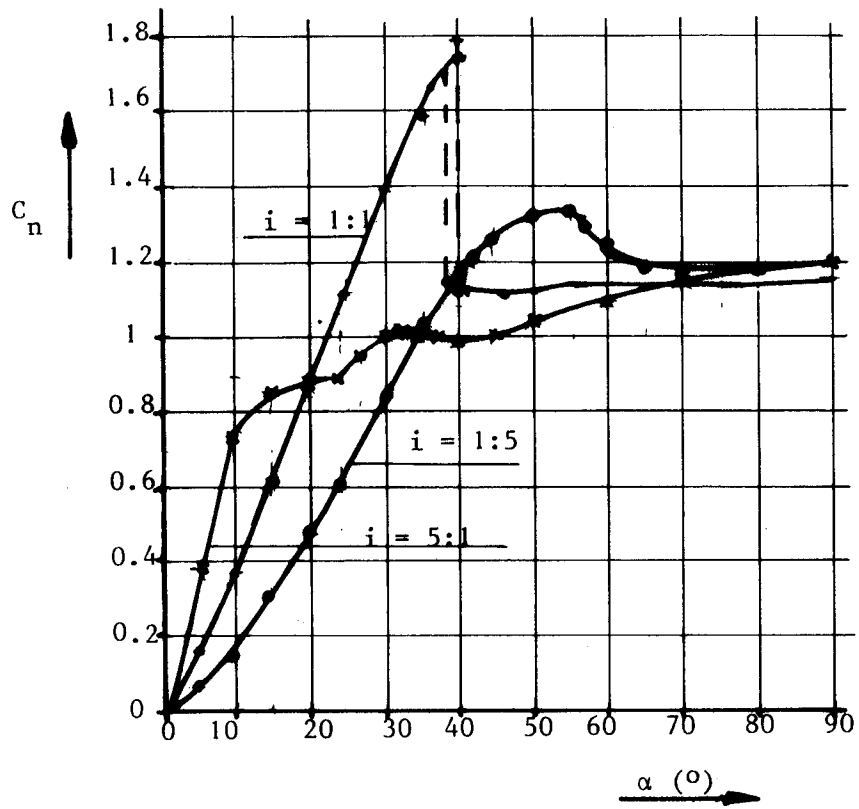

Figure 13 C_n – α curves for a square plate and for plates with aspect ratio 1 : 5 and 5 : 1

For a vane blade parallel to the rotor plane $\delta = 90^o - \alpha$ so the C_n curve as a function of δ becomes the mirror image of the $C_n - \delta$ curve.
For the square plate the $C_n - \delta$ curve is presented in figure 14.

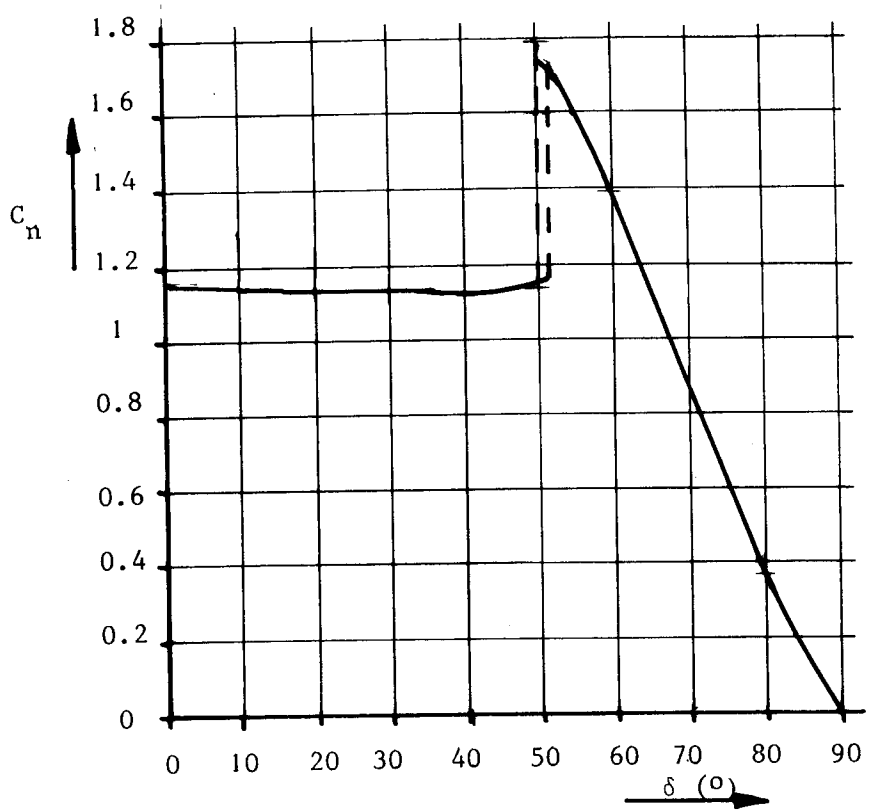

Figure 14 $C_n - \delta$ curve for a square plate parallel to the rotor plane

The $M_{av} - \delta$ curve for a certain wind speed V, a blade area A and a vane radius R_v has a shape similar to the $C_n \rightarrow \delta$ curve.
If an eccentrically placed rotor is used the relation between M_r and V is found from formula (3) and (7) $\rightarrow M_r = C_t \times 0.5\rho V^2 \cos^2\delta \pi R^2 \times e$ (11)

Both systems can be compared if they produce the same moment for the rotor perpendicular to the wind ($\cos\delta = 1$).

$M_{av} = M_r \rightarrow C_n \times A_v \times R_v = C_t \times \pi R^2 \times e$ (12)

For this condition and a certain wind speed both curves haven been drawn together in figure 15.

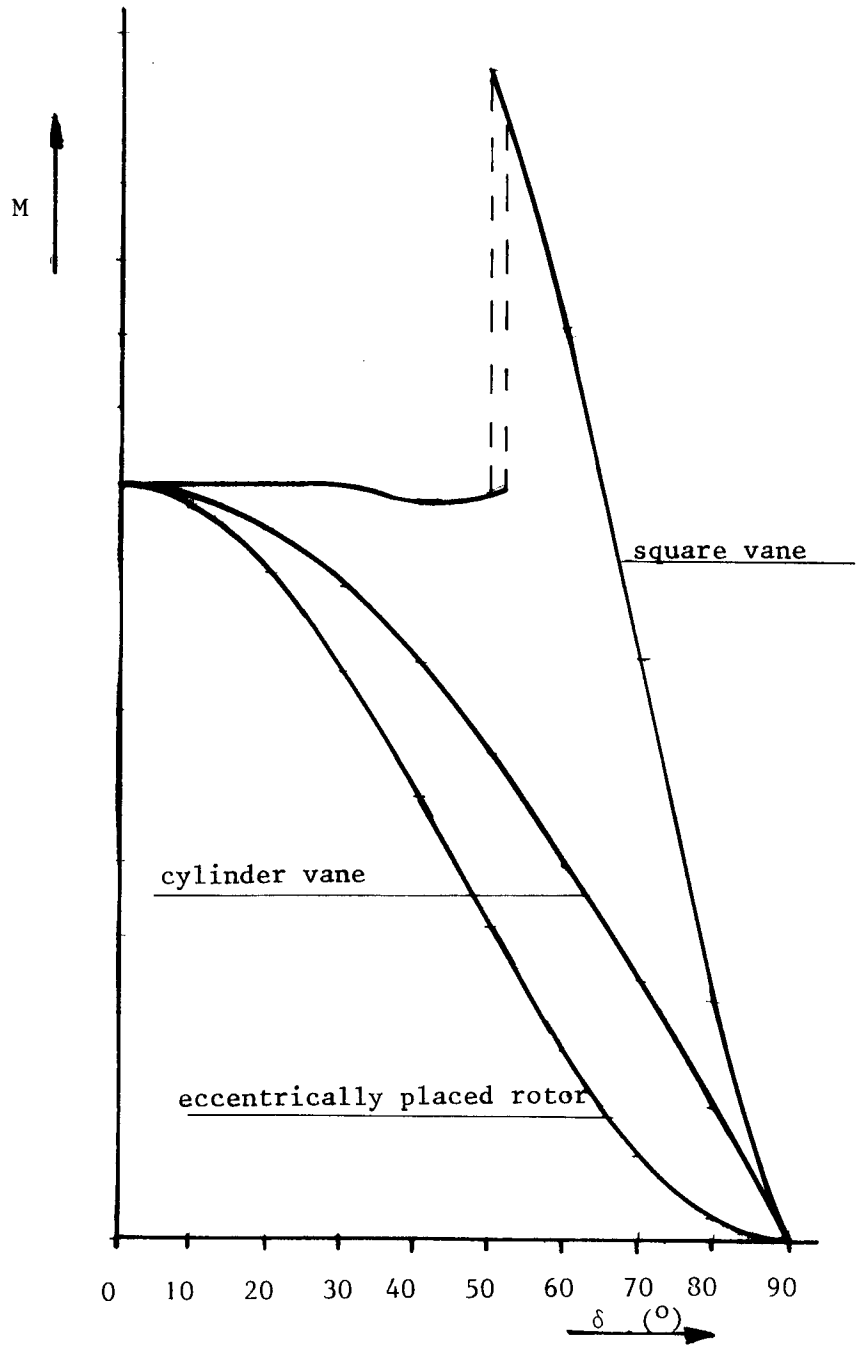

Figure 15 M – δ curves for an eccentrically placed rotor, a square plate and a cylinder

Comparison of both graphs learns that:

1. The curve of an eccentrically placed rotor is very smooth.
2. The curve of an auxiliary vane has an peak at about $\delta = 50^o$.
3. Especially at large angles δ the moment produced by an auxiliary vane is much larger than that of an eccentrically placed rotor.

This means that a safety system equipped with a square side vane will turn out of the wind more than necessary and because of the sudden rise in moment at $\delta = 50$ unstable behaviour may be expected.

By introduction of a pre-angle ξ between auxiliary vane and rotor plane the angle at which the peak occurs can be shifted. The effect of ξ on the moment is explained in chapter 7.3.

The peak itself can be made less pronounced if some turbulence is created for instance by a turbulence strip on the backside of the vane blade.

Another advantage of the eccentrically placed rotor above the auxiliary vane is that the area swept by the rotor is large with respect to the area of the auxiliary vane. Turbulence in the wind therefore gives smaller fluctuations on F_t than on N.

Unless the less favourable characteristic of an auxiliary vane it might be preferable in case centrically placing of the rotor shaft should result a simpler transmission or head construction.

Perhaps it is possible to improve the characteristic of an auxiliary vane by using a rectangular plate rather than a square plate. Maybe a vertical cylinder can be used because this one has no lift and only drag. The moment produced by a constant drag force varies with cos δ. The moment of a cylinder vane is also presented in figure 15. As far as known the use of a cylinder as vane has never been tried out on a windmill.

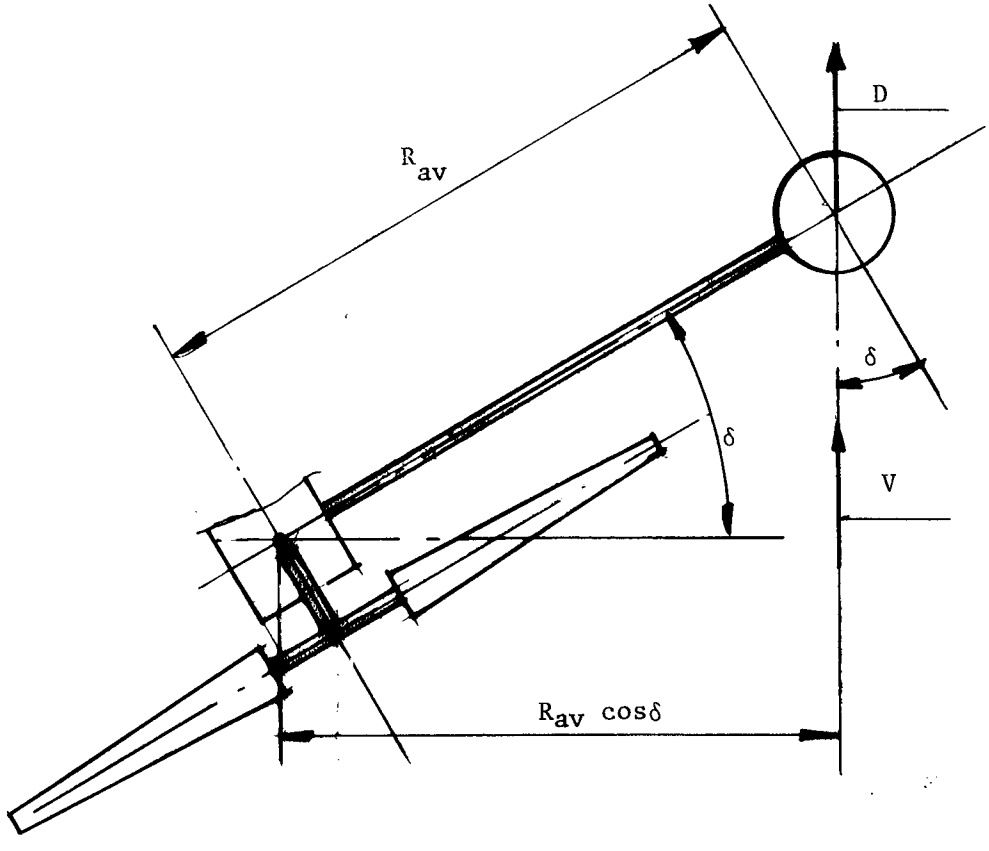

Figure 16 Cylinder as auxiliary vane

6.3 Main vane has no constant moment

Here several deviations from the optimum are possible.

If γ is the angle of rotation of the main vane around its axis the ideal main vane has a constant moment independent of γ (see curve 1 figure 17).

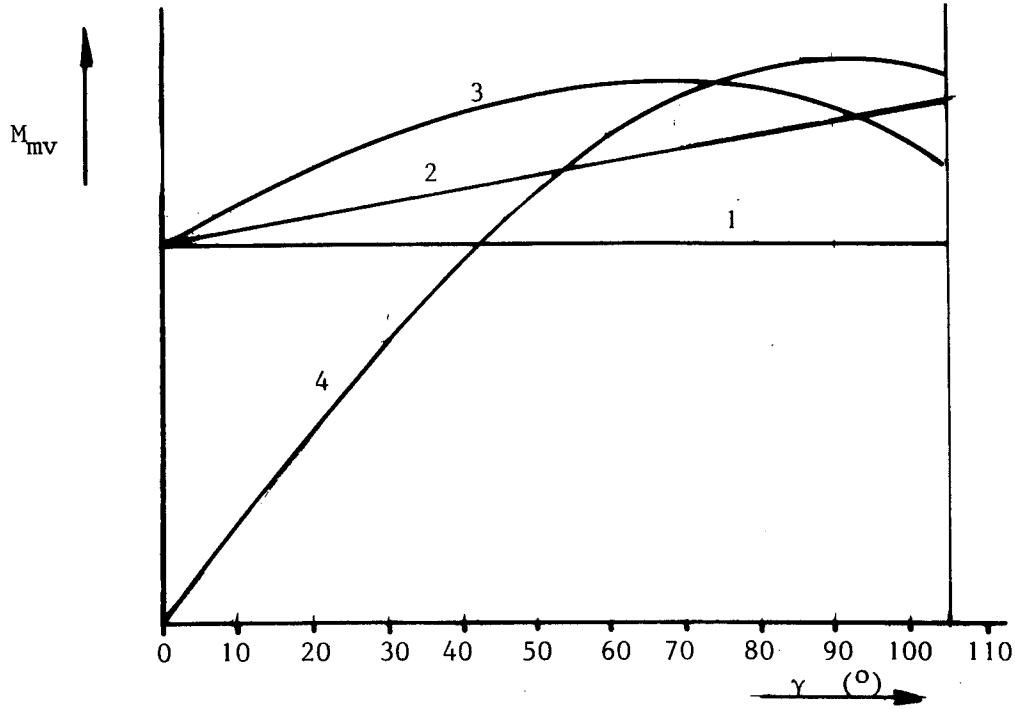

Figure 17 $M_{mv} - \gamma$ curves for four types of main vanes

If the moment is produced by a weak torsion spring there is an increase in moment proportional with γ (see curve 2 figure 17).

The effect of an increasing vane moment is an increase in rotor speed and thrust for $V > V_{rated}$.

In many commercial windmills the moment of the vane is counterbalanced with a tension spring connected to a fixed point on the head frame (see figure 18).

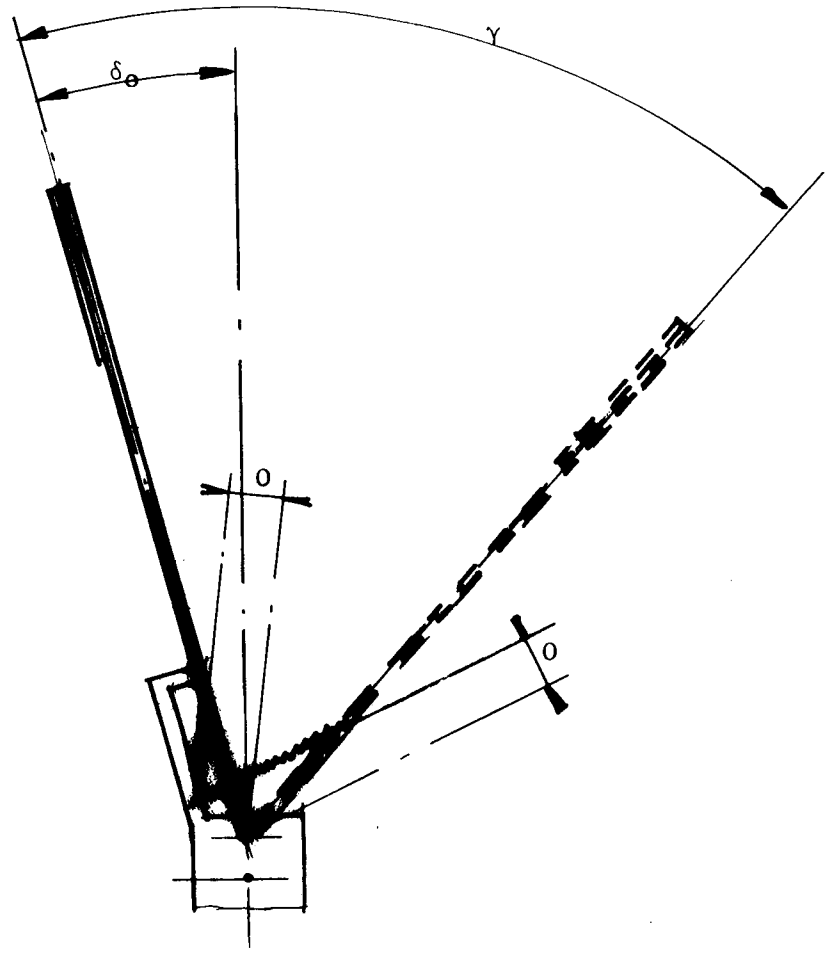

Figure 18 Spring and stop of ecliptic system

The moment of the spring is the product of the tension force in the spring and the distance o. The tension force in the spring is proportional with the stretch. The distance o depends on the position of the vane.

The product of the tension force in the spring and the distance o has a maximum at a certain angle γ. Therefore the $M_{mv} - \gamma$ line is curved (see curve 3 figure 17).

The effect of a curved vane moment with a maximum at a certain angle γ is an increase in rotor speed and thrust until this angle is reached and a decrease for higher angles γ.

The moment, for the inclined hinge main vane safety system, produced by the vane weight is zero for the vane in the lowest position and increases sinusoidally to a maximum for $\gamma = 90^o$ (see chapter 7.5). See curve 4 figure 17.

The effect of such a M - γ curve on the safety system is that the mill starts turning out of the wind at low wind speeds where it is not yet necessary.

6.4 Other disturbing effects

Even the ideal safety system of figure 11 won't have an absolute constant rotor speed above V_{rated} if placed in real wind because of the following reasons:

a. Friction in the bearings

Friction in the head bearings prevents correct orientation of the mill to the wind especially at low wind speeds.

Friction in the main vane bearings and the head bearings together causes hysteresis in the yawing movement and therefore a larger wind speed is required to turn the head out the wind. This results in a larger rotor speed and a larger thrust.

b. Inertia effects

The ideal characteristic of figure 6 only will be obtained under quasi-stationary conditions as can be realised in a wind tunnel.

In real wind there will be sudden changes in wind speed and wind direction.

Because of the inertia of head and main vane it will take some time before the head has been turned to the new position.

If the system has little damping there will be some oscillation around the new position. Because it takes some time to turn the head, the rotor will accelerate during this time but the final maximum speed depends on the rotor inertia.

Only by field measurements reliable values for the maximum rotor and yawing speed can be obtained.

Especially the maximum of the product of rotor and yawing speed is important because it determines the gyroscopic moment.

c. Inaccuracy in the used characteristics

The ideal safety system is based on the assumption that the component of the wind speed $V\cos\delta$ is determining the speed and the thrust. Measured values for speed and thrust deviate from the calculated value especially at large yaw angles.

Similarly real aerodynamic characteristics of vanes may deviate from wind tunnel measurements due to the fact that vanes are connected to vane arms by a disturbing supporting construction.

Another uncertainty may be that the wind speed and wind direction at the position of a vane is not well known.

This is special the case for vanes placed in the wake behind the rotor.

6.5 Combination of deviations

Most windmills deviate on more than one point from the ideal design and certain combinations are very unfavourable. The most unfavourable combination is a rotor which turns far before the tower, equipped with an auxiliary vane behind the rotor plane and with a main vane with a characteristic according to curve 3 of figure 17.
Such a system suddenly turns completely out of the wind above a certain wind speed and stays there until the rotor speed is almost zero. Therefore the side force on the rotor decreases and the head swings back into the wind again.
This oscillating behaviour causes strong gyroscopic moments in the rotor blades and spars and the result is that the windmill has a much lower output at higher wind speeds than compared to a stable system.

7. DETAILED DESCRIPTION OF THREE SYSTEMS

7.1 General

In this chapter the ecliptic, the inclined hinge main vane and the hinged side vane safety system are explained more in detail.

For all systems two moment equations can be set up.

1. Balance of moments around the tower axis
2. Balance of moments around the vane axis

In this publication only the stationary situation is described. Forces and moments caused by the inertia of rotor, head and vanes are neglected.

Also friction of the head and vane bearings is neglected. This means that the predicted Ω–V and F_t–V curves roughly correspond with the behaviour of well lubricated models under windtunnel conditions.

Introduction of inertia effects and friction makes all equations too complex for this publication and solution of the equations is only possible with a computer.

In [21] inertia effects and friction are included in a description of the hinged side vane system.

For the ecliptic system both axis are vertical and therefore only components of forces laying in the horizontal plane are important.

Because all forces and moments working on vane and rotor are laying in a horizontal plane the moment equations for the ecliptic system are rather simple.

The vane axis of the inclined hinge main vane system makes a certain angle with the tower axis. Therefore for balance of moments around the vane axis, components of forces acting in a plane perpendicular to this axis have to be taken. The components of forces necessary to describe the moment equation around the vane axis are different from the components of forces to describe the moment equation around the tower axis and therefore the inclined hinge main vane system is more difficult to describe exactly than the ecliptic system.

The vane axis for the hinged side vane system is positioned horizontal which results in a rather simple moment equation around the vane axis.

The moment equation around the tower axis is only simple for low wind speeds and for high wind speeds. At low wind speeds the vane blade hangs about vertical. At high wind speeds the vane blade is almost horizontal and the vane axis is about perpendicular to the wind direction.

As mentioned in chapter 4.4 to 4.9 the ecliptic system and the inclined main vane system can be used with an eccentrically placed rotor or with an auxiliary vane.

The hinged side vane system presently is only tested successfully with an eccentrically placed rotor. Before going into the specific moment equations for each of the three safety systems first the moment around the tower axis produced by the rotor and the auxiliary vane is derived.

7.2 Moment of eccentrically placed rotor around the tower axis

In figure 19 (which is similar to figure 9) the forces and moments acting on a yawing rotor have been given.

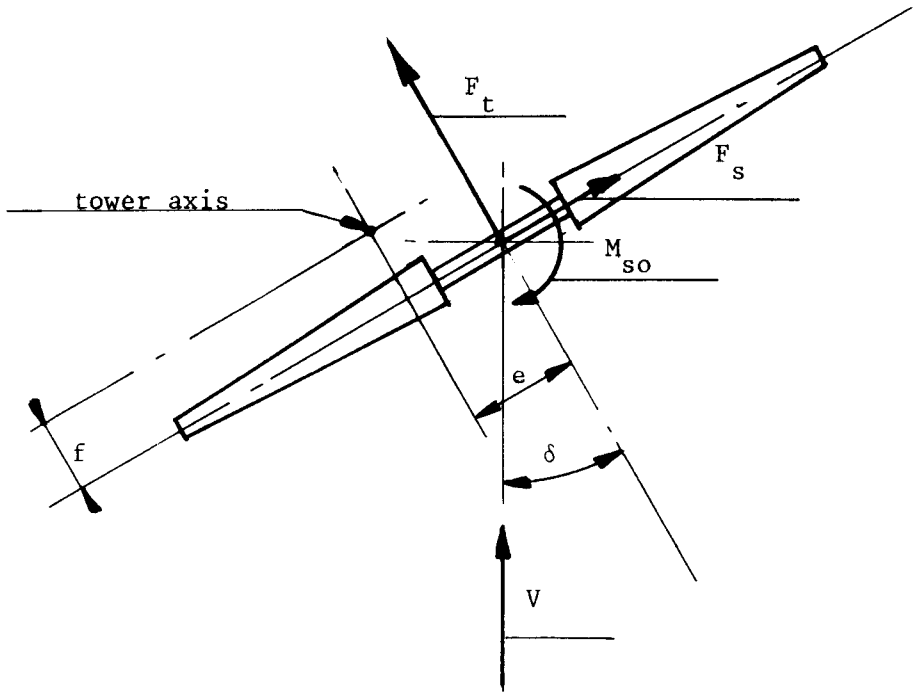

Figure 19 Forces and moments acting on a rotor in yaw

formula (6) (see chapter 5) gives the moment of the rotor M_r around the tower axis.

$$M_r = F_t \times e + F_s \times f - M_{so} \qquad (6)$$

F_t, F_s and M_{so} can be written as:

$$F_t = C_t \times 0.5\rho V^2 \pi R^2 \qquad (N) \qquad (13)$$

$$F_s = C_s \times 0.5\rho V^2 \pi R^2 \qquad (N) \qquad (14)$$

$$M_{so} = C_{so} \times 0.5\rho V^2 \pi R^3 \qquad (Nm) \qquad (15)$$

$$(6) + (13) + (14) + (15) \rightarrow M_r = 0.5\rho V^2 \pi R^2 (C_t \times e + C_s \times f - C_{so} \times R) \qquad (16)$$

The so called self orientating moment M_{so} which is caused by asymmetry in pressure on the right and the left part of the rotor is not well known. Some theory is presented in TUE report R 428 A [11] some measurements are presented in TUE report R 526 D [12]. It has been found that M_{so} is only self orientating (this means it tends to turn the rotor in the wind) for fast running rotors. For slow running rotors it is small or negative if the rotor runs almost unloaded.
However at tip speed ratios less than λ_d the self orientating moment becomes large and can not be neglected. A temporary low tip speed ratio occurs directly after a sudden jump in wind speed.

As explained in chapter 5 the change in F_t as a function of δ roughly can be found by taking only the component $V\cos\delta$ perpendicular to the rotor plane. A more accurate way is to determine the change in C_t as a function of δ at a constant V.
The dimensionless coefficients C_t, C_s and C_{so} can be determined using a scale model of the rotor in the windtunnel.
Unfortunately no good measuring device to determine these three coefficients accurately is available within CWD.
In TUE report R 763 A [13] an overview is given for several methods to determine these coefficients together with the rotor torque coefficient C_q. However the theoretical most optimal method appeared to be too complicated to build.
A very simple but time consuming method has been used for measuring the coefficients of the CWD 5000 HW rotor (see TUE report R 523 D [14] and R 575 S [15]).
This method concerns a head on which three configurations of the rotor can be realised.
The distance between rotor and tower centre f and the eccentricity e can be changed. For three different positions of the rotor the rotor moment M_r is measured for an unloaded rotor and for a constant wind speed as a function of δ. The three configurations are illustrated in figure 20, 21 and 22.
The eccentricity is zero for configuration figure 20 and 21. The distance f_1 is taken as small as possible for configuration figure 20 and 22.
The eccentricity e is taken as large as possible for configuration figure 22.

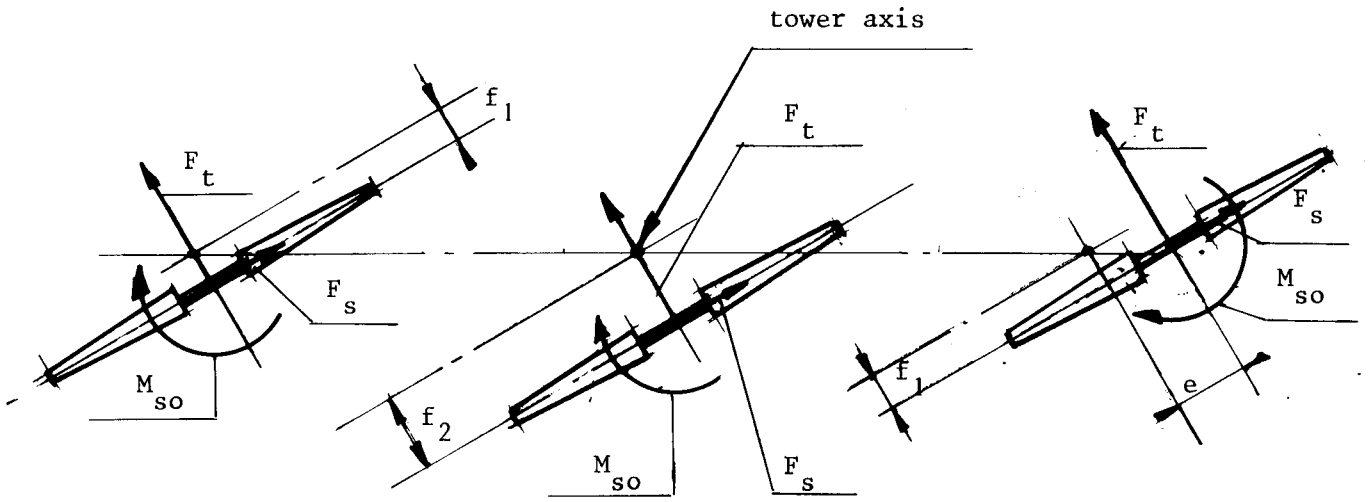

Figures 20, 21 en 22 Three configurations of the rotor with respect to the tower axis

Using formula (16) and three different values for e en f the following specific formulas are obtained.

Configuration figure 20:

$$M_r = 0.5\rho V^2 \pi R^2 (C_s \times f_1 - C_{so} \times R) \quad (17)$$

Configuration figure 21:

$$M_r = 0.5\rho V^2 \pi R^2 (C_s \times f_2 - C_{so} \times R) \quad (18)$$

Out of these two formulas C_s and C_{so} can be determined because they are the only two unknown variables.

Configuration figure 22:

$$M_r = 0.5\rho V^2 \pi R^2 (C_t \times e + C_s \times f_1 - C_{so} \times R) \quad (19)$$

Because C_s and C_{so} have already been determined C_t now can be determined with formula (19).

The $C_t - \delta$, $C_s - \delta$ and $C_{so} - \delta$ curves as presented in figure 23 have been determined this way on a scale model of the CWD 5000 HW rotor. The main parameters for the original rotor are:
Diameter D = 5 m, number of blades B = 8, tip speed ratio $\lambda = 2$, Profile 10% curved steel plate, Blade length l = 2 m, Blade chord c = 0.5 m. The scale model had a diameter of 1 m.

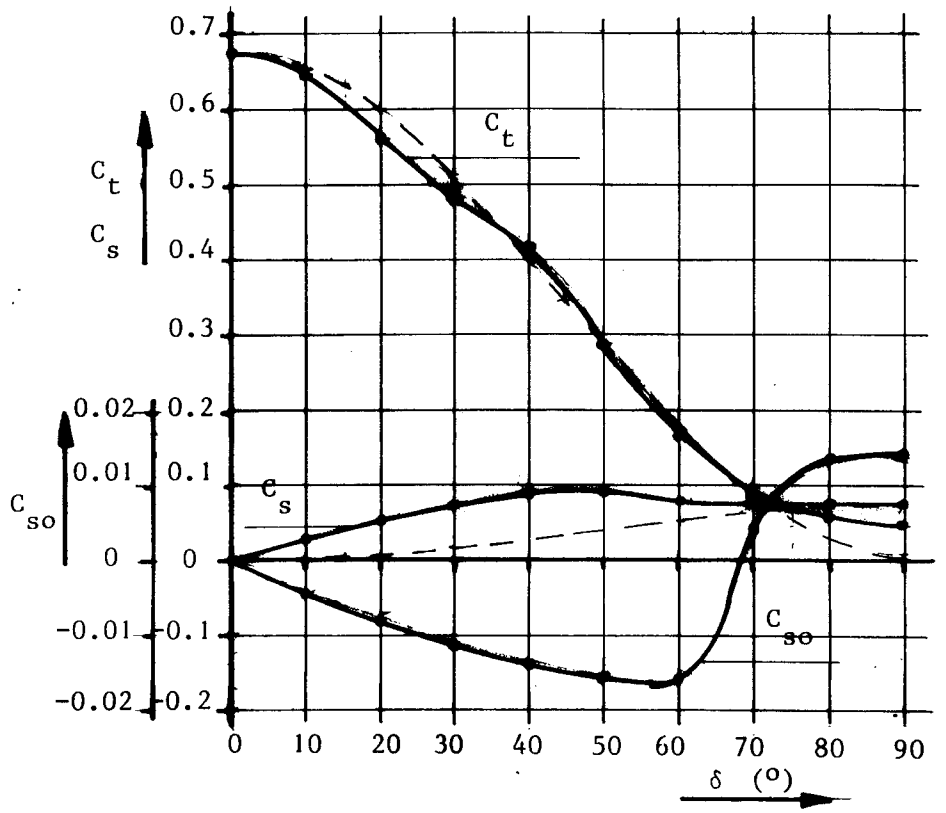

Figure 23 $C_t - \delta$, $C_s - \delta$ and $C_{so} - \delta$ curves for unloaded CWD 5000 HW rotor

The $C_t - \delta$ curve roughly looks like a $\cos^2$ function (see dotted line).
The $C_s - \delta$ curve does not look like a $\sin^2$ function (see dotted line) and especially for a low δ the measured C_s is much larger then expected according to a $\sin^2$ function.
The shape of the C_{so} curve is very strange. For $0° < \delta < 68°$ C_{so} is negative which means that it tends to turn the rotor out of the wind. For $\delta > 68°$ it becomes positive. May be this is not realistic because the accuracy in the measurement of C_{so} is small at large angles δ.
Recently the coefficients for the CWD 2000 and CWD 5000 rotor have been measured in the windtunnel of CARDC in China using a six component balance (see lit. [20]).

Dimensionless coefficients for the CWD 2000 rotor are presented in figure 24 and for the CWD 5000 rotor in figure 25. The rotors were running not really unloaded because there was some friction in the gearbox between the rotor and the electric motor even if the electric motor ran unloaded.

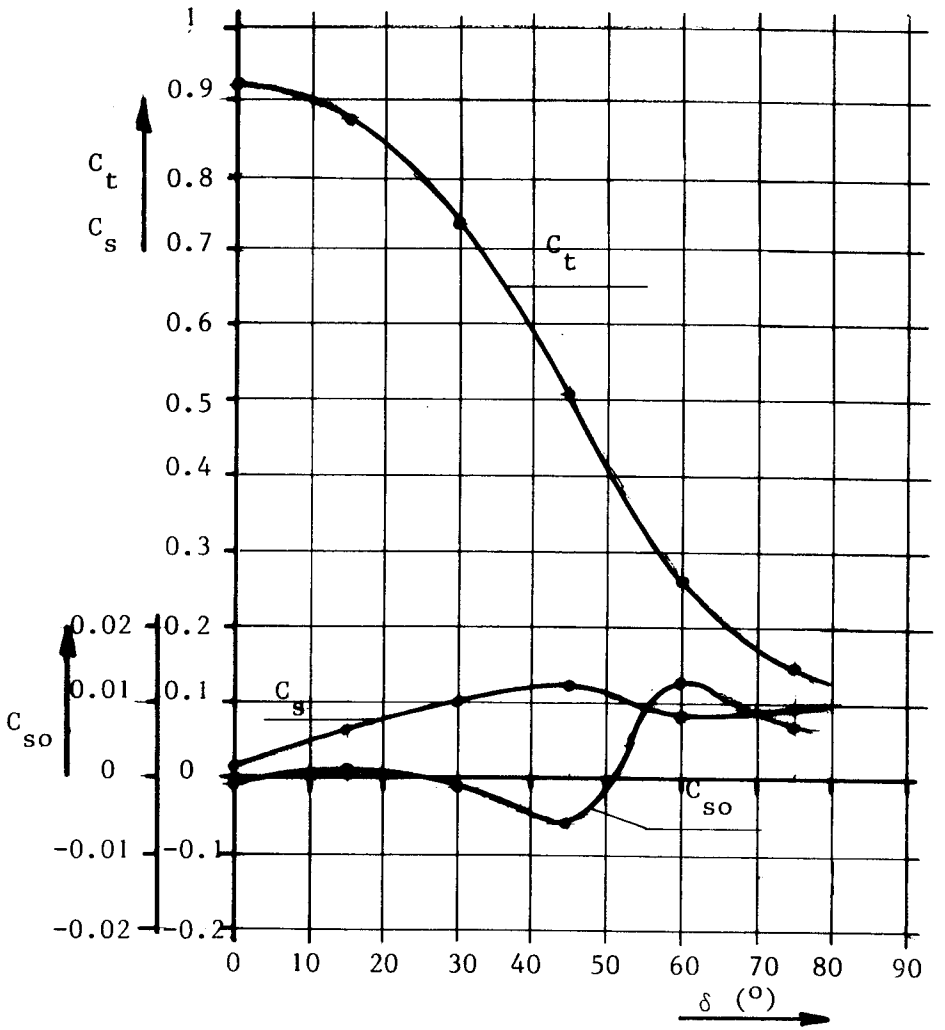

Figure 24 $C_t - \delta$, $C_s - \delta$ and $C_{so} - \delta$ curves for almost unloaded CWD 2000 rotor

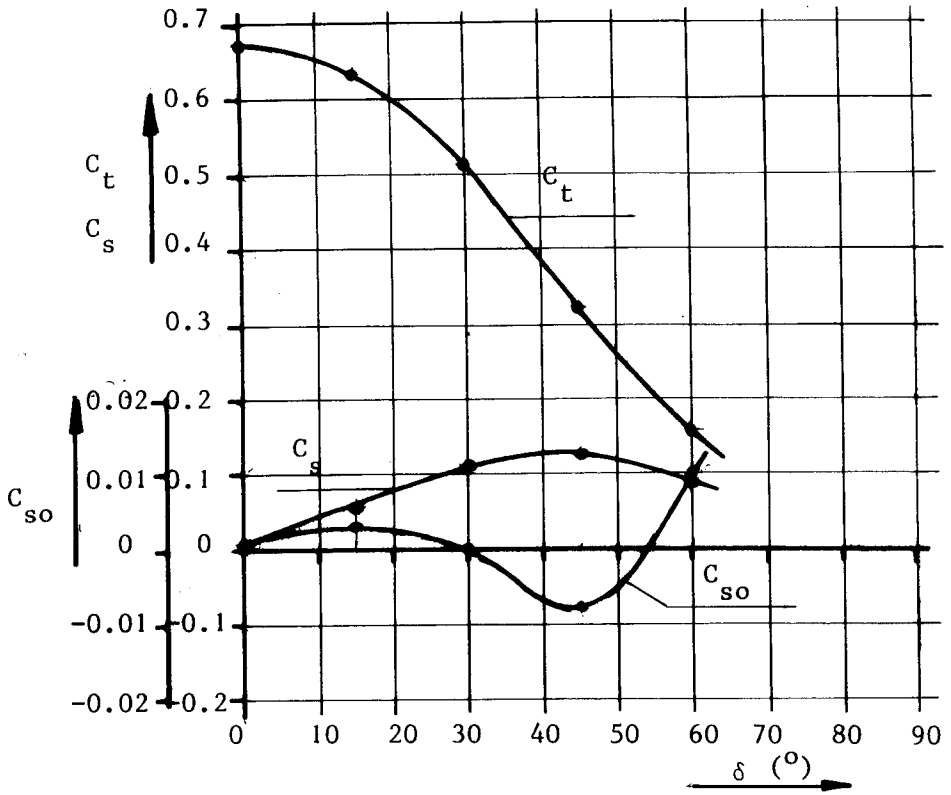

Figure 25 $C_t - \delta$, $C_s - \delta$ and $C_{so} - \delta$ curves for almost unloaded CWD 5000 rotor

The CWD 5000 rotor is almost identical to the CWD 5000 HW rotor. The main parameters for the original CWD 5000 rotor are:
Diameter D = 5 meter, Number of blades B = 8, tip speed ratio $\lambda = 1.8$, profile: 10% curved steel plate, blade length l = 1.83 m, blade chord c = 0.45 m.
The diameter of the scale model was 2 m.
The $C_t - \delta$ and $C_s - \delta$ curves are almost identical to the CWD measurements on the CWD 5000 rotor (see figure 23). The $C_{so} - \delta$ curve is different.

The CWD 2000 rotor has a much higher $C_t - \delta$ curve than the CWD 5000 HW and CWD 5000 rotors. The $C_s - \delta$ curve is about the same as the CWD 5000 rotor.
The main parameters for the original CWD 2000 rotor are:
Diameter D = 2 m, number of blades B = 6, tip speed ratio $\lambda = 1.3$, profile: 10% curved steel plate, blade length l = 0.61 m, blade chord c = 0.3 m.

Some doubts exist about the accuracy of the $C_p - \lambda$, $C_q - \lambda$ and $C_t - \lambda$ curves of the CWD 2000 rotor because after finishing the tests it appeared that the blade setting angles of the rotor were too small. Therefore the tip speed ratio and probably the thrust coefficient probably are too high.

If one knows the $C_t - \delta$, the $C_s - \delta$ and the $C_{so} - \delta$ curves and one has chosen a certain value for e × f one can determine the rotor moment M_r for a certain wind speed V as a function of δ using formula (15).

This has been done for the geometry of the head of the CWD 2000 windmill for six different wind speeds. The results of the calculations have been presented in table 1 and the $M_r - \delta$ curves have been presented in figure 26.

coefficient	$\delta = 0^o$	$\delta = 15^o$	$\delta = 30^o$	$\delta = 45^o$	$\delta = 60^o$	$\delta = 75^o$
C_t	0.919	0.875	0.735	0.505	0.257	0.152
C_s	0.015	0.062	0.101	0.121	0.080	0.098
C_{so}	–0.001	0.001	–0.001	–0.006	0.013	0.007
V (m/s)	M_r (Nm)					
2	2.2	2.2	1.9	1.5	0.6	0.5
4	8.8	8.7	7.7	5.8	2.6	1.9
6	19.8	19.5	17.3	13.1	5.8	4.3
8	35.2	34.6	30.7	23.3	10.4	7.9
10	55.0	54.1	48.0	36.4	16.2	12.0
12	79.2	77.9	68.2	52.4	23.3	17.3
14	107.8	106.1	94.2	71.3	31.7	23.5
16	140.8	138.6	123.0	93.1	41.5	30.7
18	178.2	175.4	155.7	117.9	52.5	38.9
20	220.0	216.5	192.2	145.5	64.8	48.0
22	266.2	262.0	232.5	176.1	78.4	58.1
24	316.8	311.8	276.7	209.6	93.3	68.2
26	371.8	365.9	324.8	245.9	109.5	81.1
28	431.1	424.4	376.6	285.2	127.0	94.1
30	494.9	487.2	432.4	327.4	145.8	108.0

Table 1: M_r as a function of V and δ for (almost) unloaded CWD 2000 rotor.

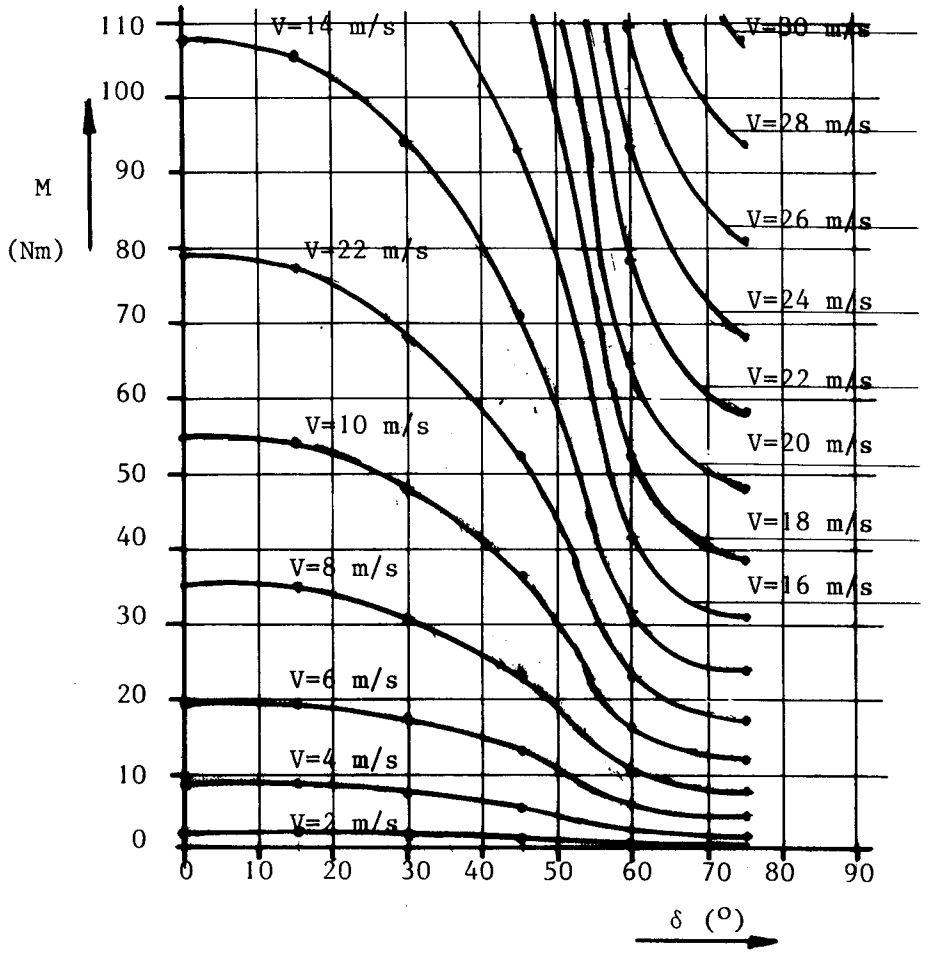

Figure 26 $M_r - \delta$ curves for different values of V for CWD 2000 rotor and head

7.3 Moment of centrically placed rotor plus auxiliary vane around the tower axis

In chapter 6.2 an auxiliary vane is compared with an eccentrically placed rotor.

If the vane blade is not parallel to the rotor plane, formula (10) can not be used because N is not perpendicular to R_v.

The formulas for the vane moment become simple if the position of the vane blade is determined by R_{av} and the angle β (see figure 27), so different from the definition of R_v in figure 12.

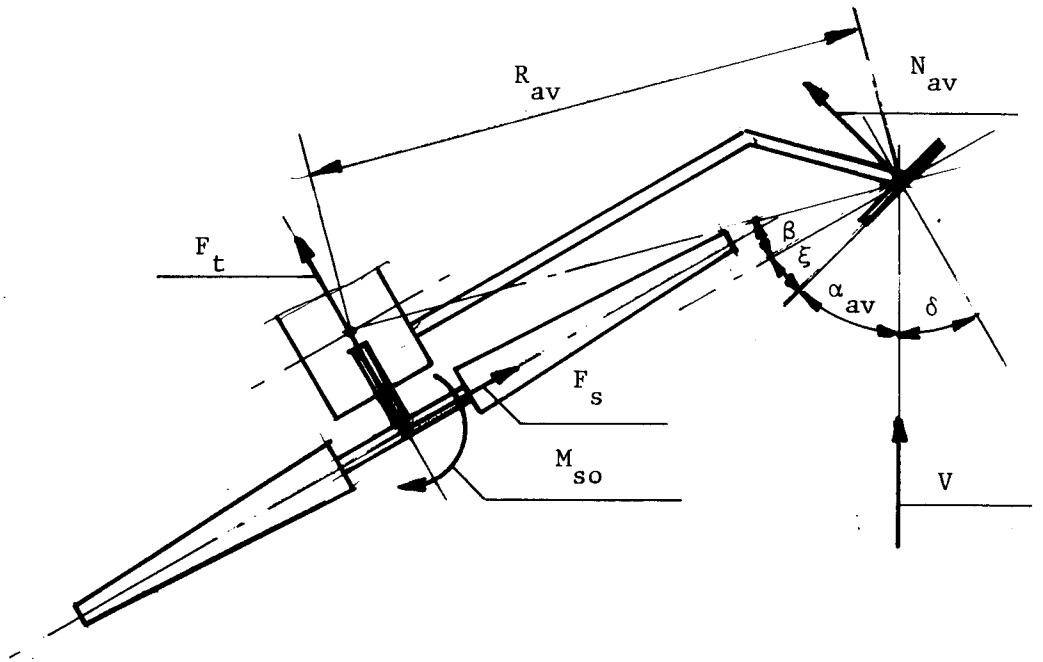

Figure 27 Forces acting on yawing rotor and auxiliary vane with pre-angle ξ

It is assumed that the normal force N acts in the middle of the vane blade. This is not true for small values of α, but because R_{av} is large with respect to the vane blade dimensions, only a small mistake in the vane moment M_{av} is made (see for accurate acting point of N figure 52). The moment of the auxiliary vane M_{av} can be written as:

$$M_{av} = N_{av} \times R_{av} \cos(\beta + \xi) \tag{20}$$

The normal force on the auxiliary vane N_{av} can be written as:

$$N_{av} = C_{n_{av}} \times 0.5\rho V^2 A_{av} \tag{21}$$

If a square vane is chosen the shape of the $C_n - \alpha$ curve is given in figure 13.

$$(20) + (21) \rightarrow M_{av} = 0.5\rho V^2 \times C_{n_{av}} \times A_{av} \times R_{av} \times \cos(\beta + \xi) \tag{22}$$

The angle α_{av} between wind direction and auxiliary vane blade can be written as:

$$\alpha_{av} = 90^{\circ} - \delta - \xi \tag{23}$$

To find the moment of rotor and auxiliary vane together we can take formula (16) and omit the term $C_t \times e$ because the eccentricity is zero if an auxiliary vane is used (see figure 27). (The effect of the aerodynamic force on the vane arm is neglected)
(16) + (22) and $e = 0 \rightarrow$

$$M_{r+av} = 0.5\rho V^2 \pi R^2 (C_s \times f - C_{so} \times R) + 0.5\rho V^2 C_{n_{av}} \times A_{av} \times R_{av} \times \cos(\beta + \xi) \tag{24}$$

The influence of M_r can be compared easily with the influence of M_{av} if written in dimensionless form. If all terms are divided by $0.5\rho V^2 \pi R^3$ formula (16), (22) and (24) are changing as follows:

$$(16) \text{ and } e = 0 \rightarrow C_{m_r} = C_s \times \frac{f}{R} - C_{so} \tag{25}$$

$$(22) \rightarrow C_{m_{av}} = C_{n_{av}} \times \frac{A_{av} \times R_{av} \times \cos(\beta + \xi)}{\pi R^3} \tag{26}$$

$$(24) \rightarrow C_{m_{r+av}} = C_s \times \frac{f}{R} - C_{so} + C_{n_{av}} \times \frac{A_{av} \times R_{av} \times \cos(\beta + \xi)}{\pi R^3} \tag{27}$$

Now $C_{m_{r+av}}$ is determined for the CWD 2740 head. The solidity and the tip speed ratio of the CWD 2740 rotor are about the same as the CWD 5000 HW rotor.
Therefore the coefficients of figure 23 can be used. The main parameters for the CWD 2740 head are:
$R = 1.37$ m, $f = 0.55$ m, $R_{av} = 2.09$ m, $\beta = 17^{\circ}$, $\xi = 0^{\circ}$ and
$A_{av} = 0.5 \times 0.5 = 0.25$ m^2.
Substitution of these values in formula (27) gives:

$$C_{m_{r+av}} = 0.401C_s - C_{so} + 0.0619C_{n_{av}} \tag{28}$$

In table 2 an overview is given for the three coefficients C_s, C_{so} and $C_{n_{av}}$. The values for C_{m_r} (which is $0.401C_s - C_{so}$), $C_{m_{av}}$ (which is $0.0619C_{n_{av}}$) and $C_{m_{r+av}}$ (see formula 28) also have been given.

	δ=0°	δ=10°	δ=20°	δ=30°	δ=40°	δ=50°	δ=60°	δ=70°	δ=80°	δ=90°
C_s	0	0.025	0.05	0.075	0.095	0.095	0.08	0.075	0.075	0.075
C_{so}	0	-0.004	-0.008	-0.011	-0.013	-0.013	-0.015	0.003	0.013	0.014
$C_{n_{av}}$	1.15	1.15	1.15	1.14	1.12	1.78	1.4	0.89	0.39	0
C_{m_r}	0	0.014	0.028	0.041	0.051	0.053	0.047	0.027	0.017	0.016
$C_{m_{av}}$	0.071	0.071	0.071	0.070	0.069	0.110	0.087	0.055	0.024	0
$C_{m_{r+av}}$	0.071	0.085	0.099	0.111	0.120	0.163	0.124	0.082	0.041	0.016

Table 2: Dimensionless coefficients for CWD 2740 head.

The values for C_{m_r}, $C_{m_{av}}$ and $C_{m_{r+av}}$ are presented in figure 28.

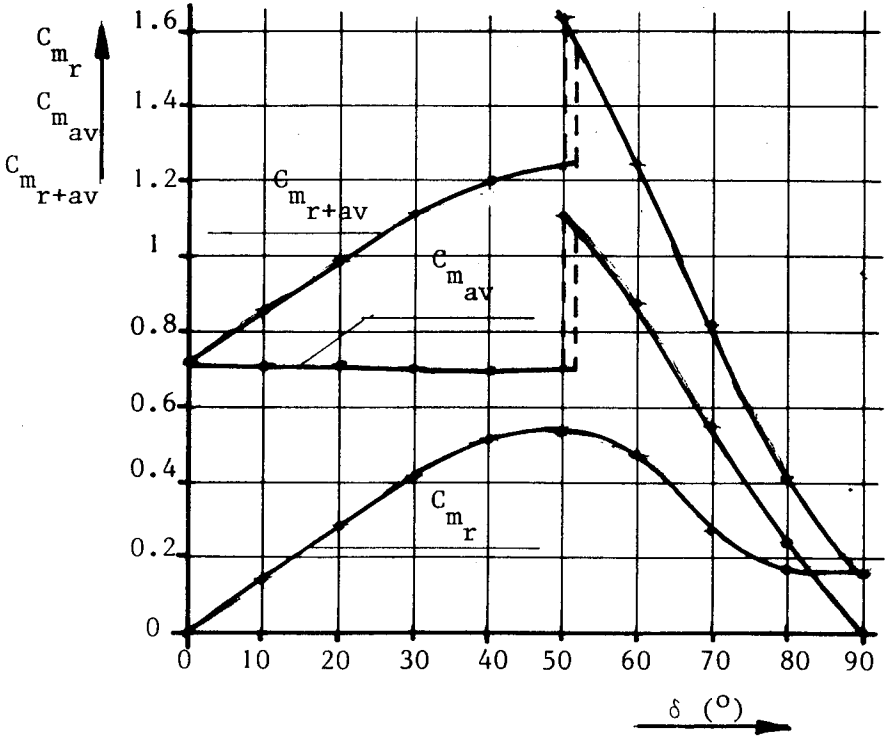

Figure 28 $C_{m_r} - \delta$, $C_{m_{av}} - \delta$ and $C_{m_{r+av}} - \delta$ curves for CWD 2740 head

It can be seen that the curve for $C_{m_{r+av}}$ is more unfavourable than the ideal $\cos^2\delta$ curve for an eccentrically placed rotor as presented in figure 15.

The moment M_{r+av} can be determined with:

$$M_{r+av} = C_{m_{r+av}} \times 0.5\rho V^2 \pi R^3 \qquad (29)$$

The result of a calculation for a certain range of wind speeds V from 2 to 30 m/s is presented in table 3 and in figure 29.

	δ=0°	δ=10°	δ=20°	δ=30°	δ=40°	δ=50°	δ=60°	δ=70°	δ=80°	δ=90°
$C_{m_{r+av}}$	0.071	0.085	0.099	0.111	0.120	0.163	0.124	0.082	0.041	0.016
V (m/s)	M_{r+av} (Nm)									
2	1.4	1.7	2.0	2.2	2.4	3.3	2.5	1.7	0.8	0.3
4	5.7	6.9	8.0	9.0	9.7	13.2	10.0	6.6	3.3	1.3
5	9.0	10.7	12.5	14.1	15.1	20.6	15.7	10.4	5.2	2.0
6	12.9	15.4	18.0	20.2	21.8	29.6	22.5	14.9	7.5	2.9
8	22.9	27.5	32.0	35.9	38.8	52.7	40.1	26.5	13.2	5.2
10	35.8	42.9	50.0	56.0	60.6	82.3	62.6	41.4	20.7	8.1
12	51.6	61.8	72.0	80.7	87.2	118.5	90.2	59.6	29.8	11.6
14	70.3	84.1	98.0	109.8	118.8	161.3	122.7	81.1	40.6	15.8
16	91.8	109.9	128.0	143.5	155.1	210.7	160.3	106.0	53.0	20.7
18	116.1	139.0	161.9	181.6	196.3	266.6	202.8	134.1	67.1	26.2
20	143.4	171.7	199.9	224.2	242.4	329.2	250.4	165.6	82.8	32.3
22	173.5	207.8	241.9	271.3	293.2	398.3	303.0	200.4	100.2	39.1
24	206.5	247.2	287.2	322.8	349.0	474.0	360.6	238.5	119.2	46.5
26	242.3	290.1	337.9	378.9	409.6	556.3	423.2	279.9	139.9	54.6
28	281.0	336.5	391.9	439.4	475.0	645.2	490.8	324.6	162.3	63.3
30	322.6	386.2	449.9	504.4	545.3	740.7	563.5	372.6	186.3	72.7

Table 3: M_{r+av} as a function of V and δ for CWD 2740 head with unloaded rotor.

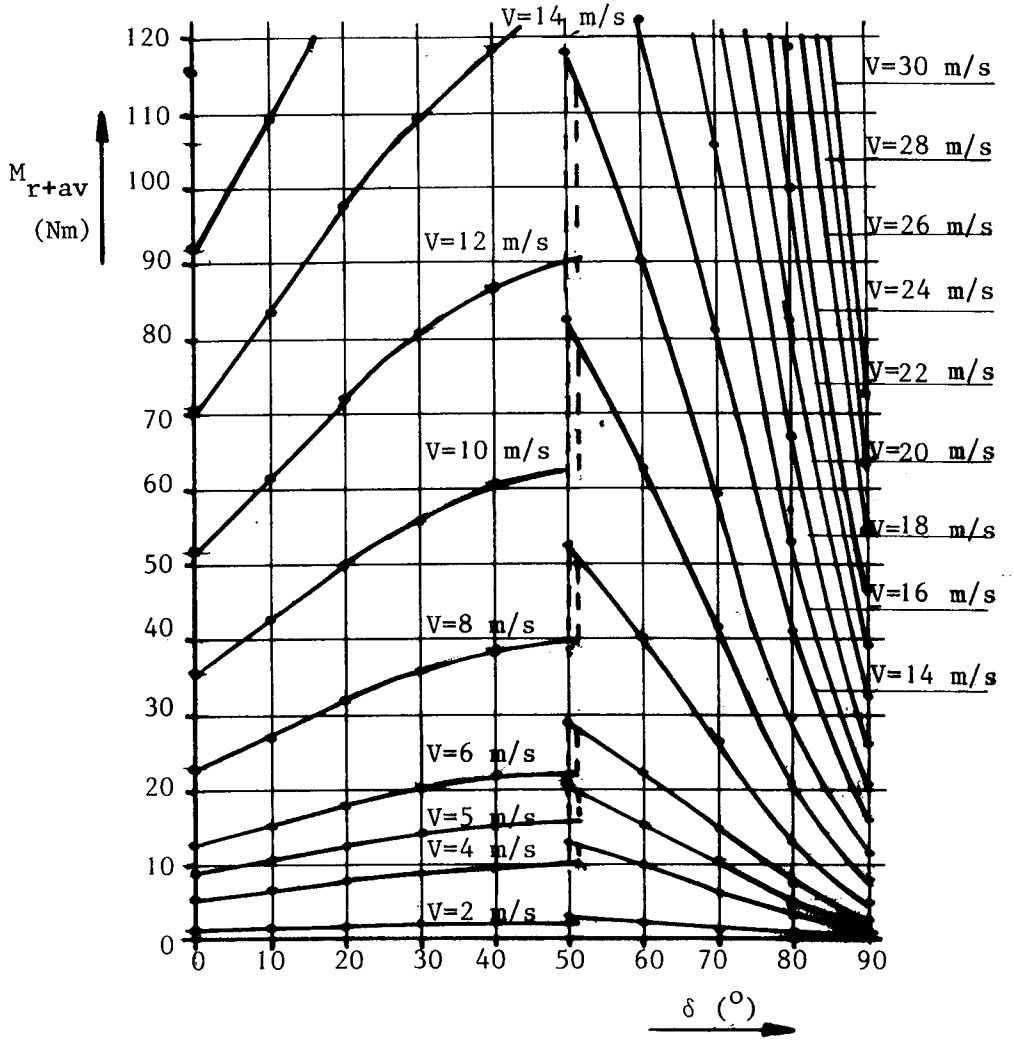

Figure 29 M_{r+av} – δ curves for different values of V for CWD 2740 rotor and head

7.4 The ecliptic system

7.4.1 General

In chapters 4.4 and 4.5 a rough description has been given for this system. The basic element of the ecliptic system is that the main vane is pulled against a stop by a spring or a weight for $V < V_{rated}$. For this condition the rotor must be perpendicular to the wind.

The moment of the aerodynamic force on the main vane around the main axis becomes the same as the moment of spring or weight at $V = V_{rated}$.
The following situations can be distinguished.

7.4.2 Ecliptic system with eccentrically placed rotor for $V \leq V_{rated}$

This situation is illustrated in figure 30.

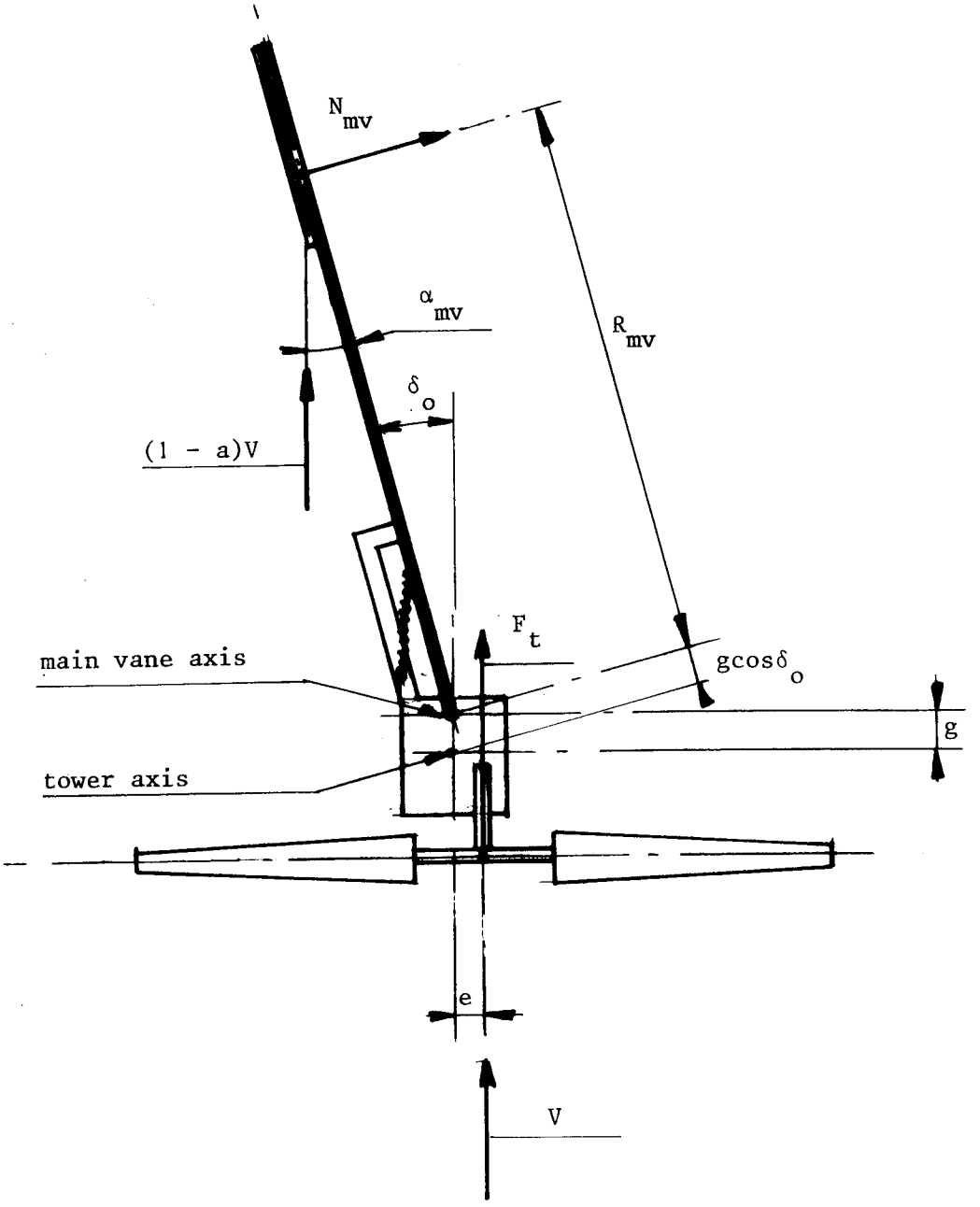

Figure 30 Ecliptic system with eccentrically placed rotor for $V \leq V_{rated}$

For this condition F_s and M_{so} both are zero. It is assumed that the aerodynamic center of the normal force on the main vane lays on about $^1/_3$ of the vane blade length from the leading edge of the vane.
Because of the influence of the wake behind the rotor the wind speed at the vane blade is reduced from V to (1 - a)V.
No exact values for the factor (1 - a) are known but it varies between about 0.4 for the rotor perpendicular to the wind ($\delta = 0$) and about 1 for the rotor full out of the wind. Suppose it is 0.5 for the configuration of figure 30.

The moment equation around the tower axis can be written as:

$$F_t \times e = N_{mv} \times (R_{mv} + g\cos\delta_o) \qquad (30)$$

The normal force N depends on the angle of attack α and the aspect ratio of the vane. The aspect ratio i is the profile length divided by the profile chord. For a vane the chord is the horizontal measure so a vane with i = 1 : 2 means that the long side of the vane is horizontal.
Often main vane blades are not square but have an aspect ratio smaller than 1.
The $C_n - \alpha$ curves for vane blades with an aspect ratio i = 1 : 2 and i = 2 : 1 are given in figure 31.
The accuracy of these curves is not as good as of the curves of figure 13 because the connection of the plate to the measuring device had an influence on the measured lift and drag (see TUE reports R 487 S [16] and R 584 S [17]).

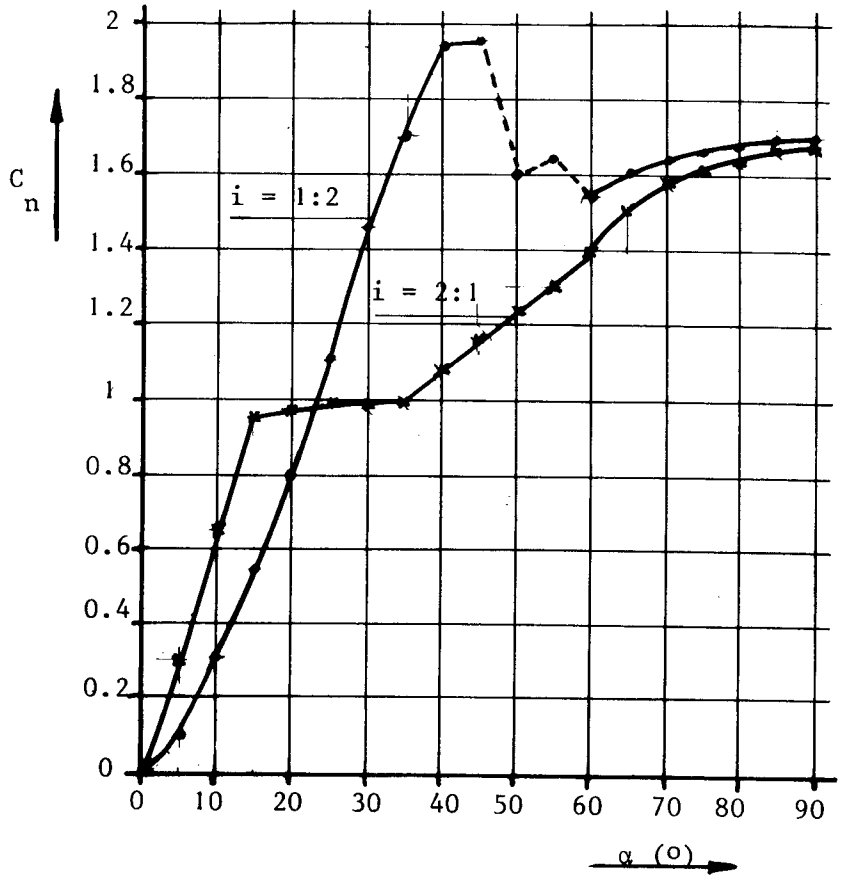

Figure 31 $C_n - \alpha$ curves for plates with aspect ratio 1 : 2 and 2 : 1

The angle α_{mv} between $(1 - \alpha)V$ and the main vane blade is equal to the pre-angle δ_o of the main vane if the rotor is perpendicular to the wind and if $(1 - \alpha)V$ is parallel with V.

The normal force on the main vane can be written as:

$$N_{mv} = C_{n_{mv}} \times 0.5\rho\,(1\text{-}a)^2 \times V^2 \times A_{mv} \qquad (31)$$

(30) + (31) + (13) →

$$C_t \times \pi R^2 \times e = C_{n_{mv}} (1 - a)^2 \times A_{mv} \times (R_{mv} + g\cos\delta_o) \qquad (32)$$

For the pre-angle δ_o normally an angle is taken about half way the rising part of the $C_n - \alpha$ curve. For a square vane this results in $\delta_o = 20^o$ and $C_n = 0.9$ and for a vane with aspect ratio 1 : 2 in $\delta_o = 23^o$ and $C_n = 1$.

The moment equation around the main vane axis for $V \leq V_{rated}$ can be written as:

$$M_{spring} > N_{mv} \times R_{mv} \quad (33)$$

$$(33) + (31) \rightarrow M_{spring} > C_{n_{mv}} \times 0.5\rho\,(1-a)^2 \times V^2 \times A_{mv} \times R_{mv} \quad (34)$$

7.4.3 Ecliptic system with auxiliary vane for $V \leq V_{rated}$

This situation is illustrated in figure 32.

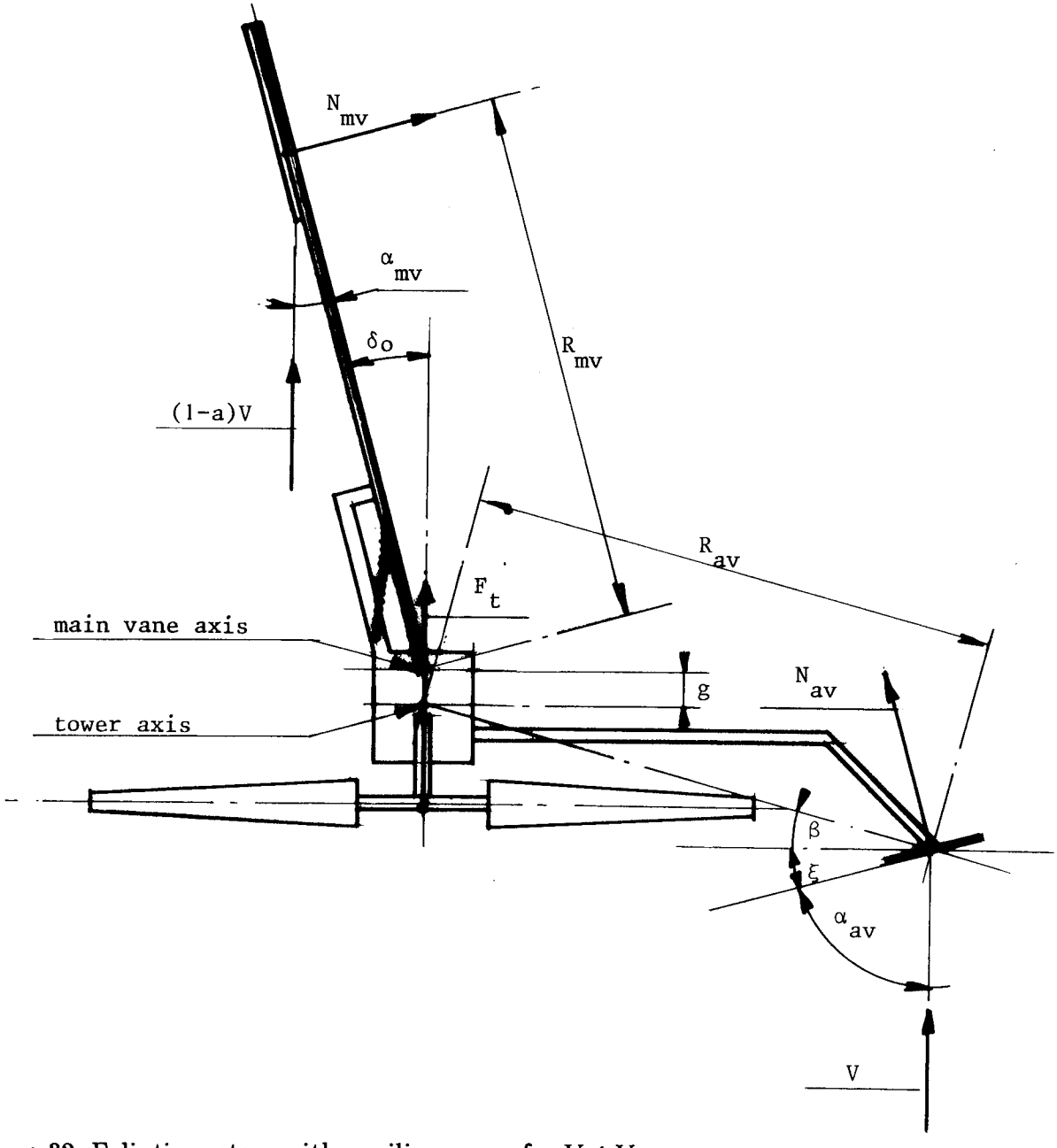

Figure 32 Ecliptic system with auxiliary vane for $V \leq V_{rated}$

Now the moment equation around the tower axis can be written as:

$$N_{av} \times R_{av} \times \cos(\beta + \xi) = N_{mv} \times (R_{mv} + g\cos\delta_o) \tag{35}$$

(35) + (21) + (31) →

$$C_{n_{av}} \times A_{av} \times R_{av} \times \cos(\beta + \xi) = C_{n_{mv}} \times (1 - a)^2 \times A_{mv} \times (R_{mv} + g\cos\delta_o) \tag{36}$$

The moment equations around the main vane axis are identical to the ecliptic system with an eccentrically placed rotor, see formulas (33) and (34).

7.4.4 Ecliptic system with eccentrically placed rotor for $V > V_{rated}$

This situation is illustrated in figure 33.

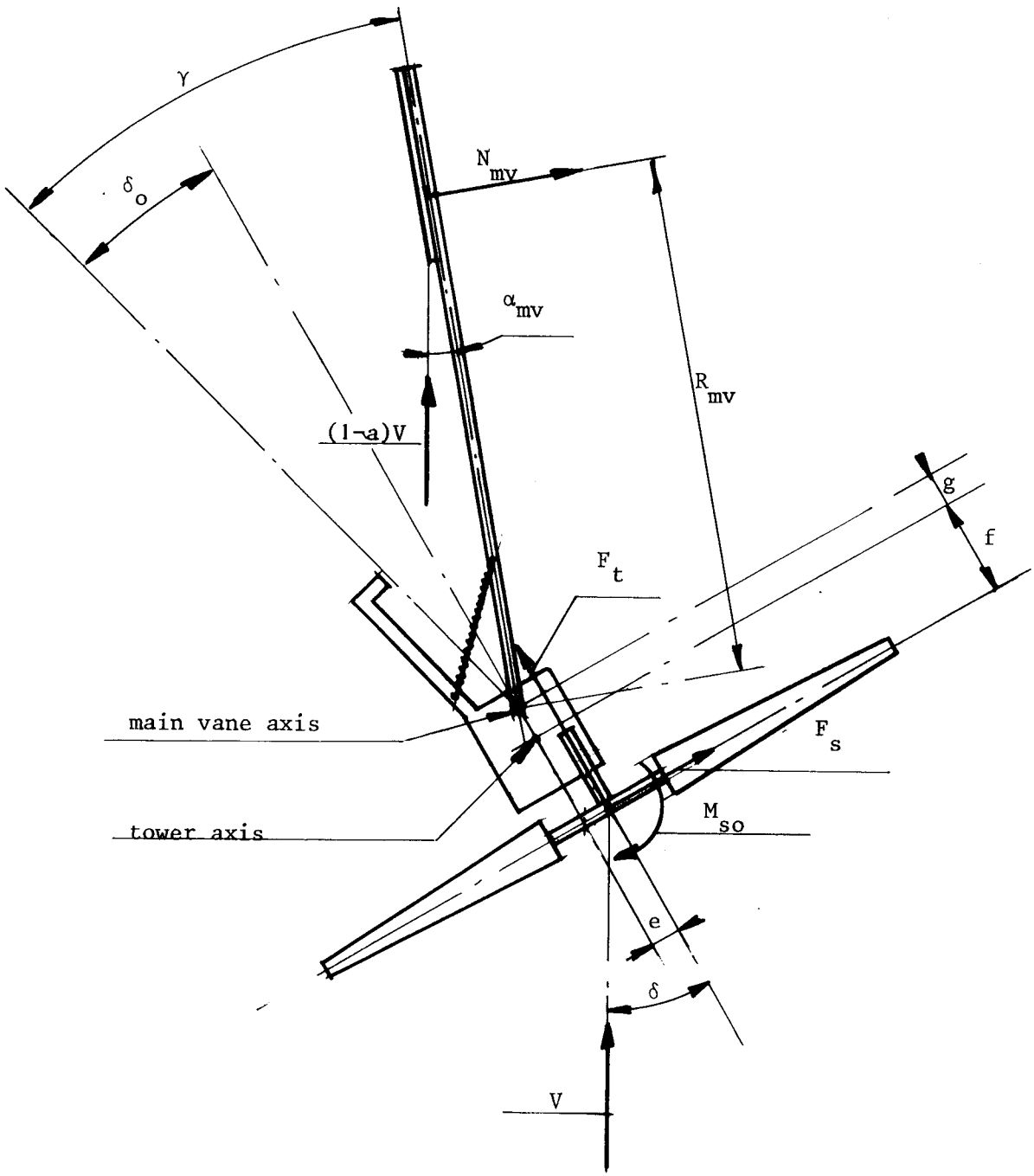

Figure 33 Ecliptic system with eccentrically placed rotor for $V > V_{rated}$

The moment equation around the tower axis can be written as:

$$M_r = N_{mv} \times (R_{mv} + g\cos(\gamma - \delta_o)) \tag{37}$$

(37) + (31) + (16) →

$$\pi R^2 (C_t \times e + C_s \times f - C_{so} \times R) = C_{n_{mv}} \times (1 - a)^2 \times A_{mv} \times (R_{mv} + g\cos(\gamma - \delta_o)) \tag{38}$$

If $V > V_{rated}$ the main vane comes free from the stop and therefore formula (34) changes into:

$$M_{spring} = C_{n_{mv}} \times 0.5\rho (1 - a)^2 \times V^2 \times A_{mv} \times R_{mv} \tag{39}$$

A formula for M_{spring} only can be given for a certain spring configuration (see also chapter 6.3 and 7.4.6).

7.4.5 Ecliptic system with auxiliary vane for $V > V_{rated}$

This situation is illustrated in figure 34.

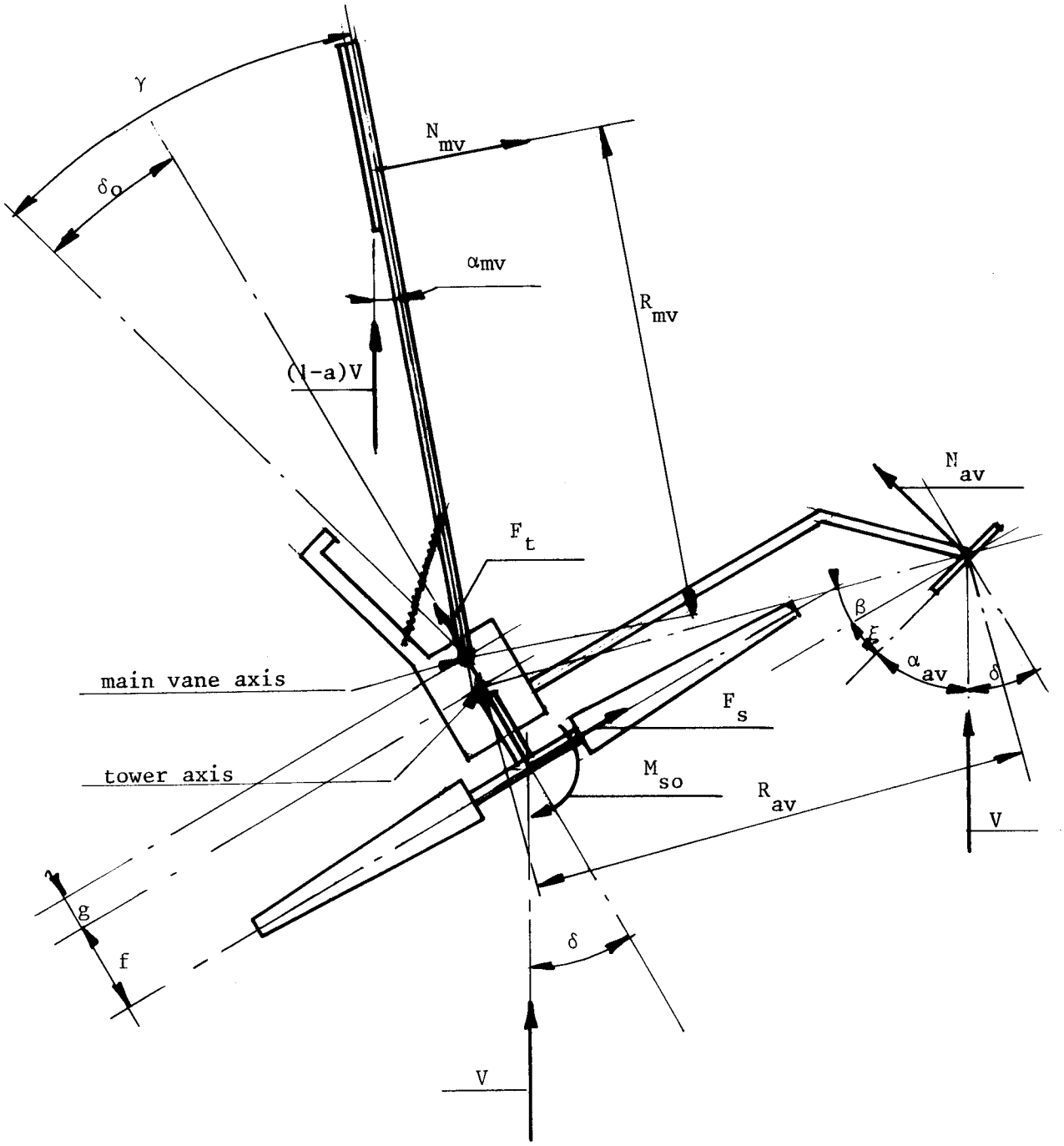

Figure 34 Ecliptic system with auxiliary vane for $V > V_{rated}$

$$M_{r+av} = N_{mv} \times (R_{mv} + g\cos(\gamma - \delta_o) \quad (40)$$

(40) + (31) + (24) →

$$\pi R^2 (C_s \times f - C_{so} \times R) + C_{n_{av}} \times A_{av} \times R_{av} \times \cos(\beta + \xi) =$$

$$C_{n_{mv}} \times (1-a)^2 \times A_{mv} \times \{R_{mv} + g\cos(\gamma - \delta_o)\} \quad (41)$$

The moment equation around the main vane axis is identical to formula (39).

7.4.6 Example

The formulas presented in the previous chapters are necessary to predict how the rotor turns out of the wind as a function of the wind speed. If this is known the rotor speed Ω_δ and the rotor thrust F_{t_δ} can be predicted with formulas (1) and (3) for $V \leq V_{rated}$ and with formulas (2) and (4) for $V > V_{rated}$. The process of designing a safety system is very complex because many parameters have to be chosen. In the following example not all parameters are variable because this results in an infinite number of possibilities.

Based on experiences with existing CWD windmills the following choices have been made:

1. Ecliptic system with auxiliary vane so the formulas of chapter 7.4.3 and 7.4.5 can be used.
2. The rotor and auxiliary vane geometry is identical to the CWD 2740 windmill so table 3 and figure 29 can be used. (The real CWD 2740 has an inclined hinge main vane safety system.)
3. Now the main vane area A_{mv} and the radius R_{mv} have to be determined in such a way that the rotor is perpendicular to the wind for $V \leq V_{rated}$. This is done with formula (36).

The parameters for the auxiliary vane of the CWD 2740 are given in chapter 7.3.

The rotor is perpendicular to the wind for $V \leq V_{rated}$. The auxiliary vane has no pre-angle ξ and therefore $\alpha_{av} = 90^o$.

In figure 13 it can be seen that $C_n = 1.15$ for $\alpha = 90^o$. The term $(1 - a)$ must be estimated. According to the aerodynamic theory $(1 - a) = {}^2/_3$ in the rotor plane and $(1-a)$ is ${}^1/_3$ far behind the rotor plane. Suppose it is 0.5 at the position of the vane. The large inaccuracy of $(1 - a)$ has a strong influence on the result of the calculation.

For some windmills (like the CWD 1000 EL) the vane is positioned above and behind the rotor to get $(1 - a) = 1$ independent of the position of the rotor.
The distance g depends on the space required for the transmission. Suppose $g = 0.2$ m.
Suppose also for the main vane a square plate is taken with $\delta_o = 20^o$; $\alpha_{mv} = \delta_o$ for the rotor perpendicular to the wind so $\alpha_{mv} = 20^o$.
In figure 13 it can be seen that $C_{n_{mv}} = 0.9$ for $\alpha = 20^o$.
So the only unknown variables now are A_{mv} and R_{mv}.

Now one has to make a choice for one of them. Suppose on takes a square vane with chord 1 m. So $A_{mv} = 1\ m^2$.

formula (36) also can be written as:

$$R_{mv} = \frac{C_{n_{av}} \times A_{av} \times R_{av} \times \cos(\beta + \xi)}{C_{n_{mv}} \times (1 - a)^2 \times A_{mv}} - g\cos\delta_o \qquad (42)$$

$C_{n_{av}} = 1.15$ $\quad$ $C_{n_{mv}} = 0.9$

$A_{av} = 0.25\ m^2$ $\quad$ $1 - a = 0.5$ $\quad$ $R_{mv} = 2.36$ m

$R_{av} = 2.09$ m $\quad$ $A_{mv} = 1\ m^2$

$\beta = 17^o$ $\quad$ $g = 0.2$ m

$\xi = 0^o$ $\quad$ $\delta_o = 20^o$

The next choice one has to make is the characteristic of the spring moment M_s around the vane axis as a function of γ. Curves 1, 2 and 3 of figure 17 give a rough impression of three different kind of characteristics. Most commercial windmills which have an ecliptic system have a characteristic like curve 3 because they use a tension spring which is connected to the vane and to a fixed point of the head (see figure 32).

The characteristic according to curve 2 is more favourable because it has no descending part. It is also easier to describe mathematically and therefore it is chosen in this example. Mechanically it can be realised by using a weak torsion spring which is mounted around the main vane axis and which connects vane and head.

Suppose the main vane can rotate over $\gamma_{max} = 105^{o}$.
Suppose the spring moment at $\gamma = 0^{o}$ is called $M_{s_{min}}$ and at $\gamma = 105^{o}$ is called $M_{s_{max}}$ (see figure 35).

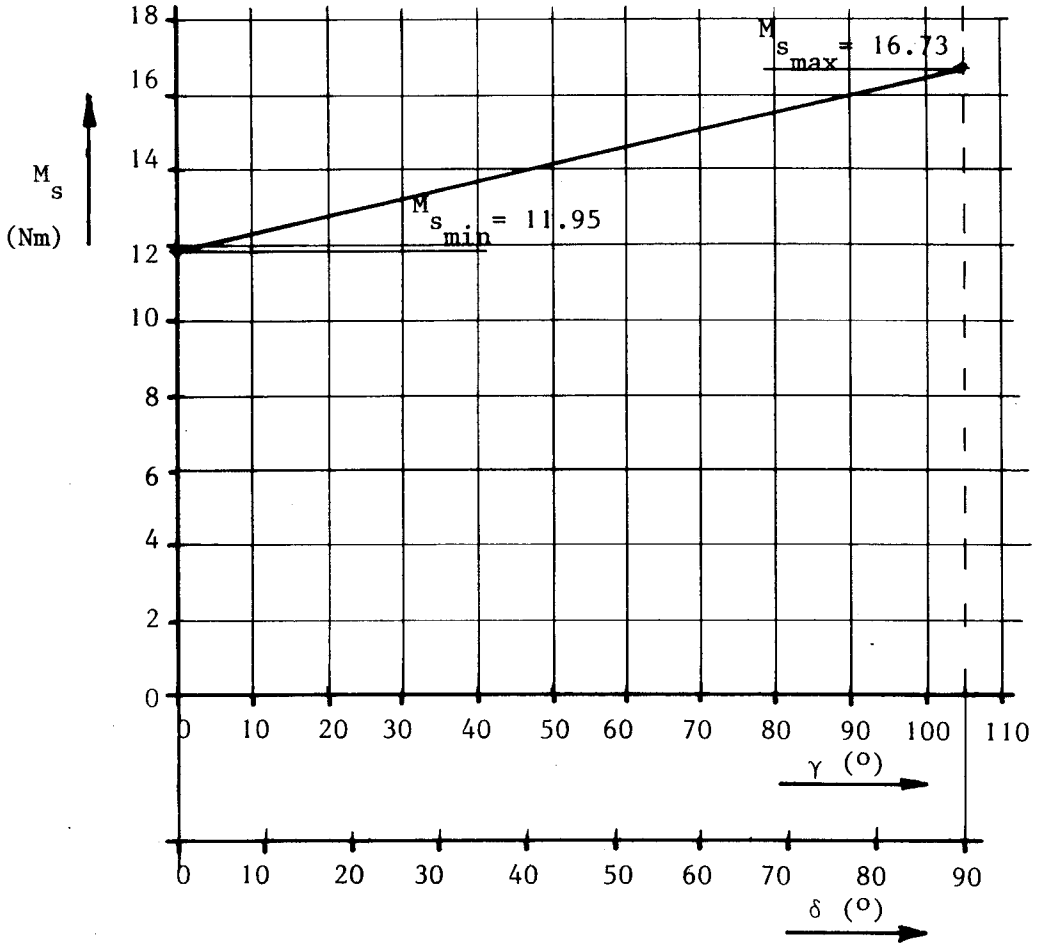

Figure 35 Moment M_s of main vane equipped with weak torsion spring as a function of γ and δ

Next the spring moment for a certain value of γ M_{s_γ} can be written as:

$$M_{s_\gamma} = M_{s_{min}} + \frac{\gamma}{105} \times (M_{s_{max}} - M_{s_{min}}) \qquad (43)$$

For static conditions and $V \geq V_{rated}$ the spring moment M_{s_γ} must be equal to the moment of N_{mv} around the vane axis $M_{mv_{va}}$ so:

$$M_{mv_{va}} = M_{s_\gamma} \quad \text{for } V \geq V_{rated} \tag{44}$$

$$M_{mv_{va}} = N_{mv} \times R_{mv} \tag{45}$$

$$(44) + (45) \rightarrow M_{s_\gamma} = N_{mv} \times R_{mv} \quad \text{for } V \geq V_{rated} \tag{46}$$

Next V_{rated} must be chosen. V_{rated} must be taken not too low because this results in loss of energy at low wind speeds and V_{rated} must be taken not too high because rotor speed and thrust must be limited.

Suppose $V_{rated} = 6$ m/s.

$M_{s_\gamma} = M_{s_{min}}$ for $V = V_{rated}$ so:

$$M_{s_{min}} = N_{mv} \times R_{mv} \quad \text{for } V = V_{rated} \tag{47}$$

(47) + (31) →

$$M_{s_{min}} = C_{n_{mv}} \times 0.5\rho\,(1-a)^2 \times V_{rated}^2 \times A_{mv} \times R_{mv} \tag{48}$$

$C_{n_{mv}} = 0.9$ (for $\delta_o = 20^\circ$) $\quad V_{rated} = 6$ m/s

$\rho = 1.25$ kg/m^3 $\quad A_{mv} = 1$ m^2

$(1-a) = 0.5$ $\quad R_{mv} = 2.36$ m

$\Rightarrow M_{s_{min}} = 11.95$ Nm

$M_{s_{max}}$ is determined by the space available for the spring. A small increase in M_s at increasing γ only can be realised for a long spring.

Suppose $M_{s_{max}}$ is 1.4 $M_{s_{min}}$ so $M_{s_{max}} = 1.4 \times 11.95 = 16.73$ Nm.

The determination of the spring geometry is beyond the scope of this publication.

The next step is to know the moment of N_{mv} around the tower axis $M_{mv_{ta}}$

$N_{mv_{ta}}$ can be written as:

$$M_{mv_{ta}} = N_{mv} \times \{R_{mv} + g\cos(\gamma - \delta_o)\} \tag{49}$$

formula (46) can be written as $N_{mv} = \frac{M_{s_\gamma}}{R_{mv}}$ (50)

(49) + (50) →

$$M_{mv_{ta}} = M_{s_\gamma} \times \frac{\{R_{mv} + g\cos(\gamma - \delta_o)\}}{R_{mv}} \quad (51)$$

The term $g\cos(\gamma - \delta_o)$ is small with respect to R_{mv}. If it is neglected formula (51) changes into:

$$M_{mv_{ta}} = M_{s_\gamma} \quad (52)$$

This means that the variation in $M_{mv_{ta}}$ as a function of γ is equal to the $M_s - \gamma$ curve of figure 35.

However if we want compare the $M_{mv_{ta}}$ with M_{r+av} as illustrated in figure 29, we must know $M_{mv_{ta}}$ as a function of δ and not as a function of γ.

The relation between γ, δ, α_{mv} and δ_o can be found from figure 34 and can be written as: $\delta = \gamma - \delta_o + \alpha_{mv}$ (53)

A problem is that α_{mv} is not constant. It is equal to δ_o for $V = V_{rated}$ (see figure 32). At higher wind speeds, α_{mv} becomes much smaller. This can be understood with formula (31) which is :

$$N_{mv} = C_{n_{mv}} \times 0.5\rho \times (1-a)^2 \times V^2 \times A_{mv} \quad (31)$$

The change in N_{mv} for $V > V_{rated}$ is proportional with the change in M_{s_γ} as illustrated in figure 35 which means that there will be only a small increase in N_{mv} for higher wind speeds. At higher wind speeds not only V is increasing but also the factor $(1-a)$ because the rotor comes out of the rotor shadow.

If N_{mv} increases only slightly and if $(1-a)^2 \times V^2$ is increasing strongly at higher wind speeds $C_{n_{mv}}$ and therefore α_{mv} will decrease strongly and goes to a small value for high wind speeds. To simplify the whole calculation it is assumed that $\alpha_{mv} \approx 5^o$ for

high wind speeds. At high wind speeds the rotor is fully out of the wind so $\delta = 90^o$.

$$(53) \rightarrow \delta = \gamma - \delta_o + \alpha_{mv}$$

$$\left.\begin{array}{l} \\ \delta = 90^\circ,\ \delta_o = 20^\circ \text{ and } \alpha_{mv} = 5^\circ \end{array}\right\} \quad \gamma = 105^o$$

Now we know:

1. $\alpha = \delta_o = 20^\circ$, $\delta = 0^\circ$ and $\gamma = 0^\circ$ for $V = V_{rated}$
2. $\alpha = 5^\circ$, $\delta = 90^\circ$ and $\gamma = 105^\circ$ for high wind speeds.

Next a second axis has been drawn in figure 35 according to these statements. It is assumed that the δ – axis is linear from $0^o \rightarrow 90^o$. An error in this assumption has only has a small influence on the δ – V curve of figure 37. Next the line for $M_{mv_{va}} - \delta$ can be drawn in figure 29.
The result is presented in figure 36.

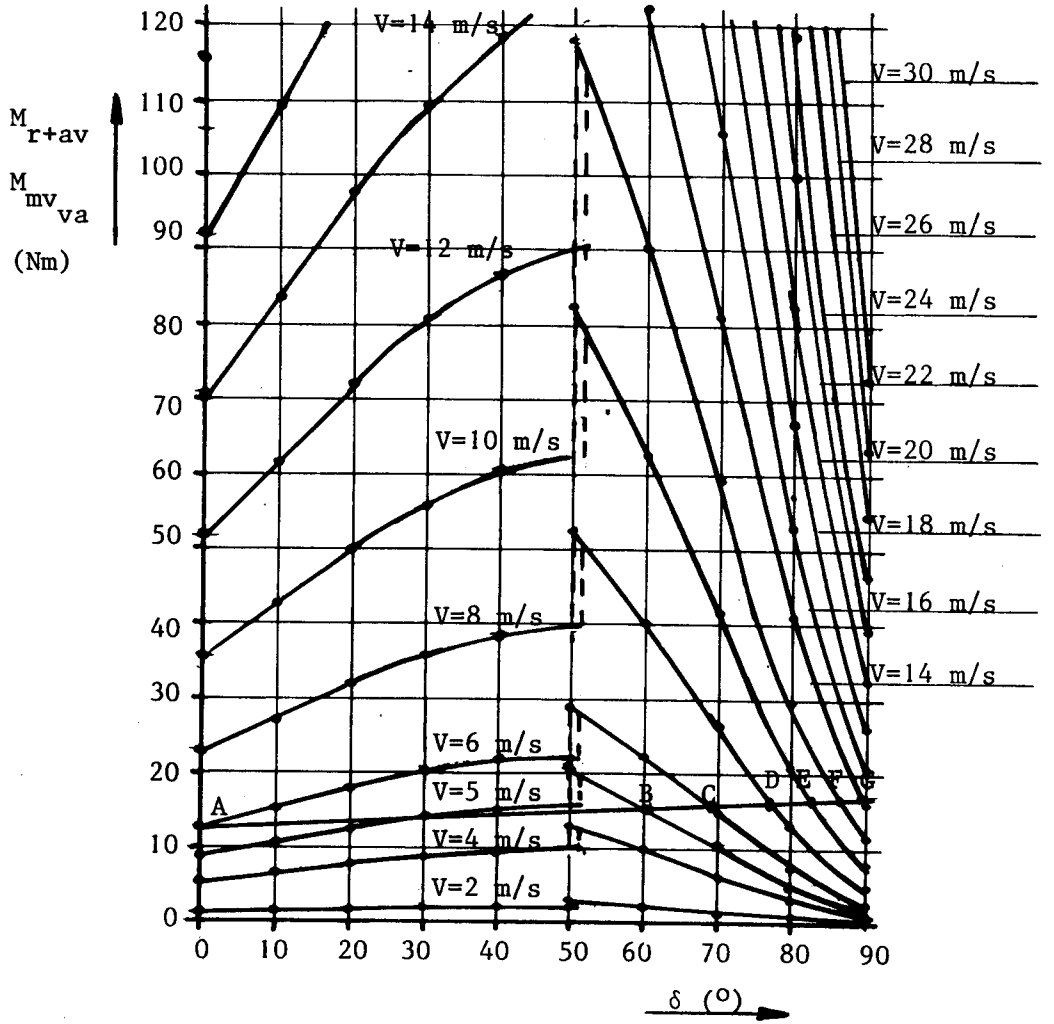

Figure 36 $M_{mv_{va}}$ – δ curve drawn in M_{r+av} – δ graph for CWD 2740 head equipped with ecliptic main vane

To be able to judge the behaviour between V = 4 and V = 6 m/s an extra M_{r+av} – δ line for V = 5 m/s has been added.

Points B, C, D, E and F are stable working points. Point A is an instable working point because M_{r+av} is increasing faster than $M_{mv_{ta}}$ at increasing δ. This is an indication for instability. From the working points of figure 36 the V – δ curve can be derived (see figure 37). There is hysteresis between a wind speed of about 4.5 m/s and 6 m/s.

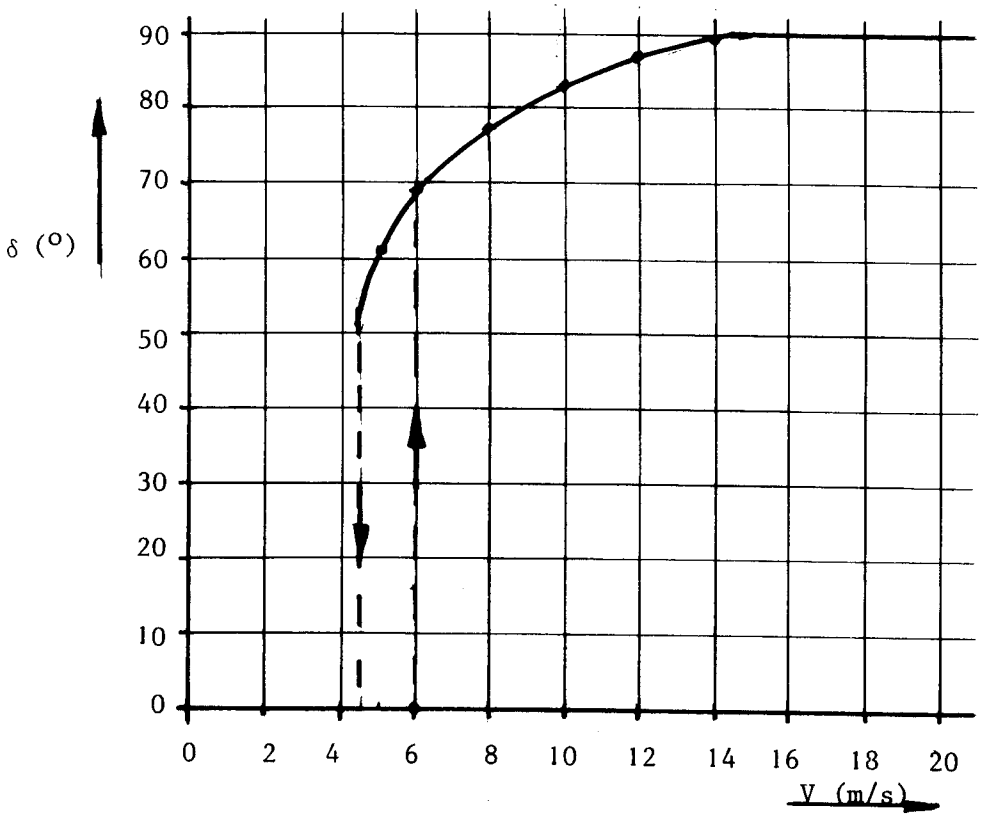

Figure 37 δ – V curve for CWD 2740 head equipped with ecliptic main vane

The results of the calculation of Ω_δ and F_{t_δ} for different values of V are presented in table 4, figure 38 and figure 39.

For the calculation formulas (1), (2), (3) and (4) have been used and the following parameters: for the CWD 2740 head $R = 1.37$ m

$C_t = 0.68$

$\lambda_{unloaded} = 3.2$

$\rho = 1.25$ kg/m^3

F_t can be calculated more accurately (especially for high wind speeds) than with formula (4) if the real measured $C_t - \delta$ values are taken.

V (m/s)	δ (°)	Ω_δ (rad/s)	Ft_δ (N)
2	0	4.7	10.0
4	0	9.4	40.1
6	0	14.2	90.2
5	61	5.7	14.7
6	69	5.1	11.6
8	77	4.2	8.1
10	83	2.9	3.7
12	87	1.5	1.0
14	89	0.6	0.15
16 and more	90	0	0

Table 4: Ω_δ and Ft_δ as a function of V for CWD 2740 head with ecliptic safety system.

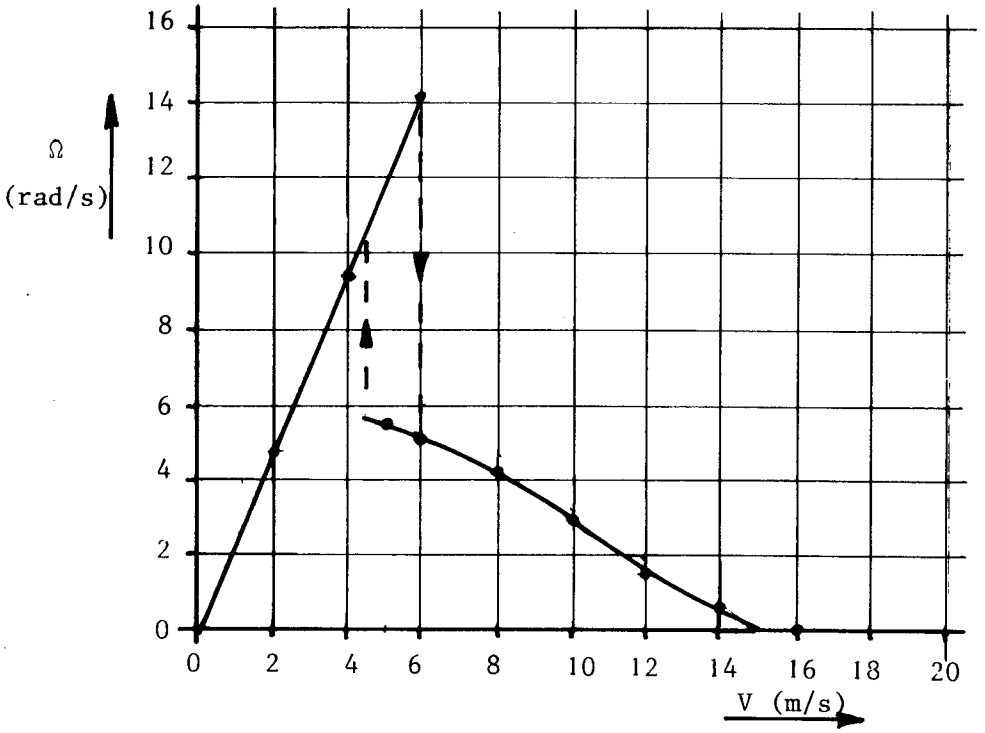

Figure 38 Ω – V curve for CWD 2740 head equipped with ecliptic main vane

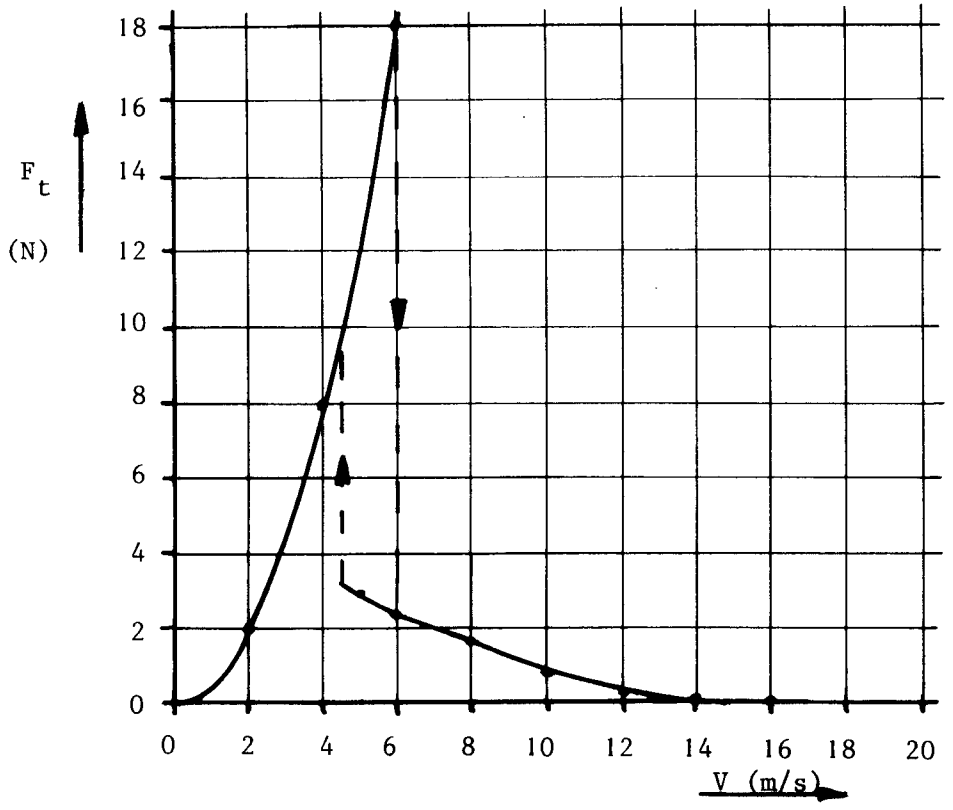

Figure 39 F_t – V curve for CWD 2740 head equipped with ecliptic main vane

It can be seen that both Ω and F_t are decreasing strongly for $V > V_{rated}$ and that there is hysteresis for $4.5 < V < 6$ m/s. Therefore the output will be reduced strongly for $V > V_{rated}$.
At $V = 6$ m/s the head turns out of the wind from $\delta = 0$ to $\delta = 68^o$ (see figure 37). Because of the inertia of the head, it will go further and oscillate around $\delta = 68^o$. In the same way it will oscillate at about $V = 4.5$ m/s when it comes back to $\delta = 0^o$. Because of the oscillation the momentary product of Ω and the yawing speed and therefore the gyroscopic moment in rotor blades and shaft can be very high. So this safety system is a bad choice.
The system can be improved on the following ways:

1. Take a torsion spring which is so stiff that $M_{mv_{ta}}$ is increasing faster than $M_{r + av}$ at increasing δ.
2. Decrease the distance f so the unfavourable effect of F_s on M_r decreases.

3. Try another shape or aspect ratio for the auxiliary vane or take a cylinder to prevent hysteresis in M_{av}.

The whole procedure of determining the Ω - V and F_t - V curves then must be repeated for the new parameters till a better result is obtained.

7.5 The inclined hinge main vane system

7.5.1 General

In chapters 4.6 and 4.7 a rough description has been given for this system. The basic element of the inclined hinge main vane system is the angle ϵ of the main vane axis with the tower axis. Because of this angle there is one position of the vane called the neutral position in which the centre of gravity of the vane is lowest.

If the vane is turned around the vane axis away from the neutral position a component of the vane weight in the plane of rotation pushes the vane back to the neutral position.

Therefore there is no stop required at the neutral position because the component of the weight is zero there. In practice a stop is required at a negative angle γ of about 65^o and at a positive angle of 105^o to prevent the vane to touch the rotor under dynamic conditions (see fig. 4).

The exact moment equations for the inclined hinge main vane system are more complex than for the ecliptic system because not all forces are working in a horizontal plane. Another complication is to find the correct angle between the main vane and the wind direction. Because of the angle ϵ the vane blade is only vertical for $\gamma = 0^o$.

For $\gamma = 90^o$ the vane blade makes an angle $90^o - \epsilon$ with the horizontal plane.

Therefore the direction of the wind speed is not parallel to the vane chord.

Also the distance g between vane axis and tower axis like it has been defined for the ecliptic system is not constant; it depends on ϵ.

In figure 40 it can be seen how it is defined for the inclined hinge main vane system.

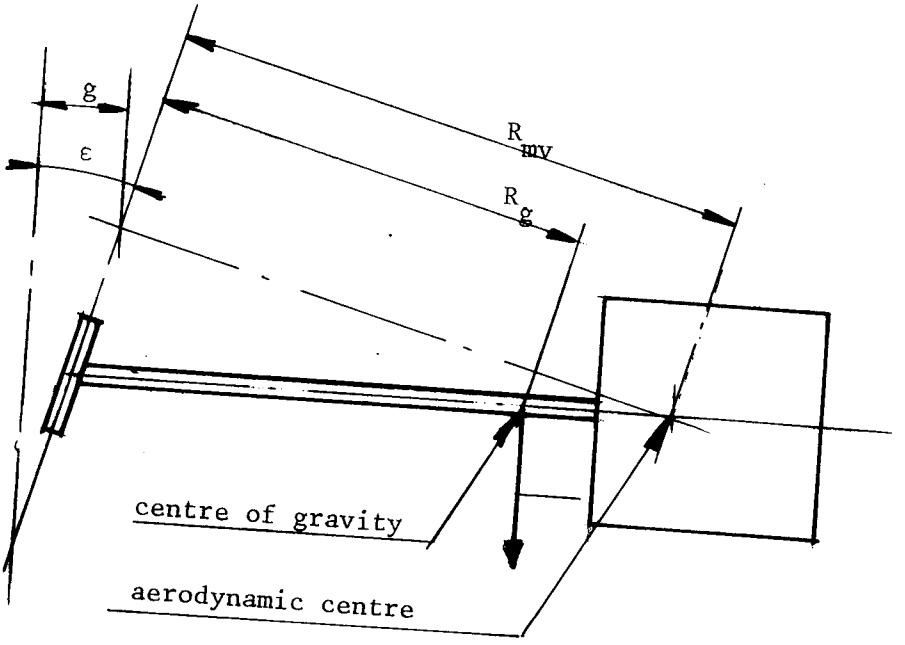

Figure 40 Parameters for inclined hinge main vane

However for small angles ϵ ($\epsilon < 20^0$) these complications can be neglected for the moment equation around the head axis and it can be assumed that all forces, arms and angles are laying in a horizontal plane.
The same formulas and figures as derived for the ecliptic system now can be used. The situation with the rotor perpendicular to the wind only exists for very low wind speeds where the main vane is almost in the neutral position.
For the moment equation around the vane axis one has to take the forces laying in a plane perpendicular to this axis. To calculate the active component of the weight first the total vane weight G is thought to be concentrated in the centre of gravity at radius R_g.
In figure 40 the vane is drawn in the neutral position and R_g, R_{mv} and g are defined. Through the centre of gravity a plane is defined perpendicular to the main vane axis (see figure 41).

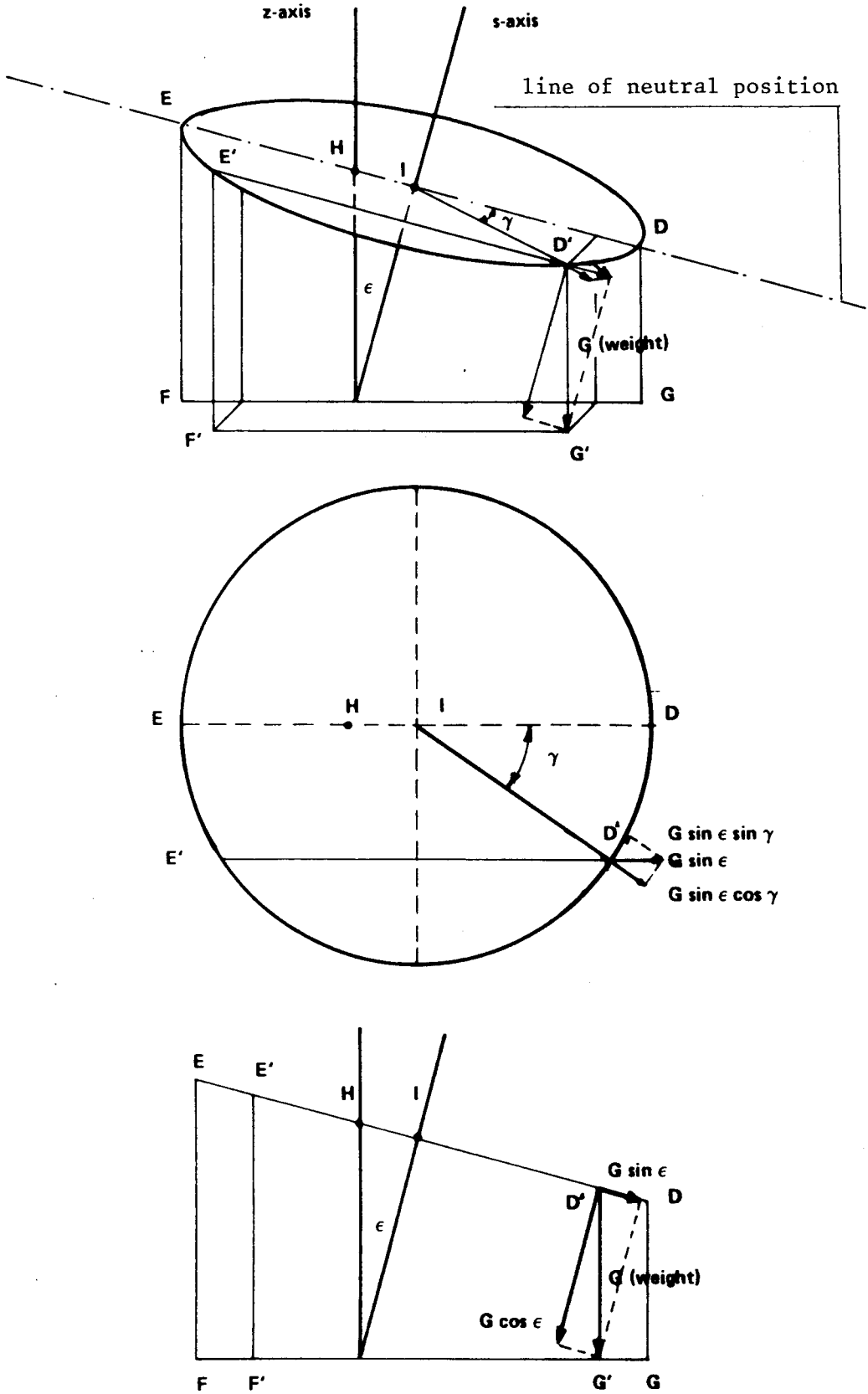

Figure 41 Force components due to the weight of the main vane

The weight vector G first is resolved into a factor G cos ϵ parallel to the main vane (s-axis) and a factor G sin ϵ parallel to the line I–D (vane in neutral position).
The latter one then is resolved in a component G sin ϵ cos γ in the direction of the main vane and a component G sin ϵ sin γ perpendicular to the main vane (line I – D').
Only this component is causing the moment of G around the main vane axis. This moment can be written as:

$$M_g = G \sin \epsilon \times \sin \gamma \times R_g \qquad (54)$$

For a certain value of G, ϵ and R_g formula (54) shows that M_g varies sinusoidically with γ.
Contrary to the ecliptic system it is not easy to define a rated wind speed for the inclined hinged main vane system. For the ecliptic system V_{rated} is the wind speed where the rotor starts turning out of the wind. For the inclined hinge main vane system V_{rated} should be the wind speed where the rotor speed is maximal but this will be the case at a certain unknown value of δ.
The following procedure is used to solve this problem:

1. Take a certain V_{rated} for instance $V_{rated} = 6$ m/s.
2. Calculate the $M_{mv_{va}}$ using formula (45) and (31) for $V = V_{rated}$ and $\delta_o = \alpha = 20^o$ (identical to the ecliptic system).
3. Take $M_{g_{max}} = 1.5 \times M_{mv_{va}}$ (55).
   Take $V = V_{rated}$ and $\gamma = 90^o$ (sin $\gamma = 1$ for $\gamma = 90^o$). This determines the term G sin $\epsilon \times R_g$ out of formula (54) and the shape of the $M_g - \gamma$ curve.
4. Determine the $M_g - \delta$ curve in the same way as it has been done for the ecliptic system.
5. Determine the $\delta - V$, the $\Omega - V$ and $F_t - V$ curves in the same way as it has been done for the ecliptic system.
6. If the maximum Ω or F_t is too high or too low this means that the factor 1.5 was not correct. Take another factor and do it again.
7. If the result is acceptable this was obtained for a certain product of G sin $\epsilon \times R_g$. Now a real vane must be drawn as light as possible and the weight G and R_g must be determined.

8. Next the angle ϵ can be determined. Commonly ϵ varies between 10^o and 15^o. If an angle larger than 15^o is found the vane can be made heavier. Angles smaller than 10^o which may be necessary for large windmills require accurate tolerances in the head and a tower which has to be placed exactly vertical.

7.5.2 Example

Suppose we take the same example as used for the ecliptic system but now an inclined main vane has been placed. Suppose the same vane blade area $A_{mv} = 1\ m^2$ and the same vane radius $R_{mv} = 2.36$ m is taken. This means the rotor is perpendicular to the wind for very low wind speeds where $\gamma \approx 0^o$. Suppose we take the same $V_{rated} = 6$ m/s.

So $M_{mv_{va}} = 11.95$ Nm (see figure 35 and (47) + (45))

$(55) \rightarrow M_{g_{max}} = 1.5 \times M_{mv_{va}}$

$M_{g_{max}} = 17.93$ Nm

$(54) \rightarrow M_{g_{max}} = G \times \sin \epsilon \times R_g$ for $\gamma = 90^\circ$ so

$G \times \sin \epsilon \times R_g = 17.93$ Nm for $\gamma = 90^\circ$

The $M_g - \gamma$ curve is drawn in figure 42.

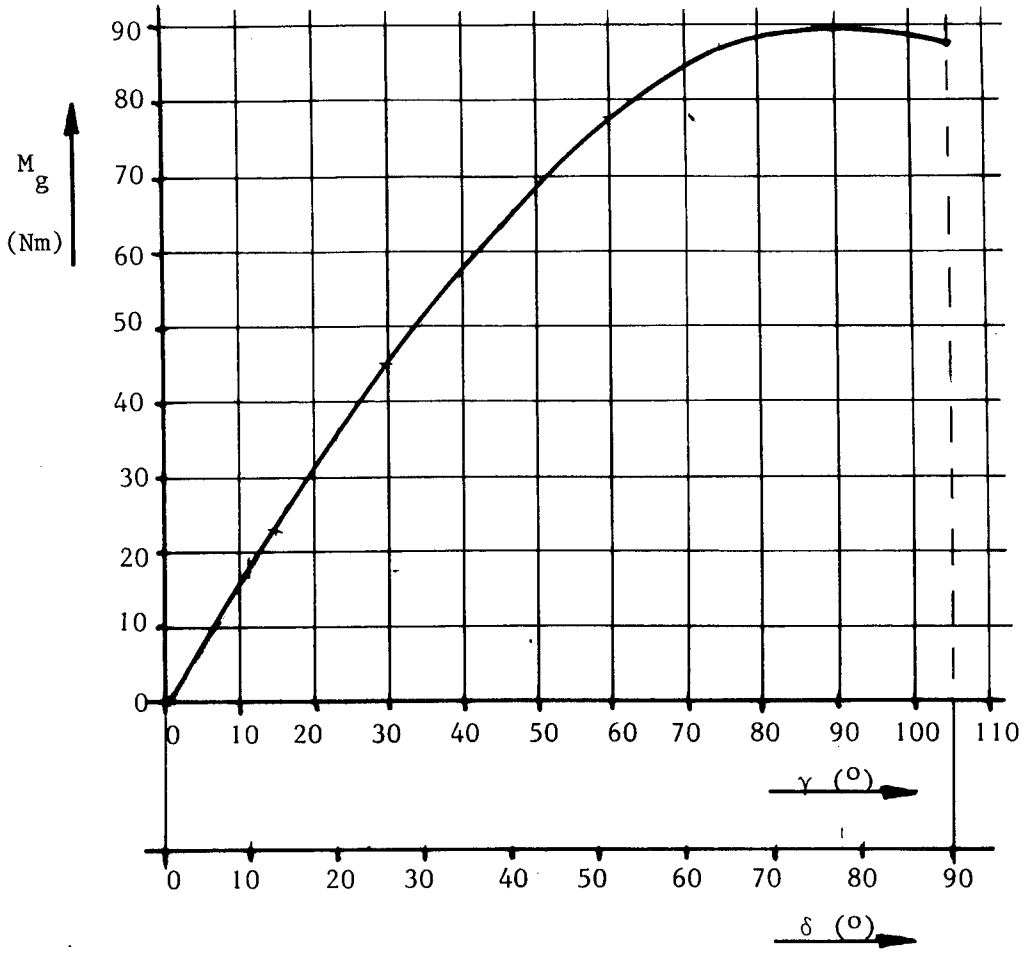

Figure 42 Moment of the vane weight M_g as a function of γ and δ

Next a second δ – axis can be added to figure 42. If g is neglected with respect to R_{mv}. M_g is equal to $M_{mv_{ta}}$ identical to the change from formula (51) to formula (52).

Next the $M_{mv_{va}} - \delta$ curve can be drawn in the $M_{r + av} - \delta$ curve of figure 29. This results in figure 43.

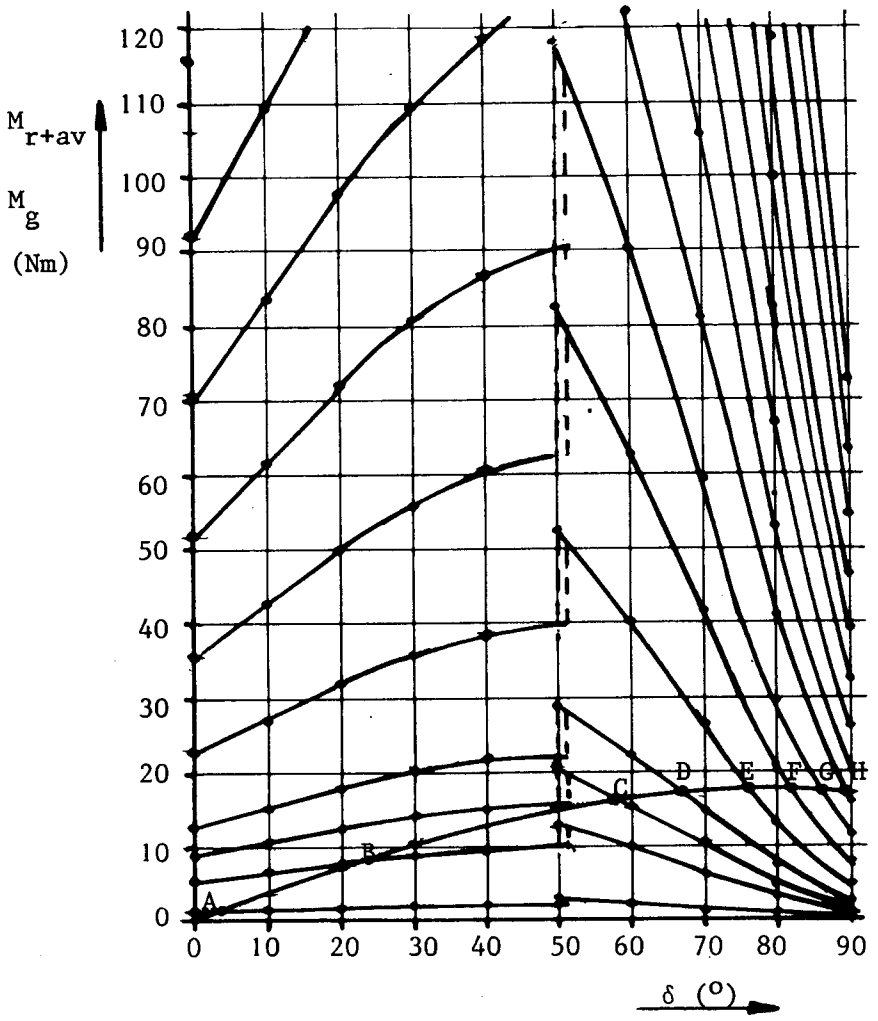

Figure 43 $M_g - \delta$ curve drawn in M_{r+av} graph for CWD 2740 head equipped with special inclined hinge main vane

Points A, B, C, D, E and F are stable working points. Out of the working points of figure 43 the $V - \delta$ curve can be derived (see figure 44).

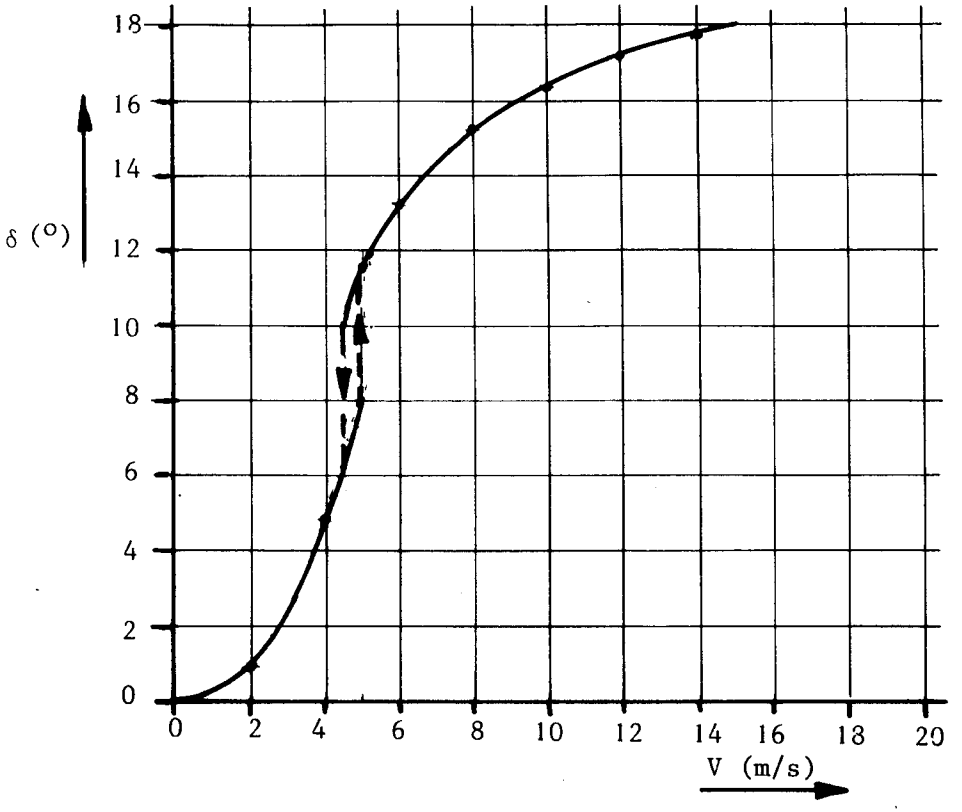

Figure 44 δ – V curve for CWD 2740 head equipped with special inclined hinge main vane

If figure 44 is compared with figure 37 the difference between both systems become clear.

The results of calculation of Ω and F_t using formulas (1), (2), (3) and (4) for different values of V are presented in table 5, figure 45 and figure 46 (F_t can be calculated more accurately than with formula (4) if the real measured C_t – δ values are taken).

V (m/s)	δ (°)	Ω_δ (rad/s)	Ft_δ (N)
2	4	4.7	9.9
4	24	8.6	33.5
5	58	6.3	17.6
6	66	5.7	14.9
8	76	4.6	9.4
10	82	3.3	4.8
12	86	2.0	1.8
14	89	0.6	0.15
16 and more	90	0	0

Table 5: Ω_δ and Ft_δ as a function of V CWD 2740 head with special inclined main vane safety

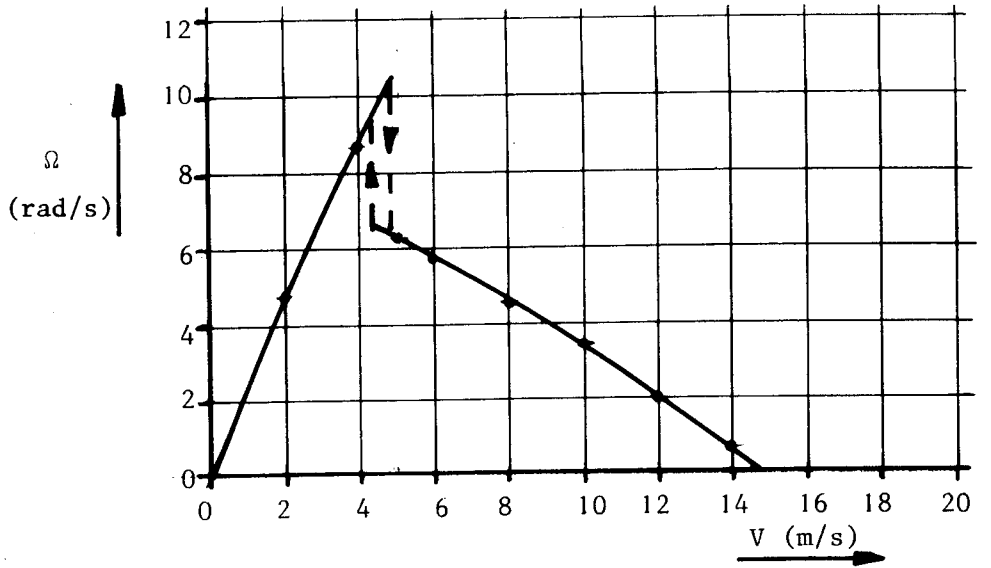

Figure 45 Ω – V curve for CWD 2740 head equipped with special inclined hinge main vane

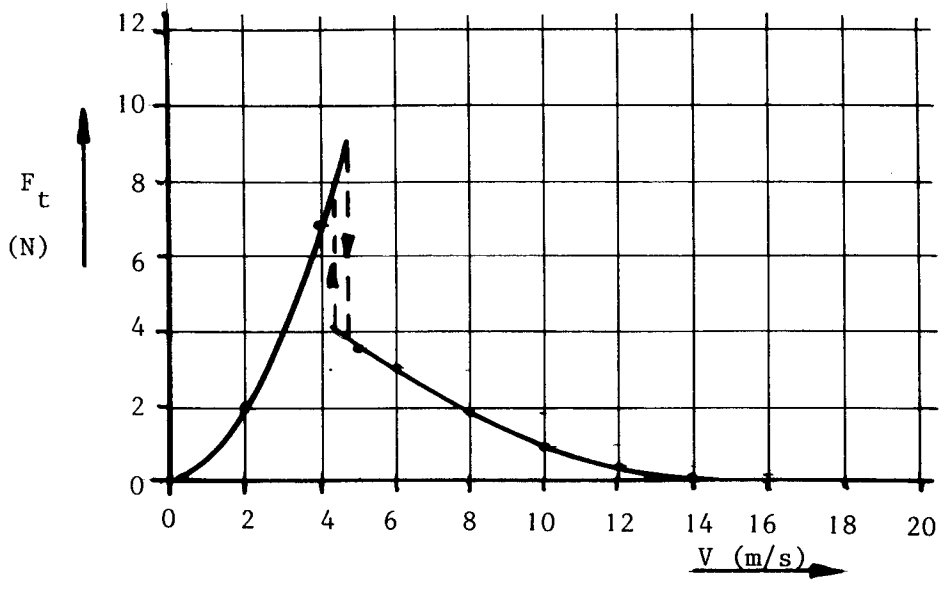

Figure 46 F_t – V curve for CWD 2740 head equipped with special inclined hinge main vane

Figure 45 learns that the maximum Ω is obtained at about V = 5 m/s. This means that the vane weight G is too low because V_{rated} should be 6 m/s.
If figures 45 and 46 are compared with figures 38 and 39 it can be seen that the effect of hysteresis is less pronounced for the inclined hinge main vane system than for the ecliptic system.
If V_{rated} = 5 m/s is found too low, the vane weight G has to be enlarged and the whole procedure has to be repeated. Suppose V_{rated} = 5 m/s is acceptable.

Next the vane is designed in such a way that R_{mv} = 2.36 m.

Suppose R_g = 1.5 m and G = 70 N → R_g × G = 105 Nm

$G \times \sin \epsilon \times R_g$ = 17.93 Nm (see figure 42) } $\epsilon = 9.8^\circ$

For results see figure 47.

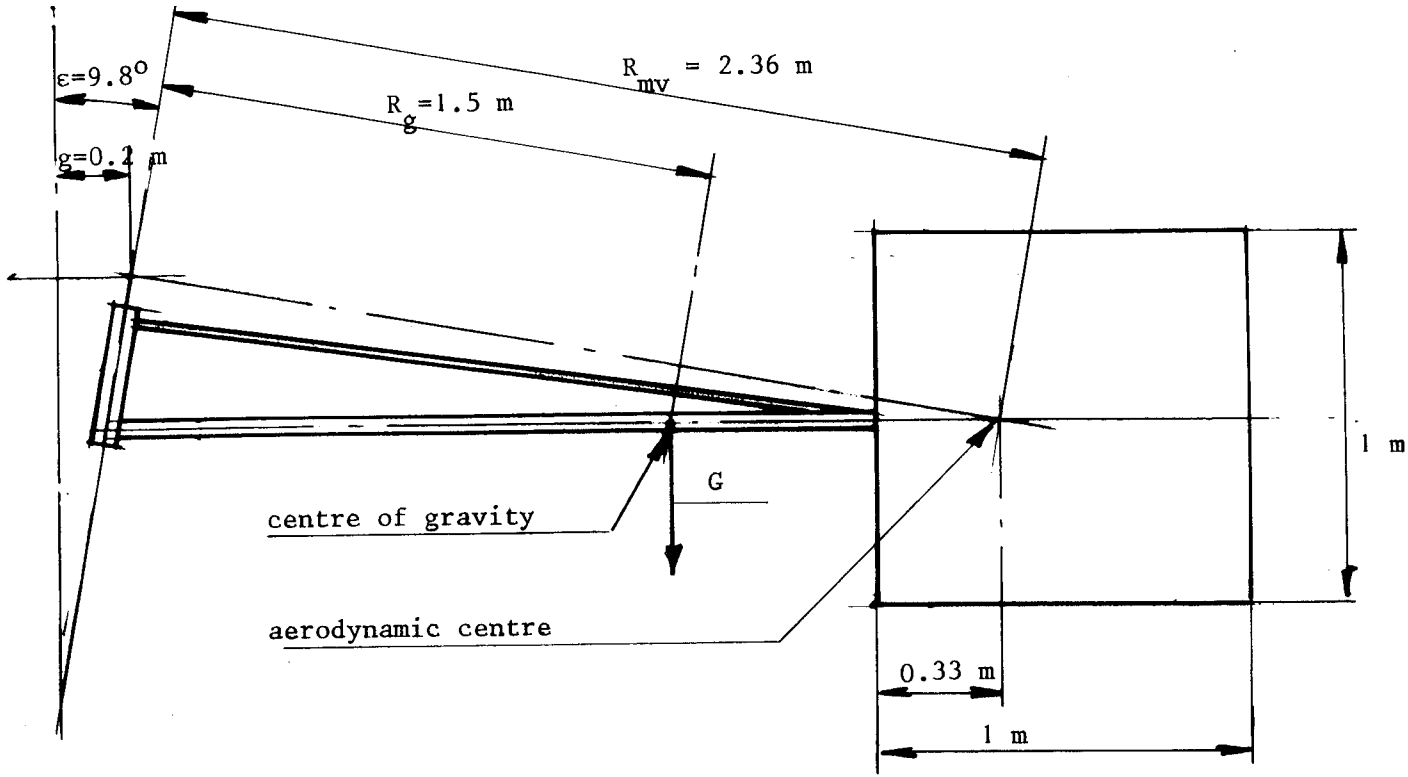

Figure 47 Vane parameters for special vane for CWD 2740 head

Note: The main vane as found in this example is not identical to the real CWD 2740 main vane. R_{mv} for the real CWD 2740 mill is shorter (R_{mv} = 1.9 m) and g is larger (0.28 m instead of 0.2 m). Despite these differences the rotor of the real CWD 2740 is about perpendicular to the wind direction at low wind speeds. This may indicate that the term (1 – a) is somewhat larger than 0.5 as assumed in the beginning of the calculations.

7.6 The hinged side vane system

7.6.1 General

In chapters 4.8 and 4.9 a rough description has been given for this system. Only the combination of hinged side vane and eccentrically placed rotor works satisfactorily and will be described.

For low wind speeds the system is positioned as illustrated in figure 48.

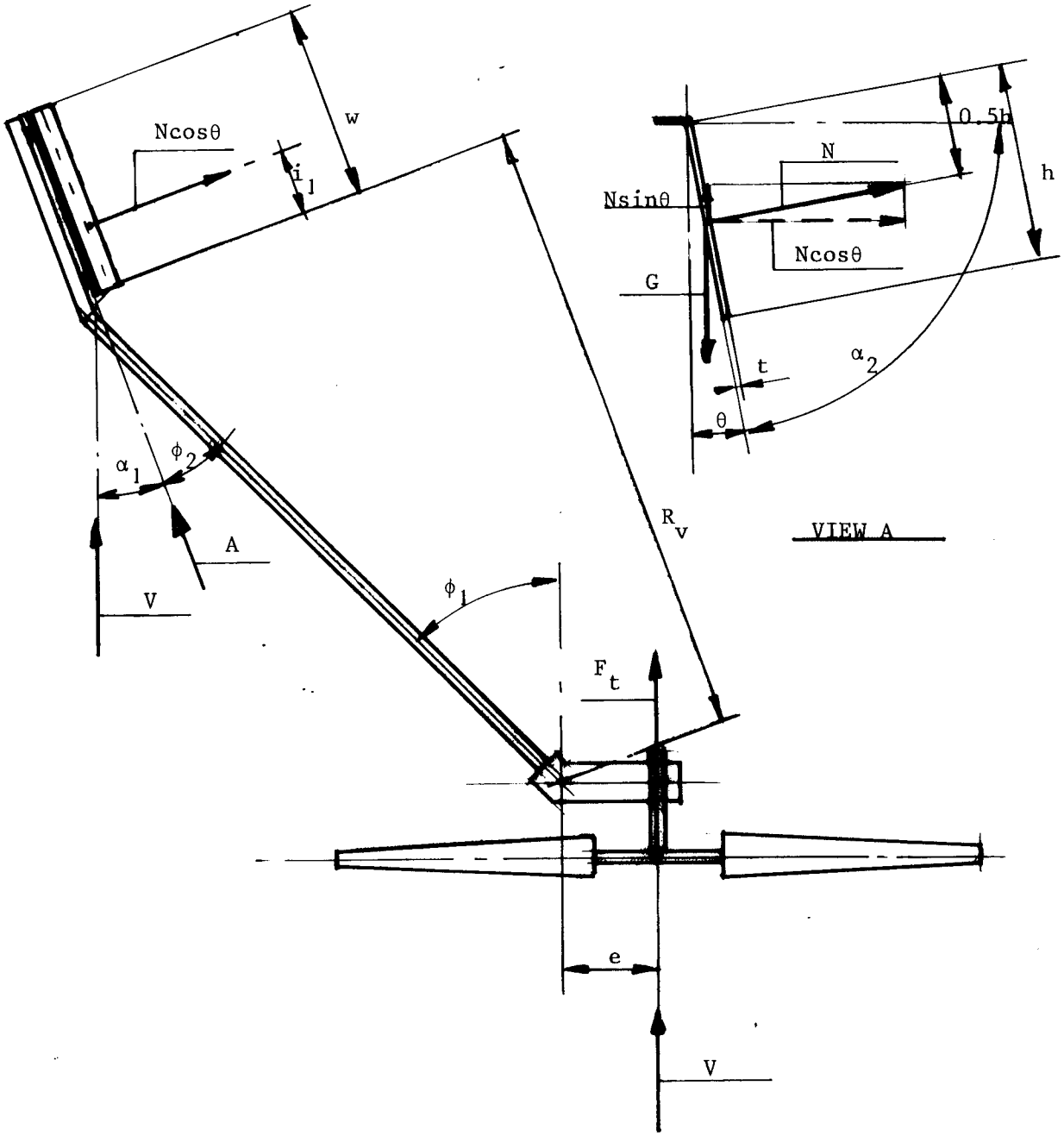

Figure 48 The hinged side vane system for low wind speeds

For the hinged side vane R_v is not taken as the distance between the tower axis and N but as the distance between the tower axis and the leading edge of the plate. This has been done because the value for i is not constant. It is about $^1/_3$w for low wind speeds where $\alpha_1 \approx 20^o$ and it is about $^1/_2$w for high wind speeds where $\alpha_1 \approx 90^o$.
The angle ϕ_1 between vane arm and rotor axis determines the position of the vane blade with respect to the rotor.
Practical experiences show that $\phi_1 \approx 45^o$ is a good choice.

It brings the vane blade out of the rotor shadow with a relative short vane arm and still R_v is only somewhat shorter than the length of the vane arm.
Therefore a relative small vane blade area can be used to get a certain moment around the tower axis.
The angle ϕ_2 is taken about 25°. This results in an angle $\alpha_1 = 20°$ for the rotor perpendicular to the wind.
At low wind speeds the direction of the wind speed is about parallel to the vane axis. This means that w can be seen as the chord and h as the width of the plate.
At high wind speeds the vane is lifted to an almost horizontal position. Now α_2 is small and because the rotor is turned out the wind the wind direction is about perpendicular to the vane axis so $\alpha_1 \approx 90°$ (see figure 49).

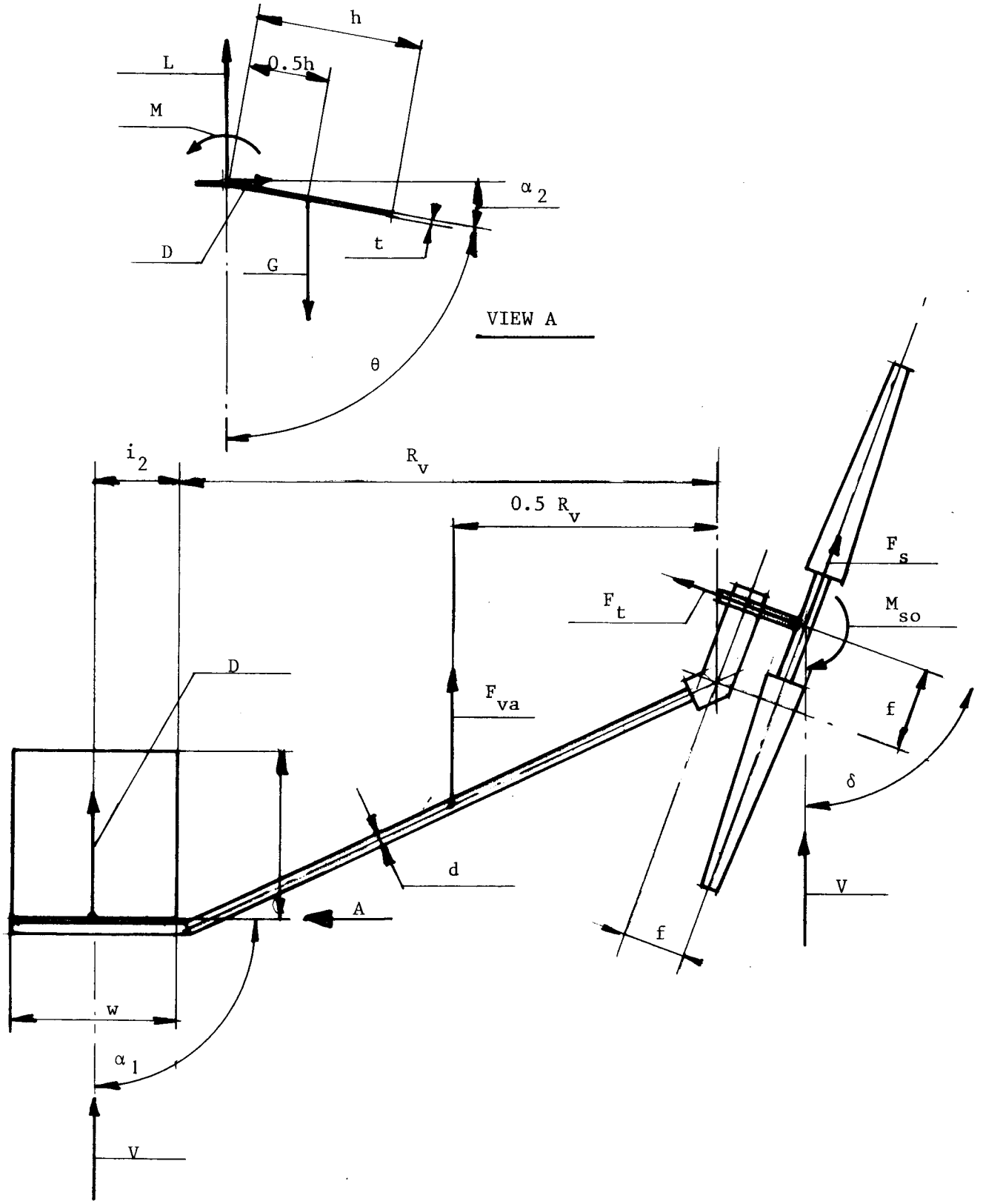

Figure 49 The hinged side vane system for high wind speeds

Now the wind direction is about parallel to h which can be seen as the chord and w becomes the width.

For the moment equations at low wind speeds it is easy to calculate with the normal force N acting on a distance i, from the leading edge of the plate. For the moment equations at high wind speed it is easier to use lift, drag and moment around the leading edge like they originally have been measured by Flachsbart [10]. The relation between both methods is as follows:
The acting point of lift, drag and pitch moment according to Flachsbart is the leading edge of the plate (see figure 50).
(Most coefficients for aerodynamic profiles are defined around the quarter chord point but Flachsbart used the leading edge.)

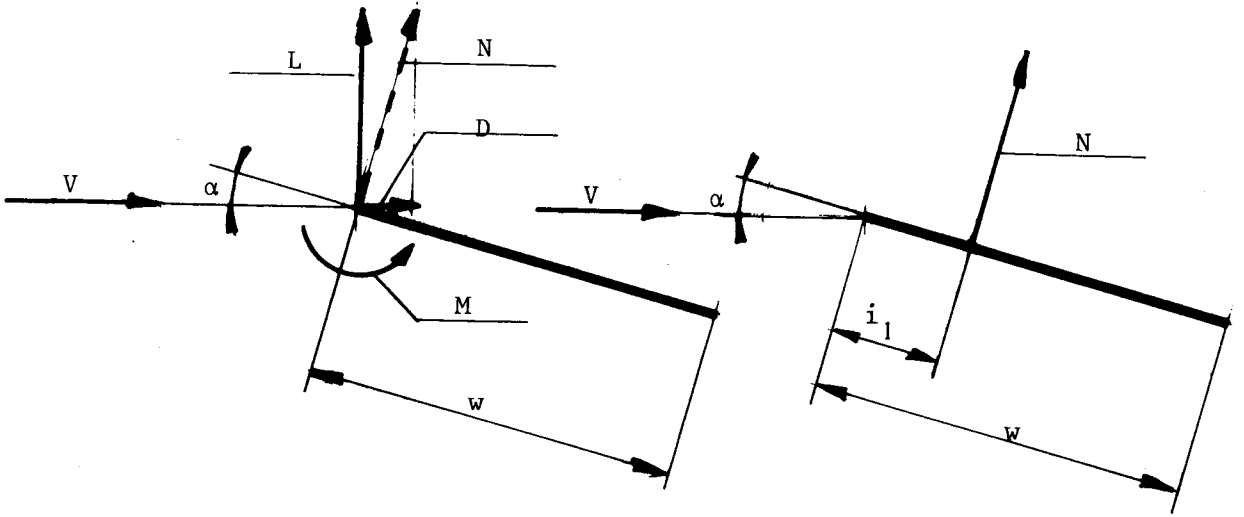

Figure 50 + 51 Lift L, Drag D, Moment M and normal force N acting on a square plate

N is the resultant of L and D

$$N = \sqrt{L^2 + D^2} \qquad \text{or} \qquad C_n = \sqrt{C_l^2 + C_d^2} \tag{55}$$

This force is perpendicular to a flat plate except for very small values of α.

Because the situation of figure 51 is equivalent with the situation of figure 50 it can be derived that:

$$\frac{i}{w}_1 = \frac{C_m}{C_n} \tag{56}$$

$$(56) + (55) \rightarrow \frac{i}{w}_1 = \frac{C_m}{C_l^2 + C_d^2} \tag{57}$$

The factor $\frac{i}{w}_1$ has been determined using the original table of Flachsbart. The result is presented in figure 52.

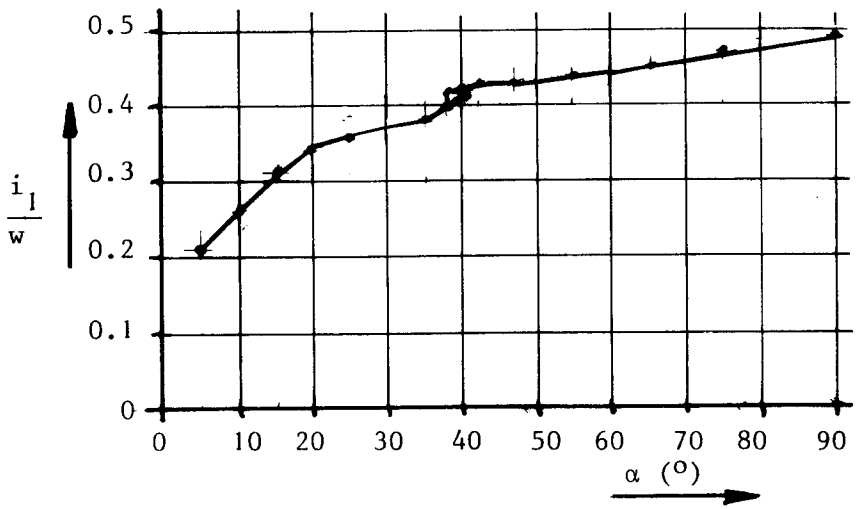

Figure 52 The $\frac{i}{w}_1 - \alpha$ curve for a square plate

It can be seen that $i_1 \approx {}^1/_3 w$ for $\alpha = 20^\circ$.

Apart from the aerodynamic force on the vane blade a drag force F_{va} is working on the vane arm. This force is neglected for low wind speeds because most of the vane arm is in the rotor shadow and because F_{va} is small with respect to the aerodynamic force on the vane blade.

At high wind speeds it is not allowed to neglect F_{va} because now the whole vane arm is in the undisturbed wind speed and because the drag component of the drag force on the vane blade D is small for small values of α.

F_{va} is supposed to act in the middle of the pipe so on a radius 0.5 R_v.

As area of the vane arm A_{va} the projected area of the pipe perpendicular to the wind direction is taken for $\delta = 70^o$ (see figure 49).

$$A_{va} = R_v \times d_p \qquad (d_p = \text{pipe diameter}) \tag{58}$$

In reality this area is not constant (it depends on δ) but at large angles δ the difference in real area and the area according to formula (53) is small and can be neglected.

7.6.2 The hinged side vane system for low wind speeds (V < 4 m/s)

The moment equation around the tower axis can be written as (see figure 48):

$$F_t \times e = N \cos\theta \times (R_v + i_1) \tag{59}$$

For low wind speeds the vane is in the almost vertical position so θ is small and $\theta \approx 1$.

Formula (59) then changes into:

$$F_t \times e = N \times (R_v + i_1) \tag{60}$$

Contrary to the ecliptic and inclined hinge main vane system the wind speed at the vane blade is not reduced by the rotor shadow so $(1 - a) = 1$.

Formula (31) changes into:

$$N = C_n \times 0.5\,\rho\,V^2 \times A_v \tag{61}$$

(The indices mv have been removed because it is not necessary to distinguish the main vane from another vane.)

(61) + (60) + (13) →

$$C_t \times \pi R^2 \times e = C_n \times A_v\,(R_v + i_1) \tag{62}$$

This formula can be used to determine the vane area and vane arm for a certain rotor and eccentricity.

For the moment equation around the vane axis it is assumed the the normal force N acts in the middle of the plate on 0.5h from the hinge axis (so the influence of the strip which forms an asymmetry is neglected).
The moment equation can be written as (see figure 48):

$$G \sin \theta = N \tag{63}$$

$$G = A_v \times t \times \rho_v \times g \tag{64}$$

(64) + (63) + (61) →

$$t \times \rho_v \times g \sin \theta = C_n \times 0.5\, \rho\, V^2 \tag{65}$$

7.6.3 The hinged side vane system for high wind speeds (V > 8 m/s)

The moment equation around the tower axis can be written as (see figure 49):

$$M_r = M_v + M_{va} \tag{66}$$

(M_v is the moment of vane blade, M_{va} is the moment of vane arm)

$$M_v = D \times (R_v + i_2) \tag{67}$$

$$D = C_d \times 0.5\, \rho\, V^2 A_v \tag{68}$$

The $C_d - \alpha$ curve for a square plate is presented in figure 53.

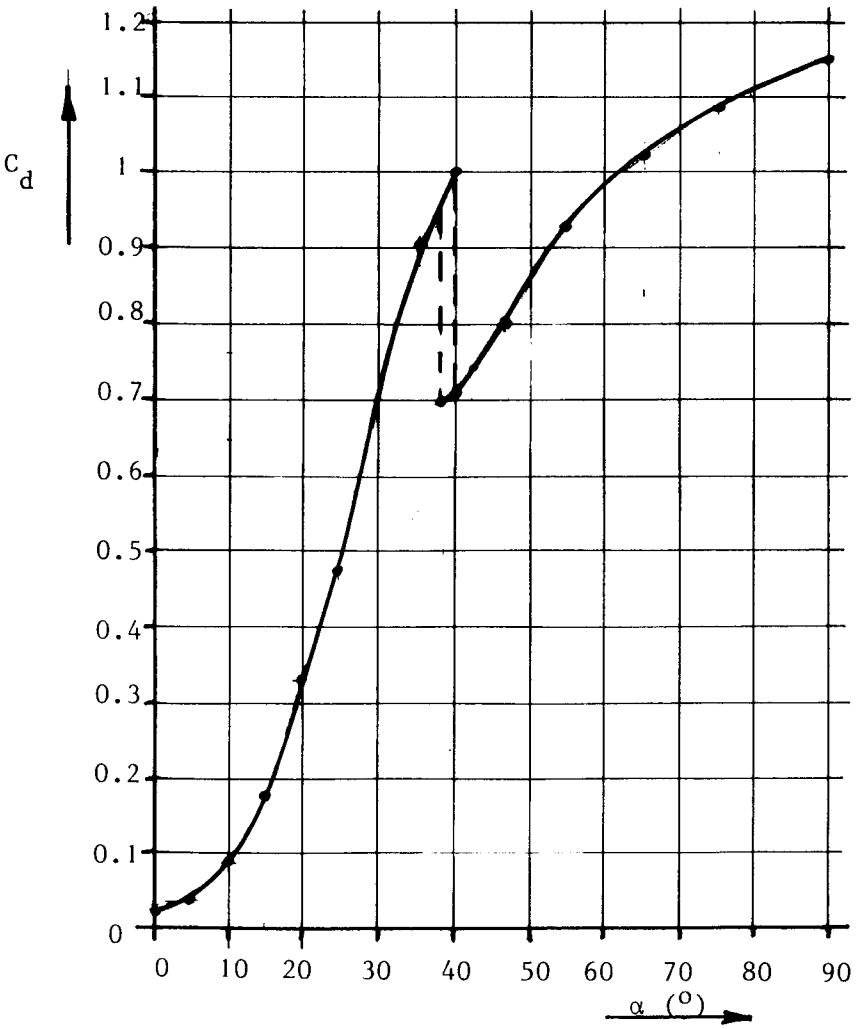

Figure 53 $C_d - \alpha$ curve for a square plate according to Flachsbart

$$M_{va} = F_{va} \times 0.5\, R_v \tag{69}$$

$$F_{va} = C_{d_{va}} \times 0.5\, \rho\, V^2 \times A_{va} \tag{70}$$

The drag coefficient C_d for a pipe depends strongly on the Reynolds number and the surface roughness. The Reynolds number for a pipe is:

$$Re = \frac{V \times d}{\nu} \tag{71}$$

d is pipe diameter (m)

ν is kinematic viscosity which is about 15×10^{-6} m^2/s for air.

The drag coefficient for a pipe is about 1.18 for $10^4 < Re < 3 \times 10^5$ (see literature [18] chapter III figure 12).

In the region $Re = 2 \rightarrow 4 \times 10^5$ it drops from 1.18 to approximately 0.3.

The effect of the surface roughness is that C_d drops at a lower Re number. Figure 54 which is a copy of figure 14 of literature [18] gives this effect for different values of k/d (k/d is the ratio between the sand - grain size k and the pipe diameter d).

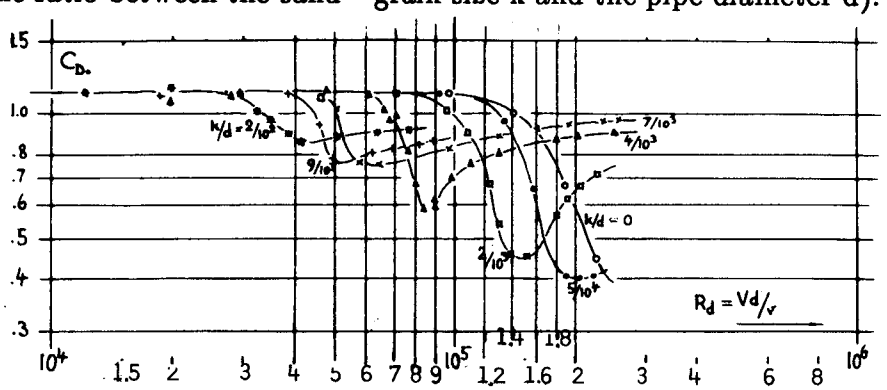

Figure 54 Drag coefficient of cylinders having various degrees of surface roughness (sand-grain size "k" as against diameter "d")

(70) + (69) + (68) + (67) + (66) + (19) $\rightarrow$

$$\pi R^2 (C_t \times e + C_s \times f_1 - C_{so} \times R) = C_d \times A_v (R_v + i_2) + C_{d_{va}} \times A_{va} \times 0.5\, R_v \tag{72}$$

The moment equation around the vane axis can be written as (see figure 49):

$$M = G \times 0.5\, h \cos \alpha_2 \tag{73}$$

$$M = C_m \times 0.5\, \rho\, V^2 \times A_v \times h \tag{74}$$

C_m is a function of α and using the original table of Flachsbart the $C_m - \alpha$ curve is derived and presented in figure 55.

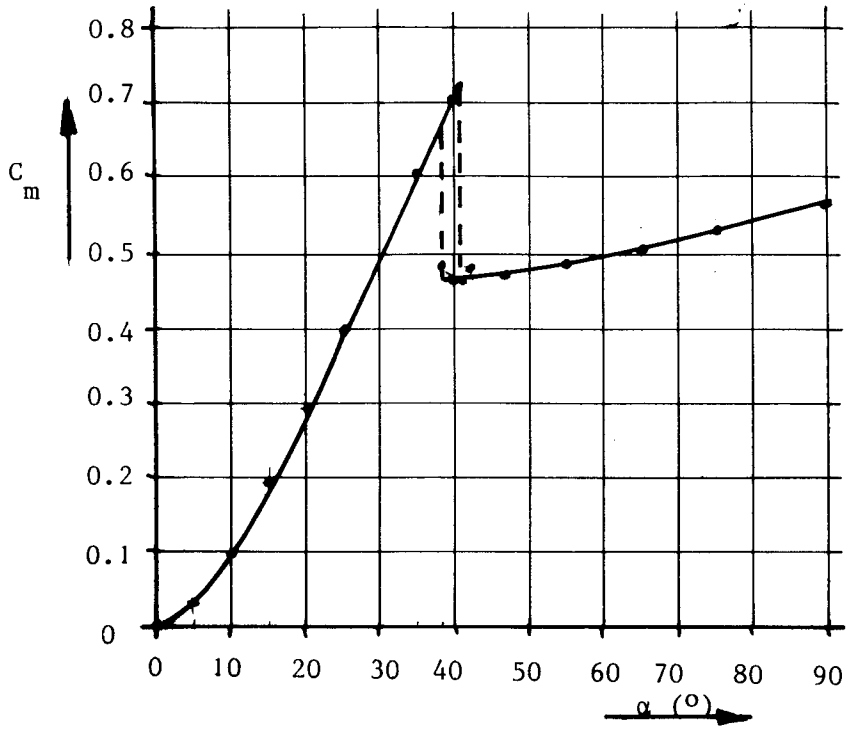

Figure 55 $C_m - \delta$ curve for a square plate according to Flachsbart

Next the moment equation around the vane axis can be derived.
(74) + (73) + (64) →

$$t \times \rho_v \times g \cos \alpha_2 = C_m \times \rho \times V^2 \qquad (75)$$

7.6.4 The hinged side vane system for moderate wind speeds

At low wind speeds ($V < 4$ m/s) and at high wind speeds ($V > 8$ m/s) the hinged side vane mechanism has been described in the previous two chapters.
At moderate wind speeds it is difficult to describe the system mathematically because the wind direction is not parallel to one of the vane edges.
Windtunnel measurements performed on an unloaded scale model of the CWD 2000 (see TUE report R 686 S [19]) show that the system is stable also at moderate wind speeds. In figure 56 the results of the windtunnel measurements are presented.

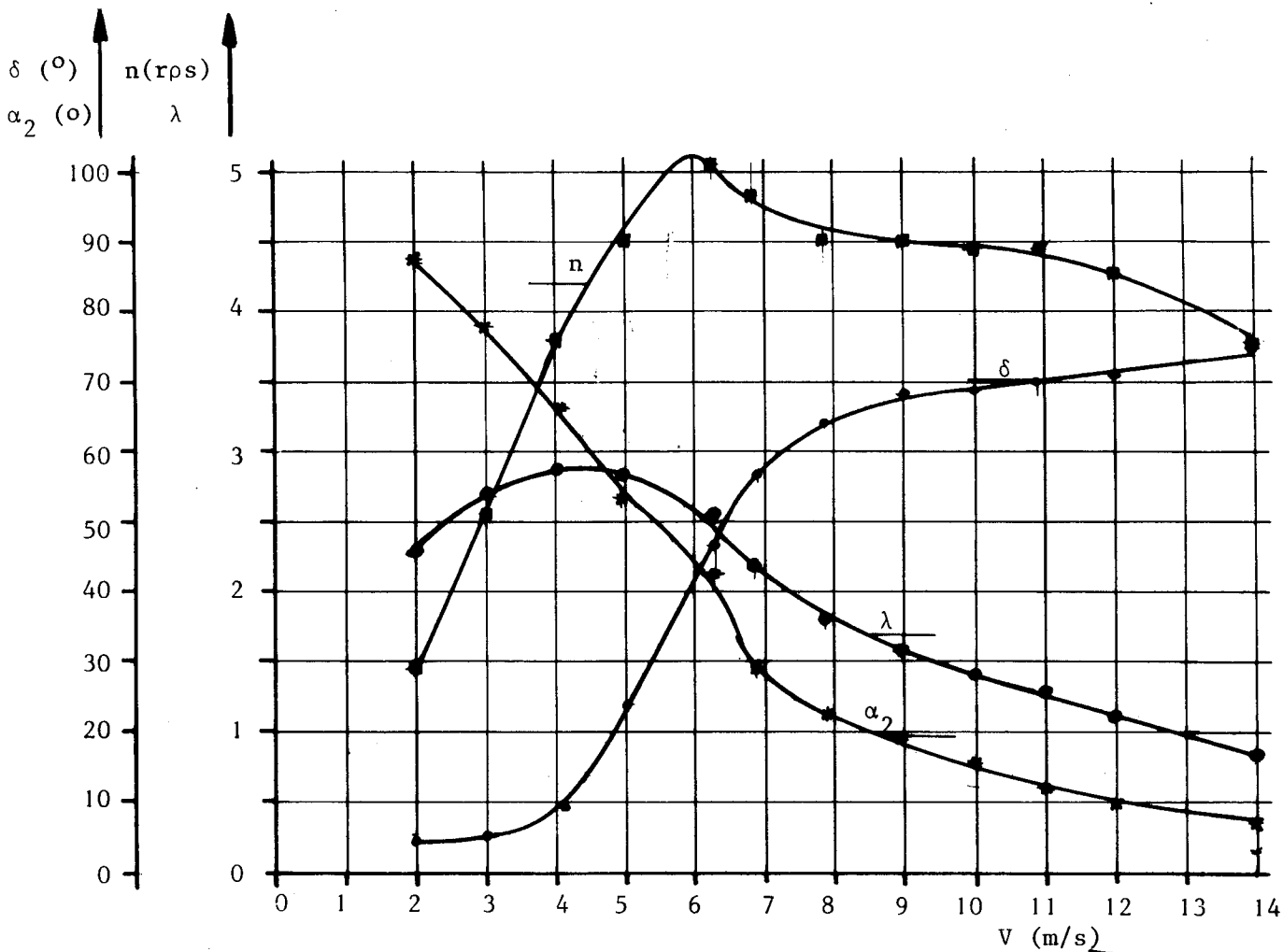

Figure 56 Measured δ -V, α_2 - V, n - V and λ - V curves for scale model CWD 2000

It can be seen that there are no discontinuities in the α_2 – V and δ – V curves which is an indication for stability.

The rotor starts to turn out of the wind at V = 4 m/s. The maximum rotor speed is reached at V = 6.5 m/s at a yaw angle $\delta = 50^{\circ}$. The rotor speed decreases slightly at high wind speeds. Field measurements on the real windmill show that the rotor speed is limited very well also for very high wind speeds (see chapter 8).

7.6.5 Example

The head and vane geometry of the CWD 2000 is taken as an example for the hinged side vane mechanism. The head geometry has already been given in chapter 7.2 and the M_r – δ curve is presented in figure 26. The vane parameters have been defined in figure 48.

With formula (62) first it is checked if the rotor is perpendicular to the wind at low wind speeds.

$$(62) \rightarrow C_n = \frac{C_t \times \pi R^2 \times e}{A_v \times (R_v + i_1)}$$

$C_t = 0.92$ (see figure 24)

$R = 1$ m

$e = 0.3$ m

$A_v = 0.61^2 = 0.372$ m^2

$R_v = 1.88$ m

$i_1 = 0.2$ m

$\rightarrow C_n = 1.12$

in figure 13 it can be seen that $C_n = 1.12$ for $\alpha = 25^\circ$

$\alpha_2 = 20^\circ$ for $\delta = 0^\circ$ so the rotor is turned 5° out of the wind for $\alpha_2 = 25^\circ$. At the windtunnel measurements in figure 56 it can be seen that $\delta = 5^\circ$ for low wind speeds. So calculations and measurements coincide (For the first geometry calculations C_t was assumed to be lower which originally resulted in $\delta = 0^\circ$).

However the effect of a small angle δ at low wind speeds on the power can be neglected so the geometry is o.k..

The assumption that the vane blade is about vertical for low wind speeds can be checked with formula (65).

$$(65) \rightarrow \sin\theta = \frac{C_n \times 0.5\rho V^2}{t \times \rho_v \times g}$$

$C_n = 1.12$

$\rho = 1.25$ kg/m^3

assume $V = 3$ m/s

$t = 5 \times 10^{-3}$ m

$\rho_v = 0.54 \times 10^3$ kg/m^3

$g = 9.81$ m/s^2

$\sin\theta = 0.2378 \rightarrow$

$\theta = 13.7^\circ$

$\alpha_1 = 90 - \theta$

$\alpha_2 = 76.3^\circ$

In figure 56 it can be seen that $\alpha_2 = 78^o$ for V = 3 m/s so almost the same as the calculated value.
$\theta = 13.7 \rightarrow \cos\theta = 0.97$ so the assumption that the vane is almost vertical and that $N \cos\theta \approx N$ is allowed.

The calculation at high wind speeds V > 8 m/s goes as follows:
Using figure 54 and figure 55, C_m and C_d are determined for a range of α_2 values between 25° and 0°. The angles have been taken according to the table of the original measurements of Flachsbart because for that angles C_m and C_d are given very accurately. Only the values for $\alpha = 3^o$ and $\alpha = 2^o$ have been estimated by interpolation.
Then V is calculated with formula (75) for each choice of α_2 and a certain choice of t.
Assume $t = 5 \times 10^{-3}$ m and $\rho_v = 0.54 \times 10^3$ kg/m³.
formula (75) also can be written as:

$$V = \sqrt{\frac{t \times \rho_v \times g}{\rho}} \times \sqrt{\frac{\cos\alpha_2}{C_m}}$$

$$V = 4.6 \times \sqrt{\frac{\cos\alpha_2}{C_m}} \qquad (76)$$

$t = 0.005$ m $\rho = 1.25$ kg/m³
$\rho_v = 0.54 \times 10^3$ kg/m³ $g = 9.81$ m/s²

Next D is calculated with formula (68)

$$D = C_d \times 0.5\,\rho\,V^2 \times A_v$$

$$D = 0.233 \times C_d \times V^2 \qquad (77)$$

$\rho = 1.25$ kg/m³ $A_v = 0.372$ m²

and M_v with formula (67)

$$M_v = D \times (R_v + i_2)$$

$$M_v = 2.18 \times D \qquad (78)$$

$R_v = 1.88$ m $i_2 = 0.3$ m

The results of the calculations are presented in table 6.

α_2	C_d	C_m	V (m/s)	D (N)	M_v (Nm)
24.6	0.479	0.402	6.92	5.34	11.65
19.9	0.313	0.299	8.16	4.86	10.59
14.9	0.176	0.193	10.29	4.34	9.47
9.9	0.0842	0.098	14.58	4.17	9.09
5.0	0.0363	0.035	24.54	5.09	11.10
3	0.028	0.02	32.50	6.89	15.02
2	0.025	0.012	41.98	10.26	22.38
0	0.0232	0	∞	∞	∞

Table 6: Calculated values for V, D and M_v as a function of α_2 for CWD 2000 vane blade.

The change in M_v as a function of V is presented in figure 57.

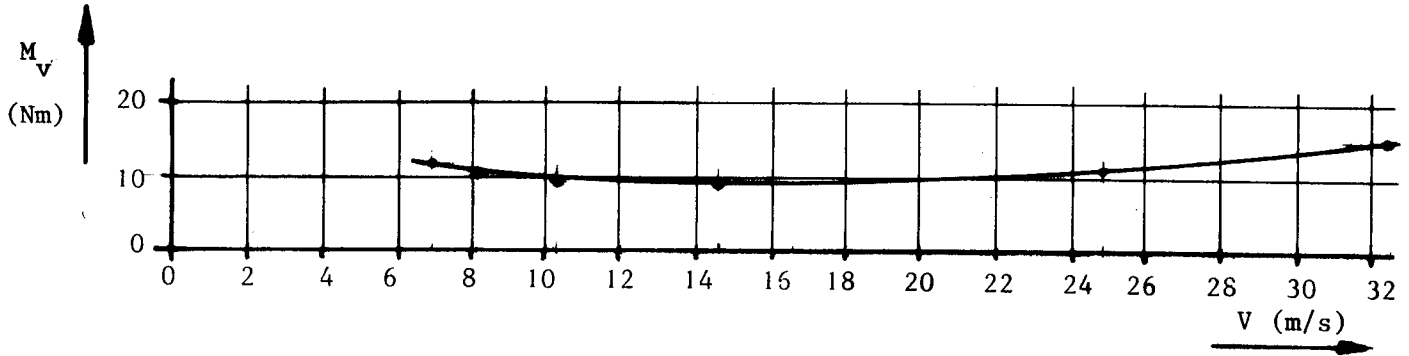

Figure 57 M_v – V curve for CWD 2000 vane blade

It can be seen that M_v is about constant for $7 < V < 25$ m/s.

The next step is to calculate the effect of M_{va} as a function of V for a certain roughness of the pipe.

As the drag coefficient $C_{d_{va}}$ is a function of the Reynolds number first the Reynolds number is calculated with formula (71) for a range of wind speeds.

$$\left.\begin{array}{l}(71) \rightarrow Re = \dfrac{V \times d}{\nu} \\ d = 48 \times 10^{3}\ m \\ \nu = 15 \times 10^{-6}\ m^2/s\end{array}\right\} \quad Re = 3.2 \times 10^{3}\ V \qquad (79)$$

Next $C_{d_{va}}$ is determined using figure 53.

Two values are tried:

1. a smooth pipe with k/d = 0
2. a pipe covered with fine sand k/d = $7/10^3$.

Next M_{va} is calculated using formulas (70), (69) and (58).

(70) + (69) + (58) →

$$\left.\begin{array}{l} M_{va} = C_{d_{va}} \times 0.5\,\rho\,V^2 \times d \times 0.5\,R_v^2 \\ \rho = 1.25\ kg/m^3 \qquad R_v = 1.88\ m \\ d = 48 \times 10^{-3}\ m \end{array}\right\} \quad M_{va} = 0.053 \times C_{d_{va}} \times V^2 \qquad (80)$$

The results of the calculation is presented in table 7.

V (m/s)	Re	$C_{d_{va}}$ for k/d=0	M_{va} (Nm) for k/d=0	$C_{d_{va}}$ for k/d=$7/10^3$	M_{va} for k/d=$7/10^3$
8	2.56×10^4	1.2	4.07	1.2	4.07
10	3.2×10^4	1.2	6.36	1.2	6.36
12	3.84×10^4	1.2	9.16	1.2	9.16
14	4.48×10^4	1.2	12.47	1.2	12.47
16	5.12×10^4	1.2	16.28	1.2	16.28
18	5.76×10^4	1.2	20.60	1.2	20.60
20	6.4×10^4	1.2	25.44	1.05	22.26
22	7.04×10^4	1.2	30.78	0.95	24.37
24	7.68×10^4	1.2	36.63	0.8	24.42
26	8.32×10^4	1.2	42.99	0.63	22.57
28	8.96×10^4	1.2	49.86	0.6	24.93
30	9.6×10^4	1.2	57.24	0.68	32.44

Table 7: calculated values for M_{va} for smooth and rough vane arms.

The M_{va} - V curves for both roughnesses are presented in figure 58. It can be seen the the pipe roughness has a significant influence of M_{va} for V > 20 m/s.

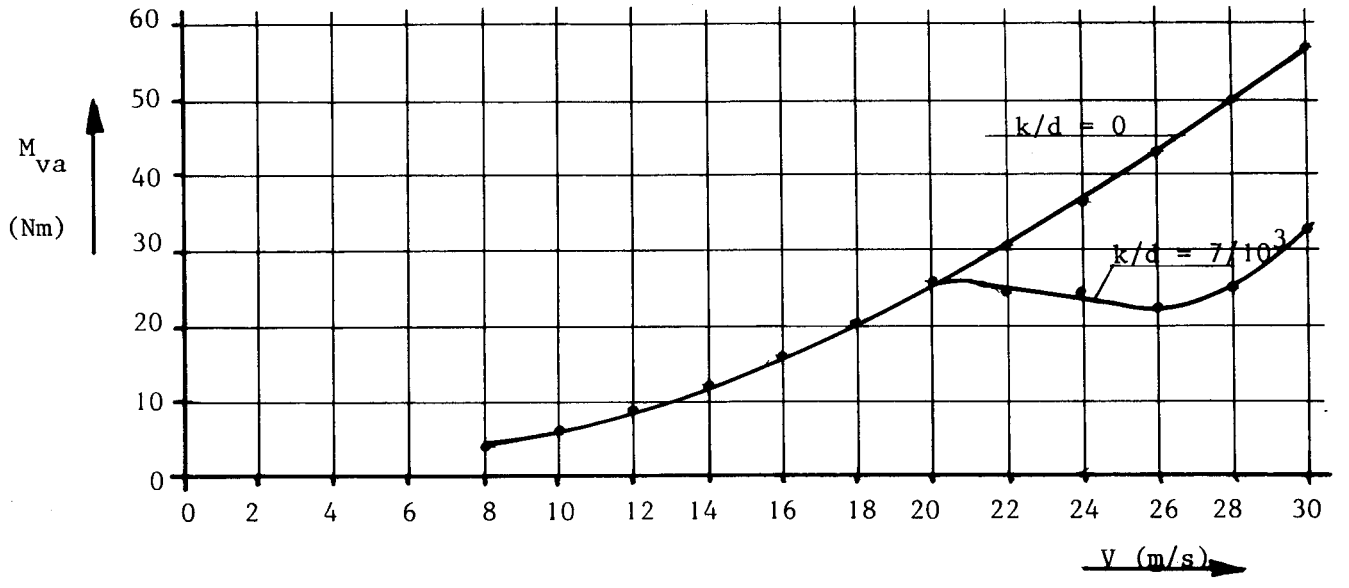

Figure 58 M_{va} – V curves for CWD 2000 vane arm for two values of the surface roughness

Next M_{va} has been added to M_v (see figure 57). The result is presented in figure 59.

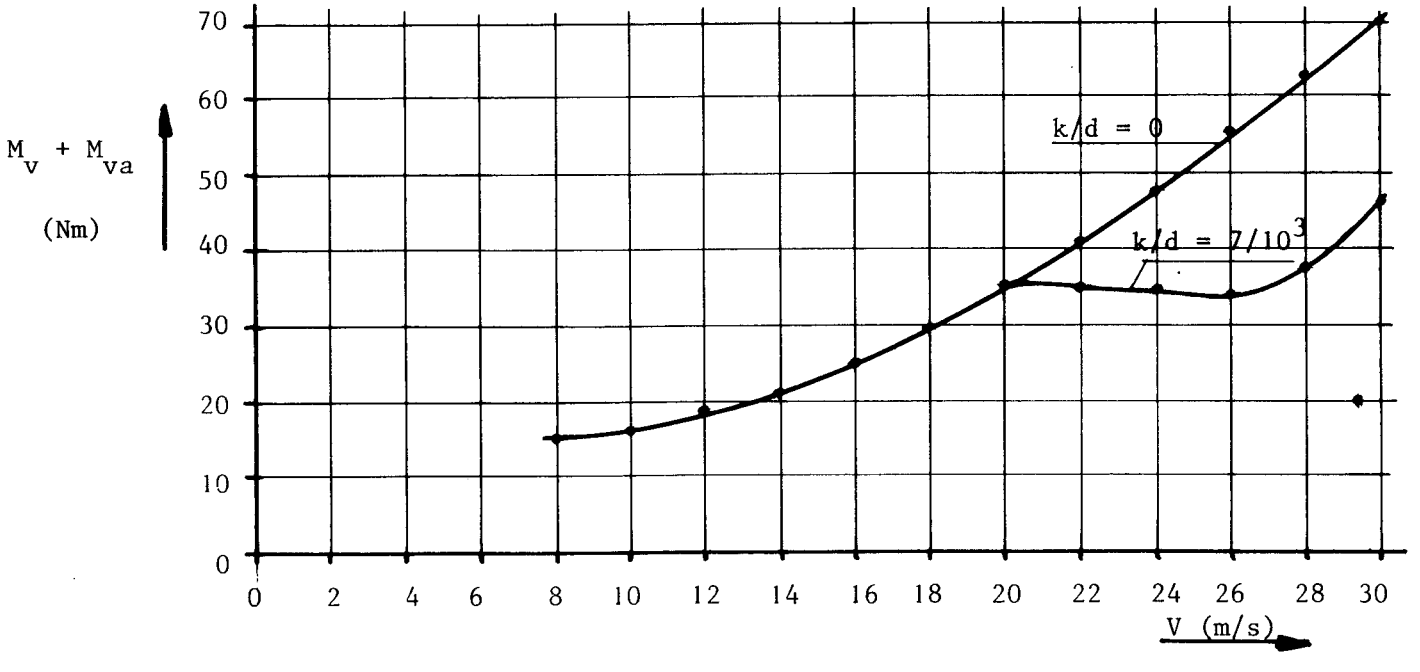

Figure 59 $(M_v + M_{mv})$ – V curves for CWD 2000 vane + vane arm for two values of the surface roughness

Now one must make a choice about the pipe roughness. Suppose one takes the smooth pipe with $k/d = 0$.

Next the $M_v + M_{va}$ must be compared with the $M_r - \delta$ curve as presented in figure 26. Therefore the values for $M_v + M_{va}$ at certain wind speeds marked with points A to L have been placed on the lines with identical wind speed. These points are the working points for those wind speeds.
The result is presented in figure 60.

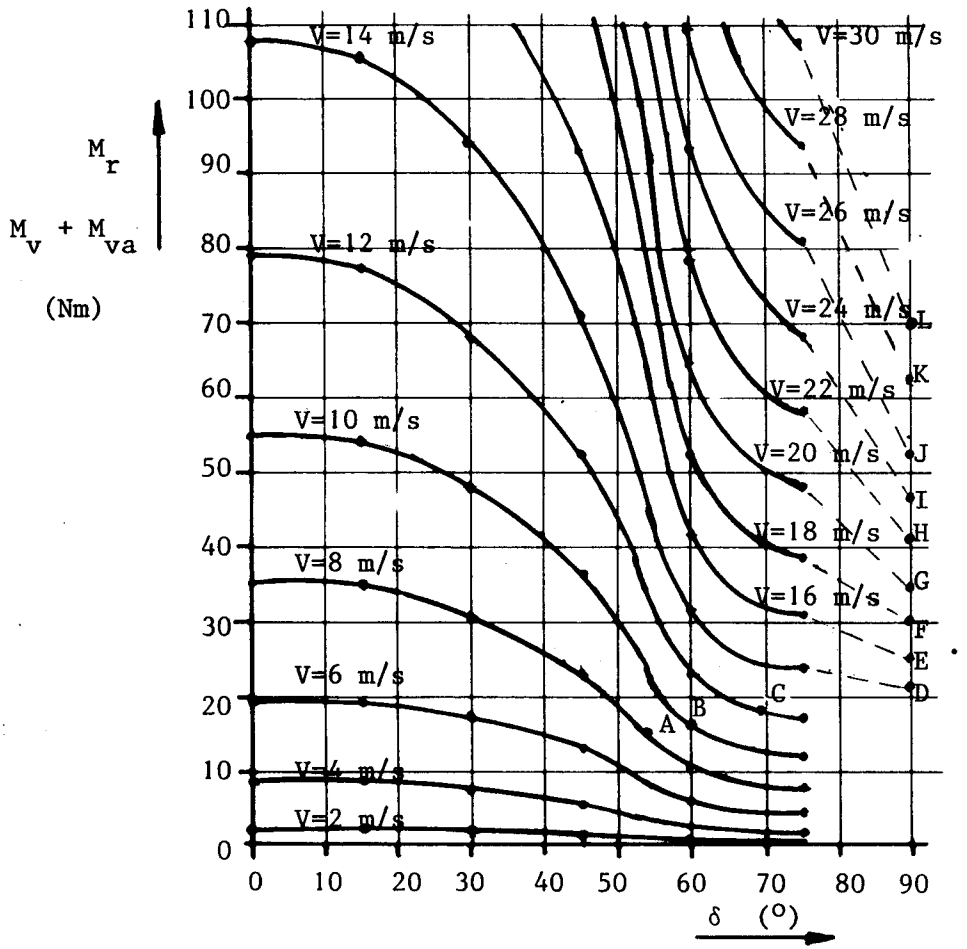

Figure 60 Points A - L for $M_v + M_{va}$ drawn in the $M_r - \delta$ graph of the CWD 2000 head

The corresponding values for δ have been listed in table 8 and in figure 61.

V	Point	M_V+M_{va}	δ (°)	Ω (rad/s)	n/rps	F_t(N)	$^1/_{2n}$ measured
8	A	15	54	13.2	2.1	39.9	2.25
10	B	16	60	14	2.2	45.2	2.2
12	C	18.5	69	12.0	1.9	33.4	2.15
14	D	21	90?	0	0	0	1.9
16	E	25	90?	0	0	0	
18	F	30	90?	0	0	0	
20	G	35	90?	0	0	0	
22	H	41	90?	0	0	0	
24	I	47.5	90?	0	0	0	
26	J	55	90?	0	0	0	
28	K	62.5	90?	0	0	0	
30	L	70	90?	0	0	0	

Table 8: Calculated and measured values for Ω and n for CWD 2000 head.

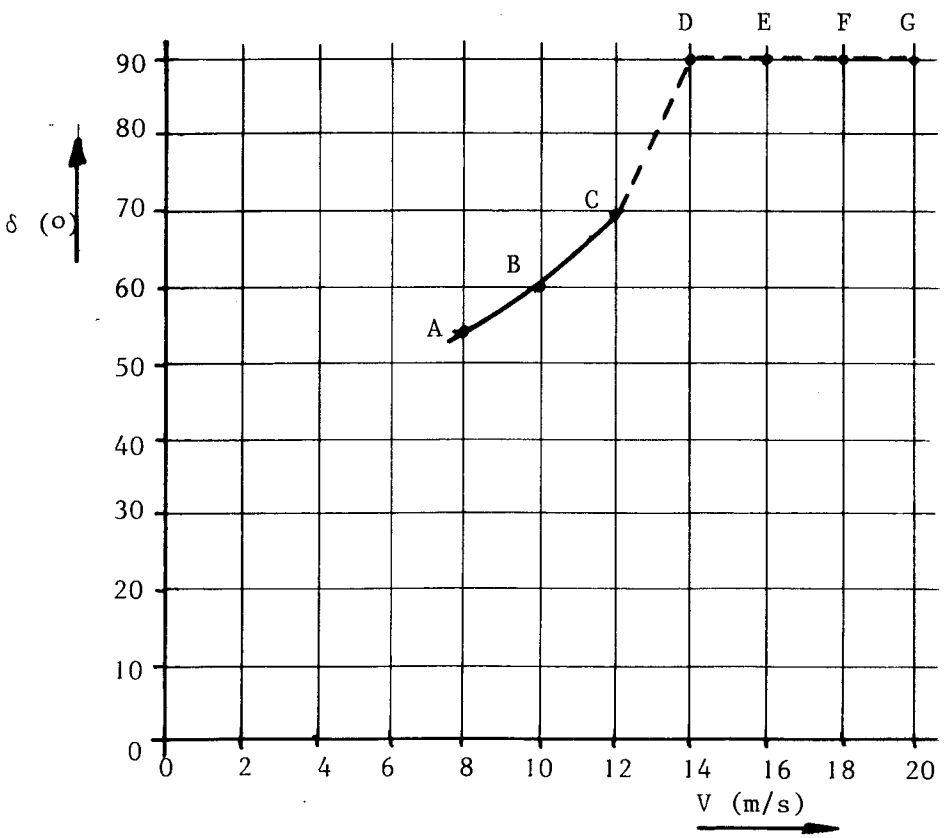

Figure 61 δ – V curve for CWD 2000 rotor + head

For wind speeds larger than 12 m/s M_r is larger than $M_v + M_{va}$ so no working points are found. It is assumed that the rotor is turned 90° out of the wind for V > 12 m/s. Field measurements however show that this is not correct. Also at wind speeds of about 20 m/s the rotor turns slowly what means that δ is smaller than 90°. Probably this is caused by inaccuracy of the dimensionless rotor coefficients at high angles δ. The reason might be:

1. A mistake has been made in the blade setting angles of the scale model and
2. The rotor was not running really unloaded during the windtunnel tests because the friction of a gearbox had to be overcome. Because of this friction the rotor stopped at angles δ just above 75° and measurements for $\delta = 90°$ have not been executed.

Next Ω, n and F_t can be calculated using formulas (2) and (4) and the following parameters for the CWD 2000: $\lambda_{unloaded} = 2.8$

$C_t = 0.92$

$\rho = 1.25$ kg/m^2

(F_t can be calculated more accurately than with formula (4) if the real measured $C_t = \delta$ values are taken.)

The results of the calculation have also been presented in table 8 and in figure 62 and figure 63.

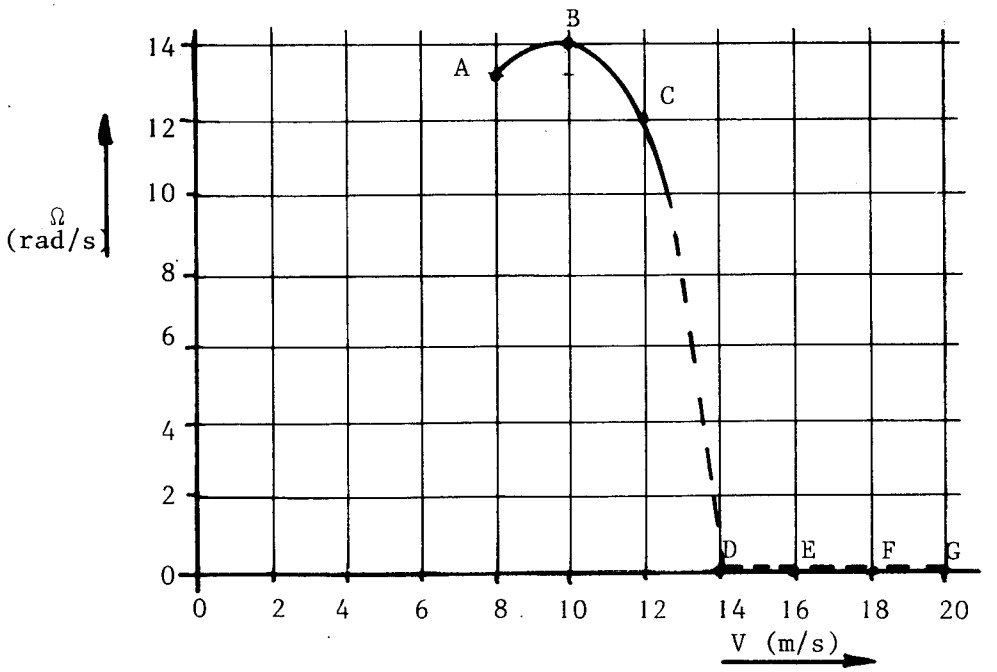

Figure 62 Ω – V curve for CWD 2000 rotor + head

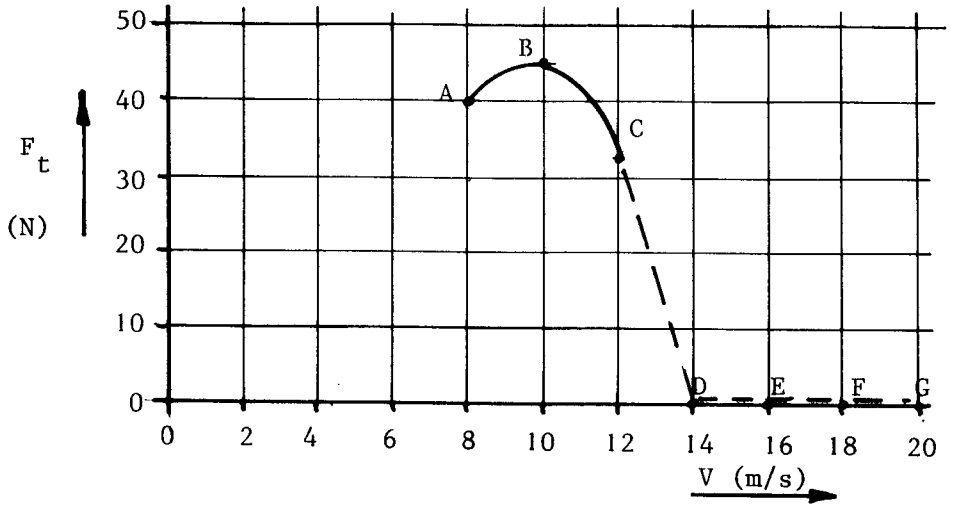

Figure 63 F_t - V curve for CWD 2000 rotor + head

The calculated rotor speed in table 8 can be compared with the measured rotor speed of the scale model in figure 56 if the scale factor is taken into account. The scale model had a diameter of 1 meter and the real CWD 2000 has a diameter of two meters. So if the measured rotor speed is divided by two it can be compared with the calculated speed. The value for $^1/_2\ n_{measured}$ is also given in table 8 and it can be seen the measured and calculated values for V = 8, 10, 12 m/s are almost the same.
The calculated values for higher wind speeds are zero but this is not realistic because of the inaccuracy of the rotor coefficient for high angles δ.

8. FIELD MEASUREMENTS

The CWD 2000 and CWD 2740 both have been measured for a long time on the CWD testfield in Almere and the measuring results have been reported in a series of measuring reports.
During the measurements as reported in report no. 57 [23] the average wind speed over the whole measuring period of two weeks was rather high. (About 4.5 m/s at the hub height of the windmills.)
The n-V curves from the CWD 2000 and CWD 2740 have been copied as fig. 64 and 65.

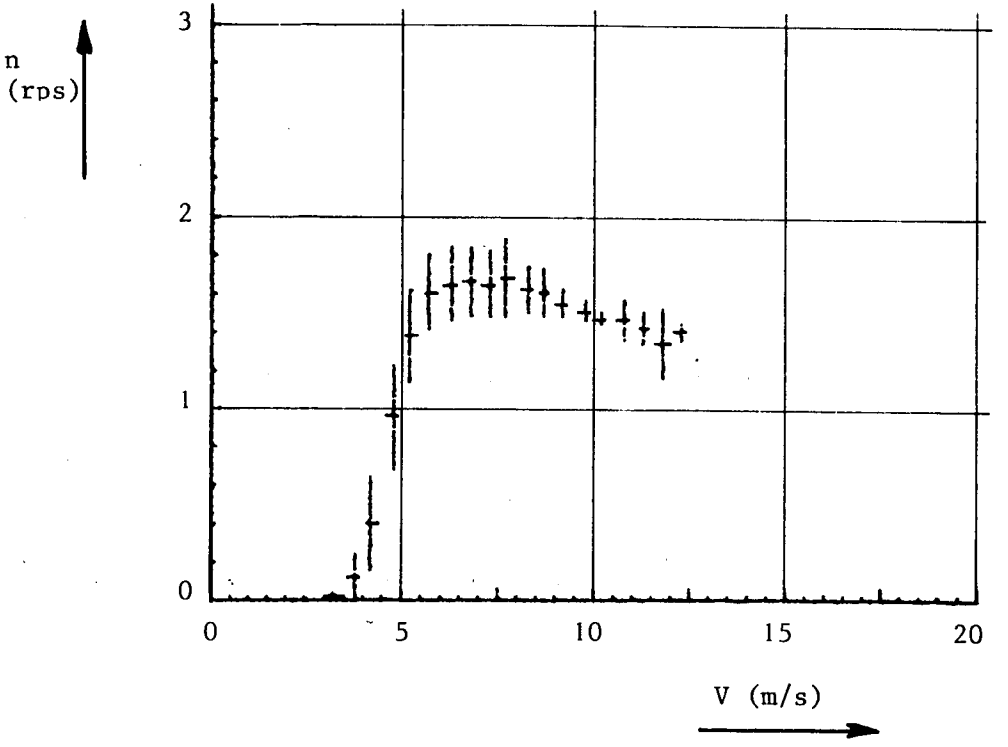

Figure 64 CWD 2000 n-V curve measured on testfield Almere.

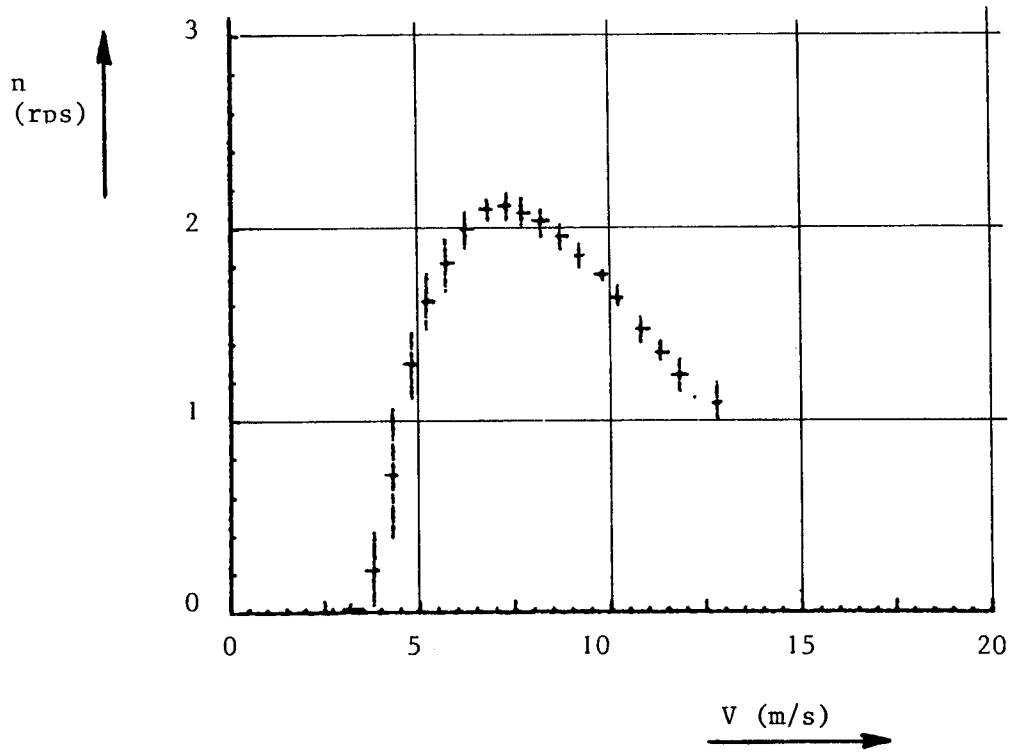

Figure 65 CWD 2740 n–V curve measured on testfield Almere.

The ten minutes average rotor speed is given as a function of the wind speed. A certain wind speed is the average of all wind speeds laying within an interval of 0.5 m/s.
This means that the presented curves may deviate from momentary curves as found from windtunnel measurements for which a certain rotor speed is gained for a certain wind speed.
The ten minutes average curves give no indication of the peak wind speed which may have occurred at a certain wind speed.
Comparing both curve learns that the average rotor speed for the CWD 2000 stays about constant for $V > 6$ m/s and that the average rotor speed for the CWD 2740 decreases for $V > 7$ m/s.

9. SCALE LAWS

In chapter 7 an example has been given for each of the three described systems. Each calculation is a lot of work and the accuracy in the result is not high because of many approximations.

Before one starts to make a windmill on full scale therefore it is advised first to make a scale model and test it in the windtunnel. If a windtunnel is not available one can use a truck and drive it on a calm day. Dynamic effects caused by turbulence and sudden changes in wind direction can be observed on a stormy day.

If one uses a scale model this must be made according to certain scale laws to simulate the same static behaviour as the original windmill.

The dynamic behaviour always will be different as the real windmill because the frequencies of all movements increase for scale models smaller than the original.

If all dimensions of a certain subject are scaled with a factor i ($i > 1$ for upscaling and $i < 1$ for downscaling) all area's are scaled with a factor i^2 and all volumes with a factor i^3. If the density is identical this means that also all masses and all weights are scaled with a factor i^3. All aerodynamic forces are proportional with the area so with i^2.

To simulate identical static behaviour it is necessary that the forces which counterbalance aerodynamic forces are scaled with the same ratio, so also with i^2. In case of the ecliptic system this means that all dimensions of the spring must be scaled with factor i. In case of the inclined hinge main vane and the hinged side vane scaling of all dimensions with a factor i results in scaling of the weight with a factor i^3 which is not correct. For the hinged side vane this problem is solved by keeping the vane thickness constant independed of the size for identical densities.

In this case the vane weight also scales with a factor i^2.

However this causes two kind of problems:

1. If the scale factor is much smaller than 1 so if for instance a windtunnel scale model is made with a scale factor of 0.2, the vane thickness becomes thick with respect to the other vane dimensions and this causes an increase of the drag coefficient at small angles of attack.

   This problem can be solved by increase of the density.

   If for instance a five mm thick wooden vane with density 0.54×10^{-3} kg/m^3 is scaled with a factor 0.2 (so 5× smaller) it can be replaced by a 1 mm thick aluminium vane with density 2.7×10^{-3} kg/m^3 (so 5× larger).

2. If the scale factor is larger than 1 which is the case if a certain windmill is scaled up to a bigger one the relative thickness of the blade with respect to the other vane dimensions becomes smaller. Therefore the relative stiffness of the blade decreases. Below a certain ratio between vane thickness and vane chord the vane itself can become instable at high wind speeds.
   This means that the vane bends upward and downward periodically and because of this bending the lift force also varies from up to down. This makes that the vane continues its oscillation see figure 66.

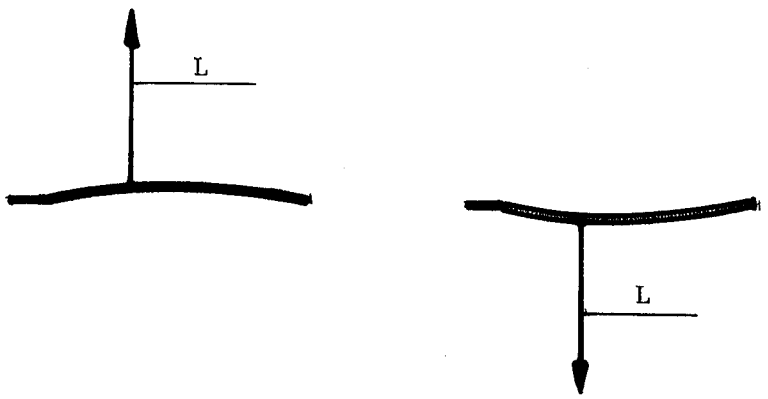

Figure 66 Oscillating lift if vane blade is not stiff enough

   Because of the oscillation the whole vane arm and tower can come in resonance which is very dangerous. The critical ratio is not exactly known but field experiment with a private prototype of an electricity generating windmill type Drieka 4 show that oscillations occur with a square wooden vane thickness 5.5 mm chord 1220 mm at a wind speed of about 20 m/s.
   The same vane with a thickness of 9 mm never showed this periodically bending of the blade.

In case of the inclined hinge main vane it is not only the vane blade but the sum of blade and vane arm which determines the weight and the position of the centre of gravity.
For scaling with a factor i smaller than 1 some extra mass can be added in the centre of gravity to realise a scale factor i^2 for the weight. For scaling with a factor i larger than 1 and a vane which already has a minimal weight one can decrease the angle ϵ between the vane axis and the vertical.

In formula (54) it can be seen the M_g is determined by the product G sin ϵ.
For small angles ϵ, sin ϵ is proportional with ϵ so if the weight is for instances a factor 1.5 too large the angle ϵ must be decreased with a factor 0.666.
Scaling also has an influence on the friction of the head bearings and the bearings at the vane axis. For scaling with factor i larger than 1 generally the weight scales up with a factor i^3 and the area with a factor i^2. This means that the specific pressure in sleeve bearings increases with a factor i. Therefore simple sleeve bearings can be used in small scale models but large heavy windmill may require roller bearings at the vane and tower axis otherwise the bearing friction would be too high.
Especially at low wind speeds where all aerodynamic forces are low bearing friction causes hysteresis in the movement of vane and head and therefore the system is not optimally orientated to the wind which causes loss in power.
Especially high friction of the head bearings can result in turning out of the wind too late or not at all.
An advantage of a large eccentricity or a large auxiliary vane is that the influence of friction at the head bearing is small.

10. CONCLUSIONS

1. An eccentrically placed rotor with a large eccentricity is preferable above an auxiliary vane because it results in δ – V, Ω – V and F_t – v curves without hysteresis.

2. The hysteresis in an inclined hinge main vane system with auxiliary vane is smaller than in an ecliptic system with auxiliary vane.

3. The hinged side vane system with eccentrically placed rotor has almost ideal characteristics. (δ – V, Ω – V and F_v – V curves.)

LITERATURE

[1] Kragten A.
Overview of literature related to safety mechanisms to limit the rotor speed and thrust.
Internal note 03–89, 1989–01–11, TUE

[2] Lysen E.H.
Introduction to wind energy.
CWD publication no 82–2, May 1983

[3] Both D. and Stelt E.R. van der
Catalogue of wind machines.
CWD publication no 84–2, February 1984

[4] Kragten A.
Overview of commercially available small water pumping windmills with D $\leq$ 1.5 meter.
Report no R 871 D, November 1986, TUE

[5] Kragten A.
Ecliptische beveiliging THE–11 (CWD 5000 HW) ontwerp.
(in Dutch)

[6] Bos K., Schoonhoven H. and Verhaar J.
Static and dynamic behaviour of mechanical control systems of slow–running windturbines.

[7] Kragten A.
The hinged side vane as a safety mechanism for windmills.
Report no R 515 D, January 1982, TUE

[8] Kragten A.
Windtunnel measurements executed on a scale model of the head of the WEU I–4 windmill.
Report no R 743 D, September 1985, TUE

[9] Schumach M.
Results of windtunnel tests on the scale model of the THE 1–2 (CWD 2740) rotor.
Report no R 408 S, December 1979, TUE

[10] Hageman A.
Catalogue of aerodynamic characteristics of airfoils in the Reynolds number range $10^4 - 10^6$.
Report no R 443 D, Juli 1980, TUE

[11] Lenssen G.
Het zelfrichtende gedrag van scheef aangestroomde snellopende windrotoren met horizontale as (in Dutch).
Report no R 423 A, Maart 1980, TUE

[12] Smulders P., Lenssen G. and Leeuwen H. van
Experiments with wind rotors in yaw.
Report no R 526 D, June 1981, TUE

[13] Vilder G.J. de
Meetopstelling voor het meten van krachten en momenten werkende op een model van een windmolen rotor (in Dutch).
Report no R 763 A, December 1985, TUE

[14] Kragten A.
Description of windtunnel measurements executed on a scale model of the head of the CWD 5000 RCV (CWD 5000 HW)
Report no R 523 D, March 1982, TUE

[15] Upperman J.M.
Krachten en momenten werkend op een scheef aangestroomde windrotor (8–bladig ontwerp snellopendheid 2) (in Dutch).
Report no R 575 S, December 1982, TUE

[16] Vermeer N.J.
Het meten met een twee-komponenten balans aan schaalmodellen in de windtunnel (in Dutch).
Report no R 487 S, April 1981, TUE

[17] Kusters R.
Aerodynamische karakteristieken van vierkante vlakke platen.
Report no R 584 S, Maart 1983, TUE

[18] Hoerner S.F.
Fluid-dynamic drag
148 Busteed Drive Midland Park New Jersey 07432 England, 1965

[19] Oers P. van
Description of windtunnel measurements of the static behaviour of the hinged side vane safety mechanism executed on a scale model of the CWD 2000 and the CWD 5001 windmills.
Report no R 686 S, November 1984, TUE

[20] Cong Xianzi, P.T. Smulders and others
The investigation on full-scale windpumps in the large low speed wind tunnel of CARDC.
October, 1987

[21] Logtenberg A.R.
On passive safety and control mechanisms for water pumping windmills.
Report no R 728 D, March 1986, TUE

[22] Beurskens, H.
Expert group study on recommended practices for wind turbine testing and evaluation part 6, Structural Safety
IEA publication, 1988

[23] Oldenkamp, H.
Almere testfield measuring report no. 57 (not yet available)
OKE Services